

TAM
C4
CER 68-69-3
COPY 2

C. E. - R. R. COPY

AD

TECHNICAL REPORT ECOM C-0423-1

GASEOUS PLUME DIFFUSION

CHARACTERISTICS WITHIN MODEL

PEG CANOPIES

TASK IIB RESEARCH TECHNICAL REPORT

DESERET TEST CENTER

BY

R. N. MERONEY

D. KESIC

and

T. YAMADA

SEPTEMBER 1968

DISTRIBUTION OF THIS DOCUMENT IS UNLIMITED

ECOM

UNITED STATES ARMY ELECTRONICS COMMAND

FORT MONMOUTH, N. J.

CONTRACT DAAB07-63-C-0423
FLUID DYNAMICS AND DIFFUSION LABORATORY
FLUID MECHANICS PROGRAM
COLLEGE OF ENGINEERING
COLORADO STATE UNIVERSITY
FORT COLLINS, COLORADO 80521

DISCLAIMER

THE CITATION OF TRADE NAMES AND NAMES OF MANUFACTURERS IN THIS REPORT IS NOT TO BE CONSTRUED AS OFFICIAL GOVERNMENT INDORSEMENT OR APPROVAL OF COMMERCIAL PRODUCTS OR SERVICES REFERENCED HEREIN.

Wind Tunnel Studies and Simulations
of Turbulent Shear Flows Related to
Atmospheric Science and Associated Technologies

TECHNICAL REPORT

GASEOUS PLUME DIFFUSION
CHARACTERISTICS WITHIN MODEL
PEG CANOPIES

TASK IIB RESEARCH TECHNICAL REPORT
DESERET TEST CENTER

PREPARED BY

R. N. MERONEY

D. KESIC

and

T. YAMADA

Fluid Dynamics and Diffusion Laboratory
Fluid Mechanics Program
College of Engineering
Colorado State University
Fort Collins, Colorado
80521

for

ATMOSPHERIC SCIENCES LABORATORY
U. S. Army Electronics Command
Fort Monmouth, N. J.

CER68-69RNM-DK-TY-3



U18401 0574954

ABSTRACT

A point source of an air-helium mixture was released continuously at various positions within a simulated canopy composed of 9 cm high pegs, 0.48 cm diameter, spaced in several arrays (2.54 x 2.54, 3.55 x 3.55, and 5.08 x 5.08 cm). Variations of the vertical location of the source revealed the strongly nonisotropic character of diffusion within a canopy with respect to the relative diffusion rates in the lateral and vertical directions. When the source was placed at various downstream distances from the edge of the canopy, it displayed a tendency to exhale the plume near the front of the model canopy and to inhale the plume at distances further downstream. Calculations of the turbulent diffusion coefficient, K , within and above the canopy from the experimental data, reveal both a constant region and a region of linear increase with height increase as suggested by previous authors.

TABLE OF CONTENTS

	<u>Page</u>
LIST OF FIGURES	iv
INTRODUCTION	1
MODELING OF A VEGETATIVE CANOPY	4
EXPERIMENTAL EQUIPMENT AND PROCEDURE	6
EXPERIMENTAL RESULTS	9
CONCLUSIONS	18
BIBLIOGRAPHY	20
FIGURES	23

LIST OF FIGURES

<u>Figure</u>		<u>Page</u>
1	Wind tunnel and artificial canopy configuration.	24
2	Continuous point source feed and sampling system.	25
3	Velocity profiles within model canopy.	26
4	Velocity profiles above model canopy.	27
5	Longitudinal turbulent intensity for model canopy	28
6	Vertical turbulent intensity for model canopy.	29
7	Shear profile for model canopy	30
8	Streamline flow in and above a model canopy.	31
9	Vertical dispersion of a continuous point source in a model peg canopy (2.54 x 2.54 cm) $x_s = 0$, $z_s = 1$ cm	32
10	Vertical dispersion of a continuous point source in a model peg canopy (2.54 x 2.54 cm). $x_s = 0$, $z_s = 0.5$ h	33
11	Vertical dispersion of a continuous point source in a model peg canopy (2.54 x 2.54 cm). $x_s = 0$, $z_s = h$	34
12	Vertical dispersion of a continuous point source in a model peg canopy (2.54 x 2.54 cm). $x_s = 6$ m, $z_s = 1$ cm	35
13	Vertical dispersion of a continuous point source in a model peg canopy (2.54 x 2.54 cm). $x_s = 6$ m, $z_s = h$	36
14	Vertical dispersion of a continuous point source in a model peg canopy (2.54 x 2.54 cm). $x_s = 6$ m, $z_s = 2$ h	37

LIST OF FIGURES - Continued

<u>Figure</u>		<u>Page</u>
15	Lateral dispersion of a continuous point source in a model peg canopy (2.54 x 2.54 cm). $x_s = 6$ m, $z_s = 1$ cm	38
16	Lateral dispersion of a continuous point source in a model peg canopy (2.54 x 2.54 cm). $x_s = 6$ m, $z_s = h$	39
17	Lateral dispersion of a continuous point source in a model peg canopy (2.54 x 2.54 cm). $x_s = 6$ m, $z_s = 1$ cm	40
18	Lateral dispersion of a continuous point source in a model peg canopy (2.54 x 2.54 cm). $x_s = 6$ m, $z_s = h$	41
19	Vertical dispersion of a continuous point source in a model peg canopy (2.54 x 2.54 cm diagonal). $x_s = 0$, $z_s = 1$ cm	42
20	Vertical dispersion of a continuous point source in a model peg canopy (2.54 x 2.54 diagonal). $x_s = 0$, $z_s = 0.5 h$	43
21	Vertical dispersion of a continuous point source in a model peg canopy (2.54 x 2.54 diagonal). $x_s = 0$, $z_s = h$	44
22	Vertical dispersion of a continuous point source in a model peg canopy (2.54 x 2.54 diagonal). $x_s = 6$ m, $z_s = 1$ cm	45
23	Vertical dispersion of a continuous point source in a model peg canopy (2.54 x 2.54 diagonal). $x_s = 6$ m, $z_s = 0.5 h$	46
24	Vertical dispersion of a continuous point source in a model peg canopy (2.54 x 2.54 diagonal). $x_s = 6$ m, $z_s = h$	47
25	Vertical dispersion of a continuous point source in a model peg canopy (2.54 x 2.54 diagonal). $x_s = 6$ m, $z_s = 1.5 h$	48

LIST OF FIGURES - Continued

Figure		Page
26	Vertical dispersion of a continuous point source in a model peg canopy (5.08 x 5.08 cm). $x_s = 0$, $z_s = 1$ cm, $x = 0.3$ m	49
27	Vertical dispersion of a continuous point source in a model peg canopy (5.08 x 5.08 cm). $x_s = 0$, $z_s = 1$ cm, $x = 0.6$ m	50
28	Traces of maximum concentration from a point source (2.54 x 2.54 cm). $x_s = 0$, $z_s = 0.5$ h	51
29	Traces of maximum concentration from a point source (2.54 x 2.54 cm). $x_s = 0$, $z_s = h$	52
30	Diffusion in the canopy-isoconcentration lines (2.54 x 2.54 diagonal). $x_s = 0$, $z_s = 1$ cm	53
31	Diffusion in the canopy-isoconcentration lines (2.54 x 2.54 diagonal). $x_s = 0$, $z_s = 0.5$ h	54
32	Diffusion in the canopy-isoconcentration lines (2.54 x 2.54 diagonal). $x_s = 0$, $z_s = h$	55
33	Diffusion in the canopy-isoconcentration lines (2.54 x 2.54 diagonal). $x_s = 6$, $z_s = 1$ cm	56
34	Diffusion in the canopy-isoconcentration lines (2.54 x 2.54 diagonal). $x_s = 6$, $z_s = 0.5$ h	57
35	Diffusion in the canopy-isoconcentration lines (2.54 x 2.54 diagonal). $x_s = 6$, $z_s = h$	58
36	Diffusion in the canopy-isoconcentration lines (2.54 x 2.54 diagonal). $x_s = 6$, $z_s = 1.5$ h	59
37	Gaseous plume cross-section of a continuous point source in a model peg canopy (2.54 x 2.54 cm). $x_s = 6$ m, $z_s = 1$ cm, $x = 0.3$ m	60
38	Gaseous plume cross-section of a continuous point source in a model peg canopy (2.54 x 2.54 cm). $x_s = 6$ m, $z_s = h$, $x = 0.3$ m	61

LIST OF FIGURES - Continued

<u>Figure</u>		<u>Page</u>
39	Gaseous plume cross-section of a continuous point source in a model peg canopy (2.54 x 2.54 cm diagonal). $x_s = 6$ m, $z_s = 1$ cm, $x = 0.25$ m	62
40	Gaseous plume cross-section of a continuous point source in a model peg canopy (2.54 x 2.54 cm diagonal). $x_s = 6$ m, $z_s = h$, $x = 0.5$ m	63
41	Gaseous plume cross-section of a continuous point source in a model peg canopy (5.08 x 5.08 cm). $x_s = 0$ m, $z_s = 1$ cm, $x = 0.3$ m	64
42	Gaseous plume cross-section of a continuous point source in a model peg canopy (5.08 x 5.08 cm). $x_s = 0$ m, $z_s = 1$ cm, $x = 0.6$ m	65
43	Variation of ground level concentration with downstream distance	66
44	Variation of characteristic plume height with downstream distance	67
45	Coefficient of turbulent diffusion	68
46	Mass and momentum turbulent diffusion coefficients	69
47	Dimensionless eddy diffusion coefficient	70

GASEOUS PLUME DIFFUSION
CHARACTERISTICS WITHIN MODEL
PEG CANOPIES

by

R. N. Meroney*, D. Kesic**
and T. Yamada**

INTRODUCTION

Agricultural meteorologists, atmospheric scientists, and many hydrologists are interested in the evaporation and exchange processes which occur in vegetative canopies. Such information permits calculation of the efficiency of water, energy, and CO₂ transport in plant metabolism and the penetration of foreign additives into or their escape out of the bulk of a canopy. As early as 1937 experimenters have made measurements of velocity, temperature, evaporation rates, and energy balance within and above such configurations^{1, 2, 3, 4} These measurements have provided a rough picture of a highly complex and turbulent flow field within the vegetation. Today, there exists a definite need for more elaborate and extensive measurements for different types of simple geometry crops.

*Assistant Professor of Civil Engineering, Colorado State University
**Graduate Research Assistants, Department of Civil Engineering,
Colorado State University

Past measurements of diffusion from point or line sources in such configurations seem to have been limited to measurements of an instantaneous line source by Bendix⁵ over a tropical rain forest, of point and line source distributions over a deciduous forest by Litton Systems,¹⁵ of instantaneous point sources in a jungle-like deciduous forest by Melpar,¹⁶ and of rates of particulate dispersion in a forest canopy at Brookhaven.⁶ These measurements are extensive and well documented; however, they must be normalized to some simplified geometry in order to determine the universal characteristics and governing parameters of vegetative penetration by a diffusing plume.

Since field measurements are not easy to obtain because of the cost of providing a perfect measuring station and the difficulty of obtaining cooperative weather, a laboratory program of modeling the flow in and above plant covers has been initiated at the Fluid Dynamics and Diffusion Laboratory at Colorado State University. Previous results from this program have been published by Quarishi and Plate, Yano, Hsi and Nath, and Kawatani.^{7, 8, 17, 18}

The purpose of this report is to discuss some measurements of diffusion from a continuous point source in and above a model peg canopy. The results of this study will consist of:

- 1) A description of the diffusion processes in and above the simulated canopy,

- 2) A description of the vertical dispersion of the tracer materials,
- 3) A determination of the effect of the initial fetch of the peg canopy on tracer dispersion, and, finally,
- 4) A determination of the vertical distribution of the eddy diffusion coefficients in and above the modeled canopy.

MODELING OF A VEGETATIVE CANOPY

The wind tunnel, long a research tool of the aerodynamicist, has recently proven its worth in atmospheric science through the success of an extensive sequence of programs to study modeling feasibility for micro-meteorological research.^{9, 10} As a result, it is now possible, for those conditions where Coriolis effects are secondary, to model many important features of the atmosphere. Suggestions concerning the applicable modeling criteria for vegetative canopies have been made by Quarishi and Plate.⁷

The intent of this program was to scale the nature of gaseous plume penetration at different points above a model crop, to determine the dispersion characteristics of a plume in such circumstances, and then to calculate and compare eddy diffusion coefficients with prototype data. Rather than model specifically all the complex characteristics of a live vegetative cover, it was proposed to retain the character of the flow while avoiding its minute complexity. Hence, short dowel pegs, approximately 0.5 cm in diameter and 9 cm long, were chosen as model elements and arranged in various geometrical patterns. This rough boundary arrangement produced turbulent flow at even small velocities; a constant drag coefficient, independent of wind speed*; and, hence, a flow independent of Reynolds' number.

*Measurements of canopy drag force were made by a shear plate described in Army Quarterly Report No. 11, 1 Nov 67-31 Jan 68, grant DA-AMC-28-043065-G20.

A logarithmic velocity profile similar to that typically found in the vertically stratified atmospheric boundary layer was reproduced in the wind tunnel by an upstream fetch of 20 meters of test section floor. It has been repeatedly shown that such an upstream boundary condition is critical for the equivalent kinematic character of a modeled flowfield.^{9, 10, 19}

A careful study of the mean velocity profiles, turbulent intensities and shear stress in and above the model peg canopy has been completed by Kawatani.¹⁸ These data were compared with prototype measurements in forests and agricultural crops. The marked functional agreement between the dynamic and kinematic behavior of the peg canopies and the live vegetative canopies provided a confirmation of the assumption of general similarity.

EXPERIMENTAL EQUIPMENT AND PROCEDURES

The experimental data were obtained in the low speed Army Meteorological Wind Tunnel in the Fluid Dynamics and Diffusion Laboratory at Colorado State University.¹¹ This tunnel was specifically designed to study fluid phenomena of the atmosphere. It has a 2 meter square by 26 meter long test section with an adjustable ceiling to provide a zero pressure gradient over the canopy crop. Model elements consisted of 0.48 cm diameter by 9 cm long dowel pegs inserted in holes in aluminum plate sections and arranged in geometric arrays the width of the test section extending for 11 meters downstream from the middle of the length dimension of the tunnel. All the various arrangements studied are summarized in Fig. 1.

A single and a cross-wire constant temperature anemometer was used to measure velocity, turbulent intensity, and shear. In addition, pitot-static tube measurements were made at each section. The sensing elements of the anemometer circuit were platinum wire 0.2 mil in diameter and approximately 0.25 cm long. The bridge circuit utilized was a CSU Solid State Anemometer and the pitot tube output went to a Transonic Model A, Type 120 electronic pressure meter. Turbulence signals were interpreted by means of a CSU designed sum and difference circuit and a Bruel and Kjaer RMS meter, Model 2416.

Helium gas was used as a tracer for the turbulent diffusion experiments. The gas was released continuously at a constant rate of 630 cc/min from a 2 mm nozzle located in or above the canopy. The sampling probe, manufactured from small diameter hypodermic tubing, was mounted on a traversing carriage, the horizontal and vertical positions of which were controlled remotely from outside the tunnel. Helium concentration was measured at ground level along a line normal to the axis of the plume and vertically at the plume centerline.

Samples were drawn into the probe at a constant rate and passed over a standard leak into a mass spectrometer (Model MS9AB of the Vacuum Electronic Corporation). Output of the mass spectrometer was an electrical voltage proportional to concentration. The mass spectrometer was calibrated periodically by a set of pre-mixed gases of research grade. Fig. 2 shows the experimental arrangement.

Since a closed-circuit wind tunnel was used, the ambient concentration level of helium built up in the wind tunnel with time. Eventually, most of the gas did leak out; therefore the amount of helium in the ambient flow was never higher than 60 parts per million. Nevertheless, an ambient concentration measurement was taken after each profile. The relative concentration was obtained

by subtracting the corresponding ambient concentration from the absolute concentration. All data presented in the figures or tables are relative concentrations.

Due to the slow response of the mass spectrometer, a period of one to two minutes was allocated for the stabilization of each reading before it was recorded. Usually, the concentration signal itself was averaged over at least 60 seconds. This method gave results that compared favorable with the average of signals taken over a period as long as 250 seconds by graphical means.

EXPERIMENTAL RESULTS

All measurements were taken at a free stream velocity of 12 m/sec. The ceiling of the test section was adjusted for zero pressure gradient, and the upstream velocity profile was measured and found to be logarithmic. And, because the temperature condition was constant, neutral stability existed.

1. Typical Velocity, Streamline, and Shear Results

Velocity and shear measurements have been compiled for pegs positioned in 1.27 x 1.27 cm diagonal, 2.54 x 2.54 cm square, 2.54 x 2.54 cm diagonal and 5.08 x 5.08 cm square arrays. In the downwind direction, the typical transformations of the wind profiles in the vertical direction are shown in Figs. 3 and 4 for flow in and above the crop respectively. Velocity profiles within the canopy agree qualitatively with prototype measurements,^{1, 2, 3, 4} and approximate the exponential profiles suggested by Inoue, Saito and Cionco, (et al).^{2, 12, 13} The profiles above the canopy are logarithmic and follow the displacement law $u/u^* = 1/k \ln \left[(y-d)/z_0 \right]$ utilized for rough surfaces since the time of Rossby and Montgomery (1935).

Typical intensity and shear profiles shown in Figs. 5, 6 and 7 indicate the growth of the inner boundary layer over the rough surface. The shear profile growth compares favorably with the measurements of transition made by Schlichting for flow from a smooth to a rough

surface.¹⁴ Values of intensity from 0.5 to 0.8 within the canopy correspond to field measurements in crops and forests but suggest that a linearized interpretation of the hot-wire anemometer output is extremely doubtful. Hence, measurements of velocity, intensity or shear may err as much as 20% at the lower velocities.

Streamline calculations over the model canopy as shown in Fig. 8 indicate the tendency for the approach flow to initially accelerate upward away from the floor and then to subsequently re-penetrate the canopy ceiling. This flow behavior was also evidenced in the diffusion measurements. It was concluded that the flow field was probably quasi-established within 60 h of the inception of the canopy. The dynamic behavior of the flow over the peg canopies is described in greater detail in Reference 18.

2. Diffusion Plume Results

Diffusion measurements were made over pegs positioned in the 2.54 x 2.54 cm square, 2.54 x 2.54 cm diagonal (3.60 x 3.60 cm) and 5.08 x 5.08 cm square arrays (see Table I). The plume source was located either at the canopy inception ($x_s = 0$) or six meters downstream ($x_s = 6$ m). It was located at various times at heights of 1 cm, 4.5 cm, 9 cm and 13.5 cm ($z_s = 1$ cm, $h/2$, h , $3/2 h$). Vertical and horizontal traverses along the plume were made at varying distances downstream.

Source and sampling tube locations studied are summarized in Table 1. The most extensive data are available for the 2.54 x 2.54 diagonal (or center filled square) matrix. Unfortunately, the program of diffusion measurements was instituted some time after the inception of the dynamic measurements (mean velocity, turbulence, etc.), and therefore only a limited number of data are presented for the other peg matrices.

Figures 9 to 18 display the longitudinal variation of the vertical profiles for the 2.54 x 2.54 cm peg matrix. Figures 15 to 27 display the longitudinal variation of the vertical profiles for the 2.54 x 2.54 cm diagonal peg matrix. The lateral profiles for the 2.54 x 2.54, 2.54 d x 2.54 d and the 5.08 x 5.08 cm peg matrices are displayed as isoconcentration lines on Figs. 37-38, 39-40 and 41-42, respectively.

The more extensive concentration data for the 2.54 x 2.54 diagonal peg matrix have been converted into isoconcentration profiles for a longitudinal section along the plume centerline. Figures 30 to 32 indicate the tendency of a point source to exhale out of the canopy when the source is located at half canopy height or above and near the inception of the vegetative cover. Farther downstream, the plume tends to dip down into the vegetative cover when released above the canopy, as is shown in Figures 33 to 36.

Figures 28 and 29 show how the plume maximum concentration rises abruptly upward at the canopy inception and subsequently is

displaced downward slightly as the flow re-penetrates the canopy ceiling. In the same figures, the maximum concentration line is compared with the meandering of the streamlines passing through the source position.

TABLE I

Summary of Data Collection Program

Peg Array	Source Release x_s m	Source Release z_s cm	Vertical profiles at longitudinal distances x m	Longitudinal distances at which lateral profiles measured m	
2.54 x 2.54 cm	0	0	0.3, 0.6, 0.9		
		4.5	0.3, 0.6, 0.9		
		9.0	0.3, 0.6, 0.9		
	6	1.0	0.3, 0.6	0.3	
		9.0	0.3, 0.6	0.3	
		18.0	0.3, 0.6		
3.60 x 3.60 (2.54 x 2.54 diagonal)	0	1.0	0.25, 0.5, 0.75, 1.0, 1.5, 7.0, 7.5		
		4.5	0.25, 0.5, 0.75, 1.0, 1.5, 7.0, 7.5		
		9.0	0.25, 0.5, 0.75, 1.0, 1.5, 7.0, 7.5		
		6	1.0	0.25, 0.5, 0.75, 1.0, 1.5, 7.0, 7.5	0.25
		4.5	0.25, 0.5, 0.75, 1.0, 1.5, 7.0, 7.5		
		9.0	0.25, 0.5, 0.75, 1.0, 1.5, 7.0, 7.5	0.50	
	13.5	0.25, 0.5, 0.75, 1.0, 1.5, 7.0, 7.5			
		0.25, 0.5, 0.75, 1.0, 1.5, 7.0, 7.5			
	5.08 x 5.08	0	1.0	0.3, 0.6	0.3, 0.6
			9.0	0.3, 0.6	0.3, 0.6

The consequences of this effect on crop dusting penetration are obvious. Yano has suggested this effect may be accelerated by differences in eddy diffusion coefficient profiles; however, calculations of K from velocity data do not suggest that any large changes do occur.⁸ It was found that the vertical position of the maximum concentration of plumes released at $x_s = 6$ m tended to drift downward. This is probably a joint effect of streamline re-penetration and the gradient in K .

The growth in the characteristic width of the vertical dispersion of a continuous point source plume has frequently been found to be proportional to a power function of the longitudinal downstream distance, x^n . Similarly, it is generally observed that the maximum concentration at ground level decreases at a rate proportional to x^{-m} . For a plume dispersing in or above the vegetative canopy, the rate of dispersal appears to be a function of the fetch distance from the canopy inception position (see Table II). This marked variation is evident near the canopy edge as is shown in Figs. 43 and 44. These rates of dispersion may be compared with values of $x^{0.7}$ and $x^{-1.5}$ for plumes dispersing over a smooth surface.²⁰

The nonisotropic character of the horizontal versus vertical plume dispersal is evident in cross-sections of the plume plotted as isoconcentration lines (see Figs. 37 to 42). For a source located

TABLE II

Coefficients of Concentration Dispersal Rate for Canopy*

x_s	n	-m
0	1.66	3.6
6	1.42	2.5

*2.54 x 2.54 diagonal case

$z_s = 1$ cm only

within the canopy, lateral diffusion is very strong, while for a source at the top of the canopy, vertical dispersion predominates. Rapid diffusion in the vertical direction is very evident within the canopy since gradients in concentration are quickly reduced to a uniform vertical distribution.

3. Eddy Diffusion Coefficient

The concept of a macroscopic equation of turbulent dispersion of some property C results generally in the equation

$$\frac{\partial C}{\partial t} + \frac{\partial}{\partial x_i} (u_i C) = \frac{\partial}{\partial x_i} (K_{x_i} \frac{\partial C}{\partial x_i}) \quad (1)$$

where K_{x_i} is the coefficient of turbulent diffusion. The coefficient K_{x_i} incorporates within itself the complexities of the actual transport process. Hence, most analytical studies of fluid mechanics require some theoretical or empirical expression for the variation of K_{x_i} with other parameters. Several scientists have studied the nature of K_{x_i} for plant communities, but further data are still needed. 1, 2, 3, 8, 12, 13

The eddy diffusion coefficient for transport of the injected gas in the model canopy has been determined utilizing concentration and velocity profiles and a finite difference interpretation of Equation (1). In order to accomplish the calculations with the limited data, it was assumed that K_y and K_z were equal at all levels. Calculations were performed on a CDC 6400 computer at Colorado State University

using input data taken from lines fared through the concentration measurements, from vertical velocities calculated from the slope of streamlines, and from the following equation:

$$K(x, z) = \frac{u \left(\frac{\partial C}{\partial x} \right) + v \left(\frac{\partial C}{\partial z} \right) + \left(4K(x, z - \Delta z) - K(x, z - 2\Delta z) \right) \left(\frac{\partial C}{\partial z} \right)}{\left(\frac{\partial^2 C}{\partial z^2} \right) + \frac{1.5}{\Delta z} \left(\frac{\partial C}{\partial z} \right)} \quad (2)$$

The resulting profiles in $K(z)$ are displayed on Fig. 45.

Three distinct regions of variation of K are noticeable. Immediately adjacent to the wall is a zone where K increases exponentially. In the area from 2 to 5 cm, K remains essentially constant; and, finally, K increases linearly with z in the region beyond 5 cm.

A number of authors have suggested that K should remain constant in vegetative cover; others have suggested that K should vary linearly.^{2, 3} It is interesting to note that for the case of the model peg canopy, both conditions of K exist, although in different regions. Figure 47 compares the distribution of K within the canopy with typical results of the distribution of K for a corn crop as measured by Uchiyama and Wright.³

The momentum vertical eddy transport coefficient K_m has been calculated from the velocity and shear data found in Reference 18 by use of

$$K_m = \frac{-\overline{u'w'}}{\left(\frac{du}{dz} \right)} \quad (3)$$

Figure 46 compares the variation of the momentum, K_m and mass K_c eddy diffusion coefficients in and above the artificial canopy. Above the canopy, K becomes proportional to $(z-d)$ where d is a displacement height. Similar behavior has been observed for prototype canopies.^{1, 2, 3, 12, 13, 21}

As a result of calculations by Denmead, the eddy diffusivity in a pine forest might also be interpreted to behave in a similar manner.²¹ Wright and Lemon reported K distributions in a canopy of corn; however, they reported results in terms of a wind profile classification which does not permit direct comparison.²² Finally, these K profiles may also be described as qualitatively similar to the peg data.

CONCLUSIONS

It is apparent that the general character of flow in and above vegetative canopies may be satisfactorily simulated in the meteorological wind tunnel. In addition, these new data suggest that even the micro-structure transport phenomena behave in a manner similar to that of the prototype. Therefore, it is possible to conclude that:

1) The basic trends of the dynamic and kinematic behavior of a complex vegetative cover may be simulated by a simple porous geometry in a wind tunnel.

2) The initial fetch of the peg canopy affects tracer dispersion of a continuous point source in a unique manner: Vertical convective motions exhale the gases released at the beginning of the canopy, and subsequently, the canopy appears to re-inhale the products farther downstream.

3) The dispersive characteristics of the canopy are non-isotropic. For a source near ground level, lateral mixing is strong; for a source located at the top of the canopy, vertical transport predominates.

4) The eddy diffusion coefficient varies linearly as $(z-d)$ above a vegetative cover and has a growth rate proportional to ku^* .

5) The eddy diffusion coefficient, K , within the artificial vegetative cover, appears to develop into three regions: Initially K

grows exponentially, next it remains constant, and, finally, K grows at a linear rate.

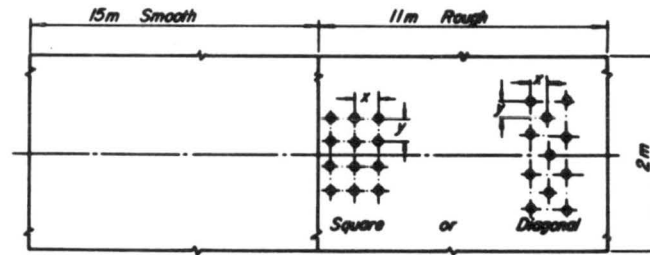
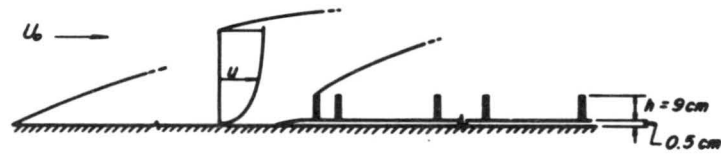
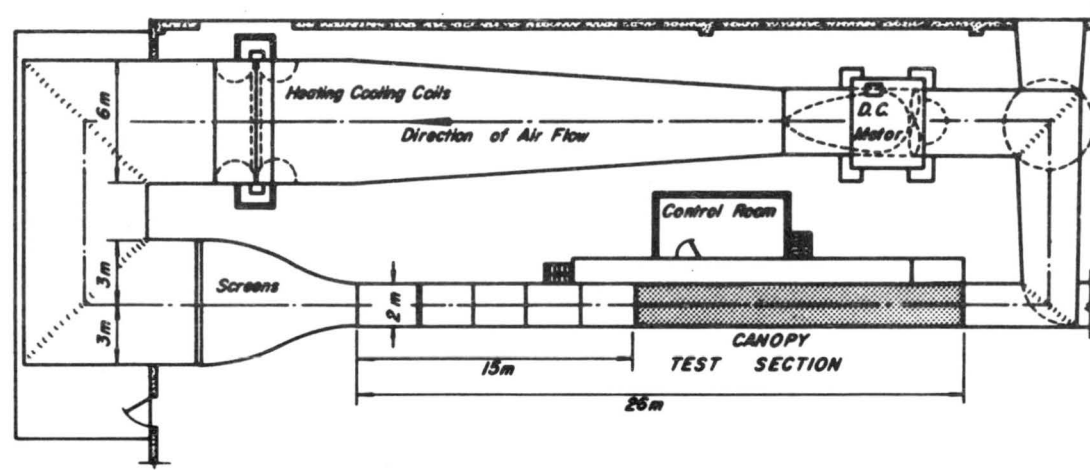
6) The experimental law for attenuation of boundary concentration was obtained as $x^{-2.5}$ for gas source releases far from the canopy inception. (Rates of dispersion are somewhat larger near the edge of the vegetative cover.)

BIBLIOGRAPHY

1. Penman, H. L. and I. F. Long, "Weather in Wheat," Quarterly Journal of Royal Meteorological Society, Vol. 86, pp. 16-50, 1960.
2. Inoue, E., "On the Turbulent Structure of Airflow Within Crop Canopies," Journal of Meteorological Society of Japan, Series II, Vol. 41, #6, December 1963.
3. Uchijima, Z. and J. L. Wright, "An Experimental Study of Air Flow in a Corn Plan-Air Layer," Bulletin of the National Institute of Agricultural Sciences (Japan), Series A, #11, February 1964.
4. Lemon, E. R., (ed.), "The Energy Budget at the Earth's Surface," Part II, Production Research Report No. 2, Agricultural Research Service, U. S. Dept. of Agriculture, 49 p, 1962.
5. Bayton, H. W. "The Penetration and Diffusion of a Fine Aerosol in a Tropical Rain Forest," Ph.D. Thesis, University of Michigan, Ann Arbor, 1963.
6. Raynor, G. S., "Effects of a Forest on Particulate Dispersion," USAEC Meteorological Information Meeting, Chalk River, Canada, September 1967.
7. Plate, E. J. and A. A. Quarishi, "Making of Velocity Distributions Inside and Above Tall Crops," Journal of Applied Meteorology, Vol. 4, #3, pp. 400-408, June 1965.
8. Yano, Motoaki, "Turbulent Diffusion in a Simulated Vegetative Cover," Fluid Dynamics and Diffusion Laboratory Tech. Rept. CER66MY25, Colorado State University, 1966.
9. Hidy, G. M., (ed), "On Atmospheric Simulation: A Colloquium," NCAR Technical Note NCAR-7N-22, Boulder, November 1966.
10. McVehil, G. E., et al., "On the Feasibility of Modeling Small Scale Atmospheric Motions," Cornell Aeronautical Laboratory, Tech. Rept. ZB-2328-P-1, April 1967.

11. Plate, E. J. and J. E. Cermak, "Micro-Meteorological Wind Tunnel Facility: Description and Characteristics," Fluid Dynamics and Diffusion Laboratory, Tech. Rept. CER63EJP-JEC9, Colorado State University, 1963.
12. Saito, T., "On the Wind Profiles in Plant Communities," Bulletin of the National Institute of Agricultural Science (Japan), Series A, #11, February 1964.
13. Cionco, R. M., W. D. Ohmstede and J. F. Appleby, "Model for Wind Flow in an Idealized Vegetative Canopy," Report ERDAA-MET-7-63, Electronics Research and Development Activity, Ft. Huachuca, June 1963.
14. Schlichting, H., Boundary Layer Theory, McGraw Hill Book Co., Inc., New York, 1960.
15. Tourin, M. H. and W. C. Shen, "Deciduous Forest Diffusion Study," Final Report to U. S. Army, Dugway Proving Grounds, Contract DA42-007-AMC-48(R), August 1966.
16. Allison, J. K., L. P. Herrington and J. P. Morton, "Diffusion Below and Through a Dense, High Canopy," Paper PRC 68-3, Melpar, Inc., Arlington, Virginia. (Paper presented at Conference on Fire and Forest Meteorology of the American Meteorological Society and the Society of American Foresters, March 1968.)
17. Hsi, G. and J. H. Nath, "A Laboratory Study on the Drag Force Distribution Within Model Forest Canopies in Turbulent Shear Flow," Fluid Dynamics and Diffusion Laboratory Report No. CER67-68GH-JHN-50, Colorado State University, 1968.
18. Kawatani, Takeshi, and R. N. Meroney, "Structure Of Canopy Fluid Flow," Fluid Dynamics and Diffusion Laboratory Report CER67-68TK-RNM-33, Colorado State University, 1968.
19. Jensen, M. and N. Frank, "Model-Scale Test in Turbulent Wind, Part I," The Danish Technical Press, Copenhagen, 1963.
20. Malhotra, R. C. and J. E. Cermak, "Mass Diffusion in Neutral and Unstably Stratified Boundary-layer Flows," International Journal of Heat and Mass Transfer, Vol. 7, pp. 169-186, 1964.

21. Denmead, O. T. "Evaporation Sources and Apparent Diffusivities in a Forest Canopy," Applied Meteorology, Vol. 3, pp. 383-389, 1964.
22. Wright, J. L. and E. R. Lemon, "Estimation of Turbulent Exchange within a Corn Crop Canopy at Ellis Hollow (Ithaca, N. Y.), 1961," Internal Report 62-7, N. Y. State College of Agriculture, Cornell University, July 1962.



PEG ARRAYS STUDIED

x, cm	y, cm	ARRAY
1.27	1.27	DIAG.
2.54	2.54	SQ.
2.54	2.54	DIAG.
5.08	5.08	SQ.

Fig. 1. Wind tunnel and artificial canopy configuration

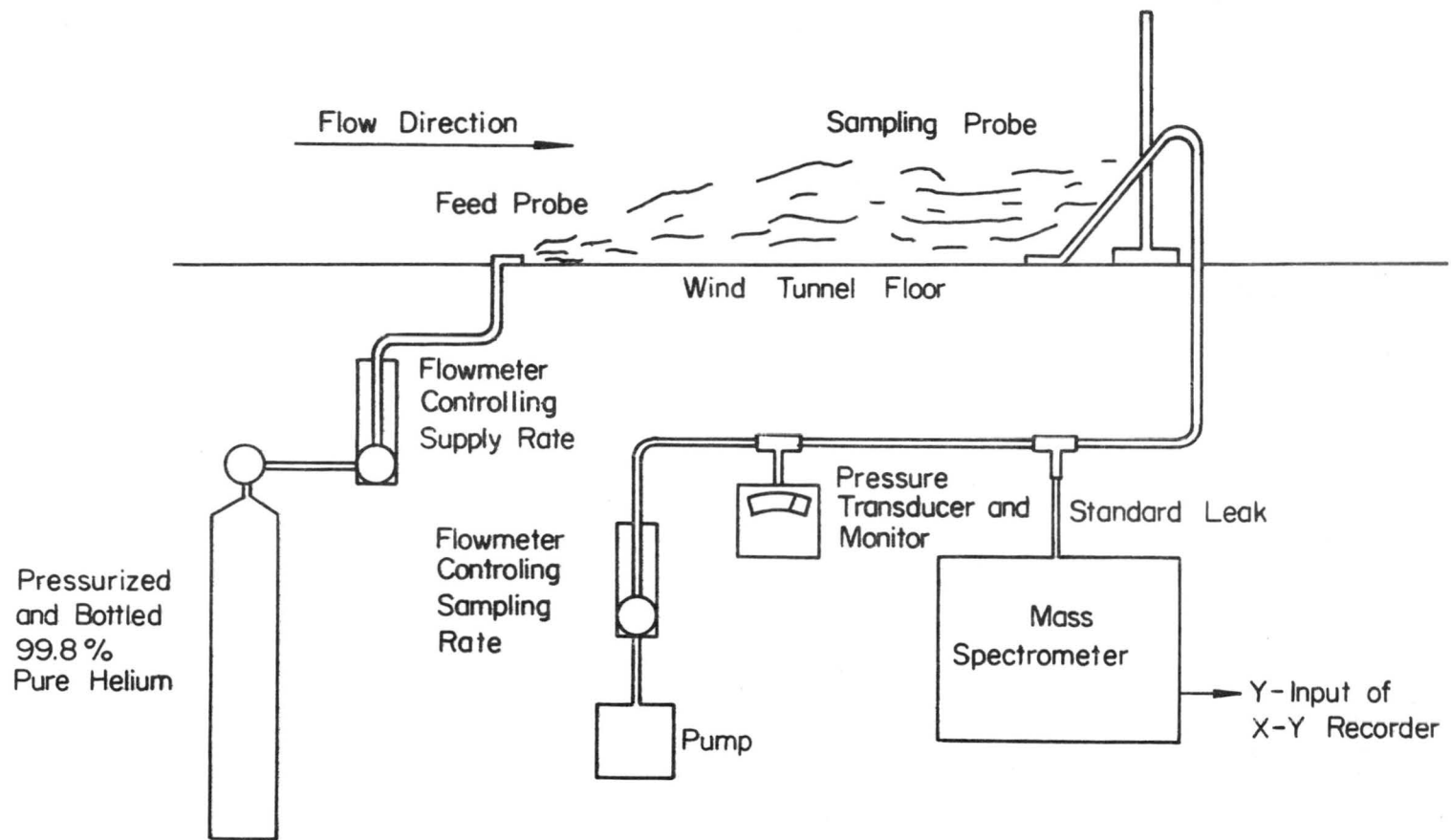
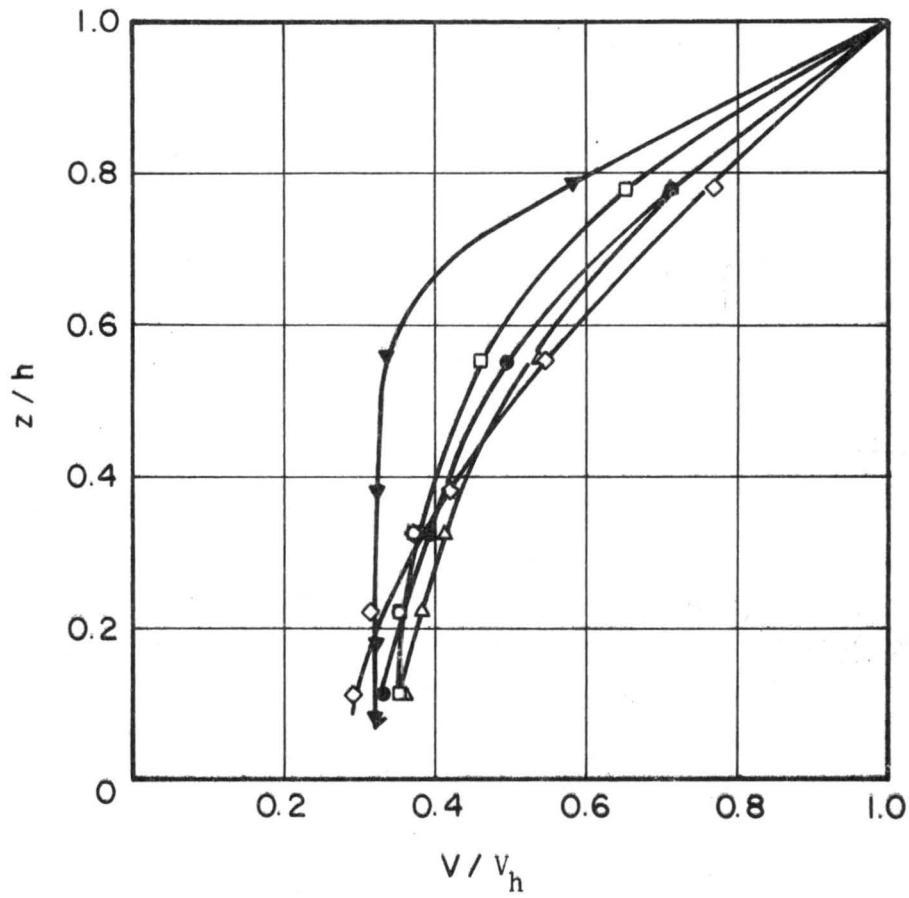


Fig. 2. Continuous point source feed and sampling system



$$\nabla \quad \frac{x}{h} = 11.1$$

$$\triangle \quad \frac{x}{h} = 94.5$$

$$\bullet \quad \frac{x}{h} = 44.4$$

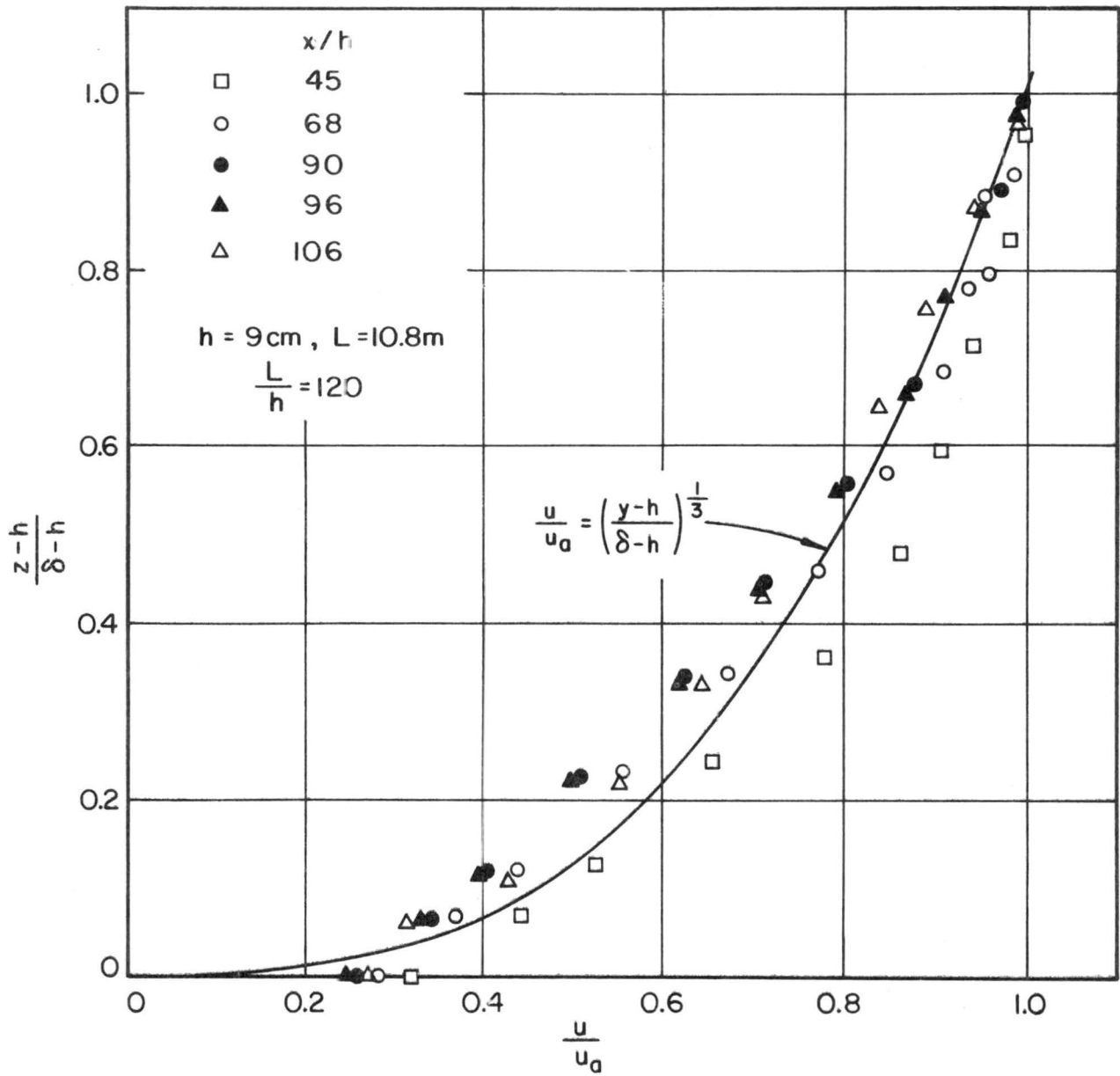
$$\diamond \quad \frac{x}{h} = 111.0$$

$$\square \quad \frac{x}{h} = 66.7 \sim 83.0$$

Pegs $\phi = 0.48$ cm, $h = 9$ cm, $L = 10.8$ m, $\frac{L}{h} = 120$

Spaced 2.54×2.54 cm, $V_\infty = 12$ m/s

Fig. 3. Velocity profiles within model canopy



Canopy Study: Flow Above Canopy
 Pegs ϕ 0.48, Spaced 2.54 x 2.54 cm

Fig. 4. Velocity profiles above model canopy

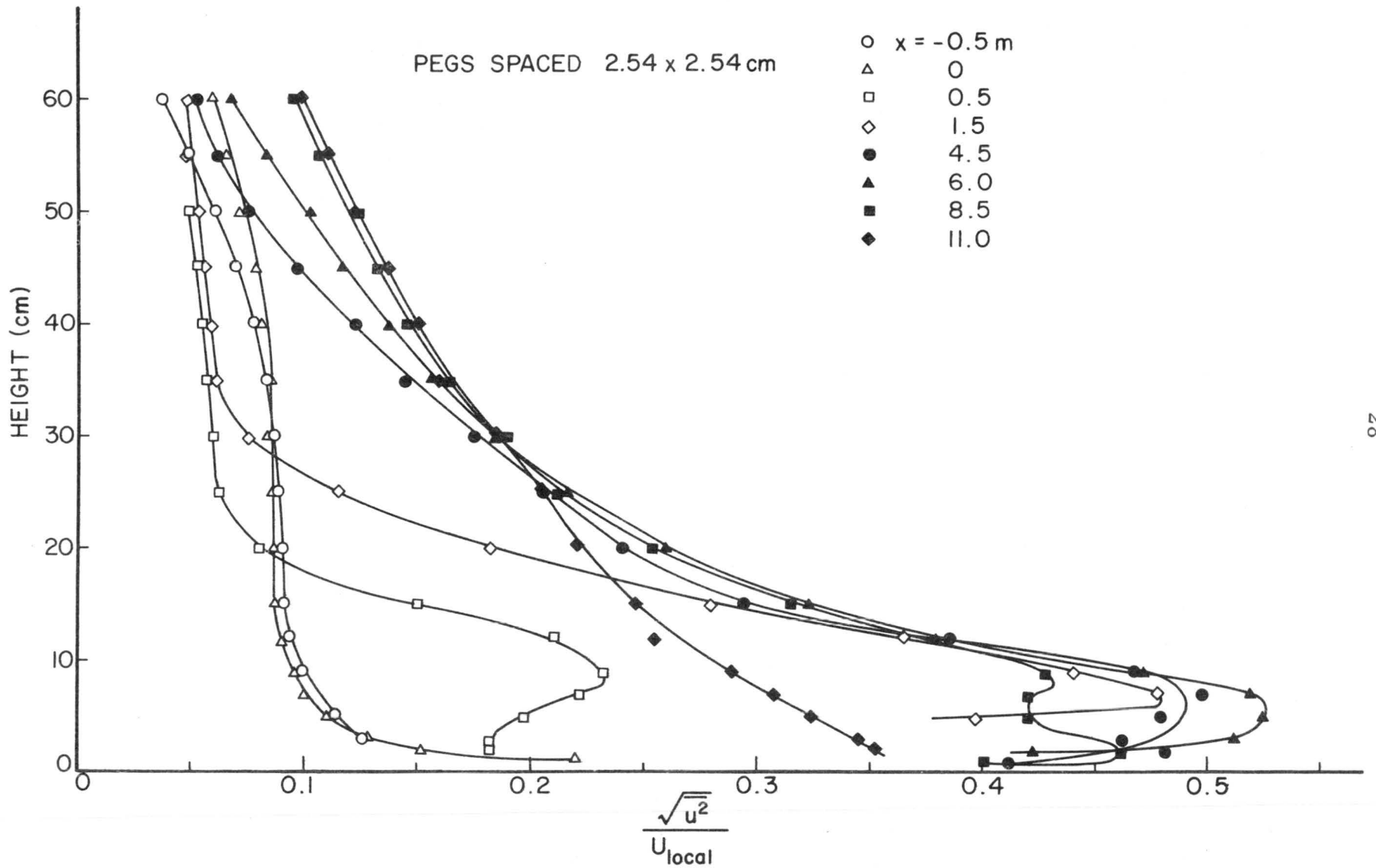


Fig. 5. Longitudinal turbulent intensity for model canopy

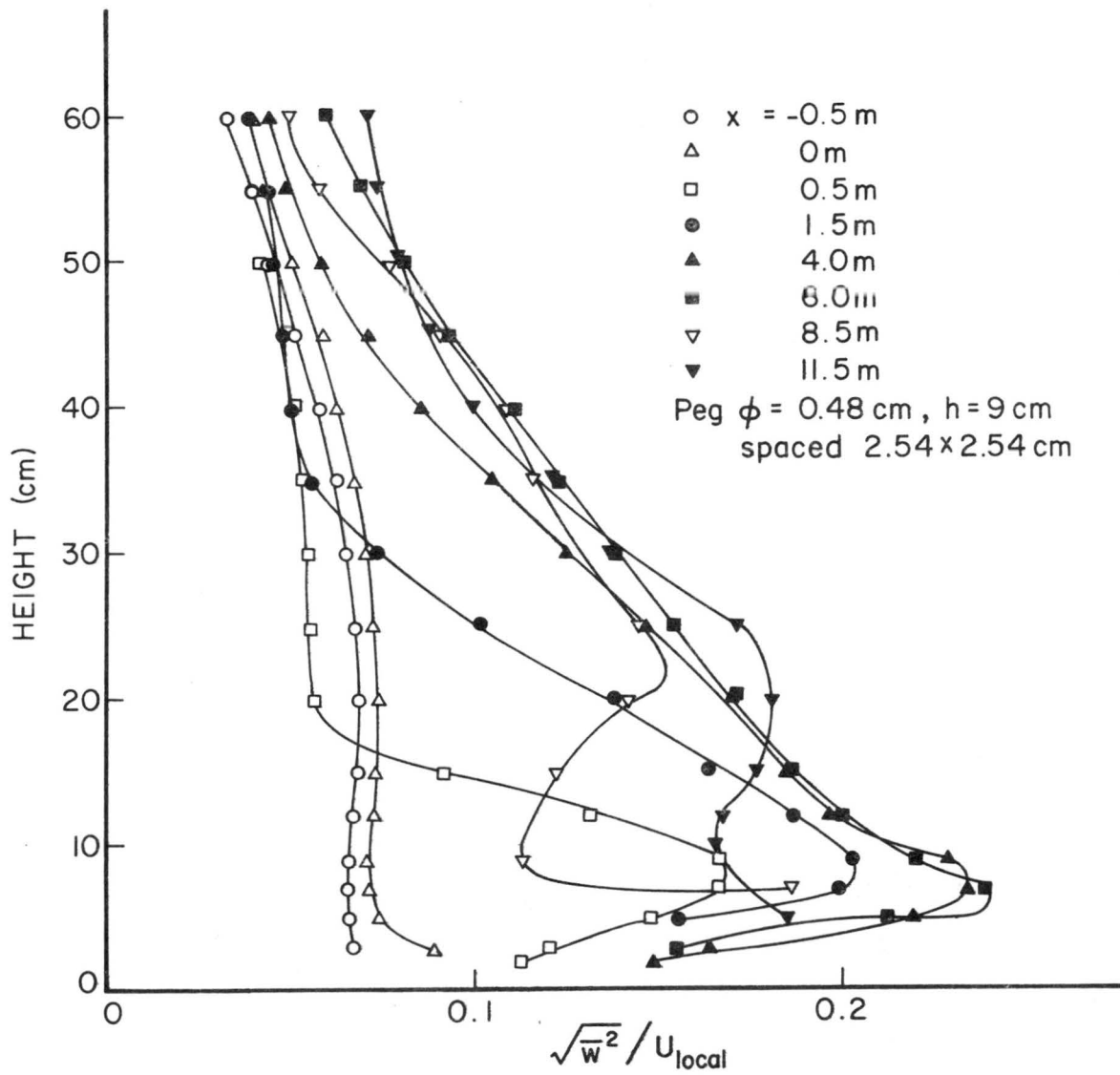


Fig. 6. Vertical turbulent intensity for model canopy

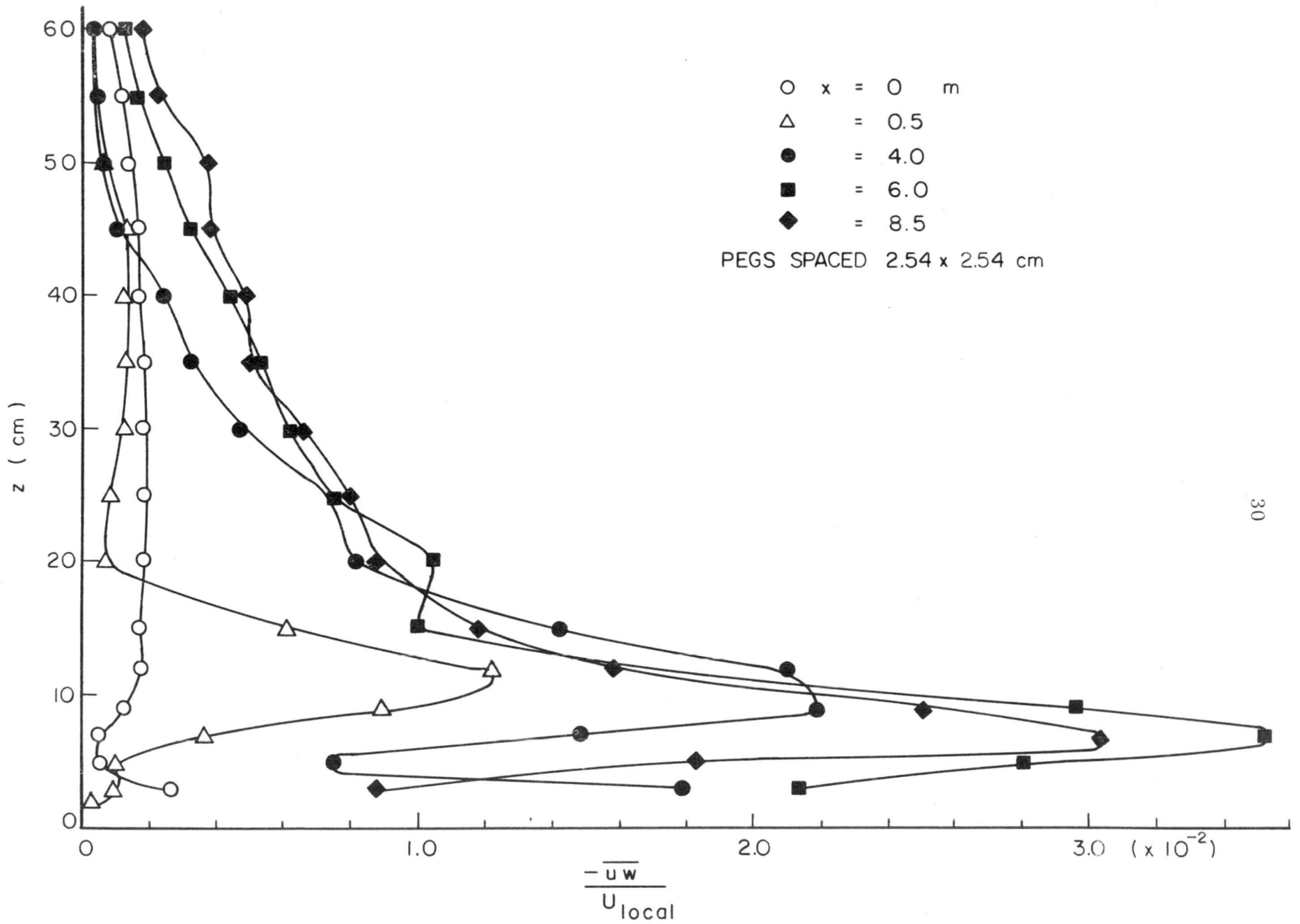


Fig. 7. Shear profile for model canopy

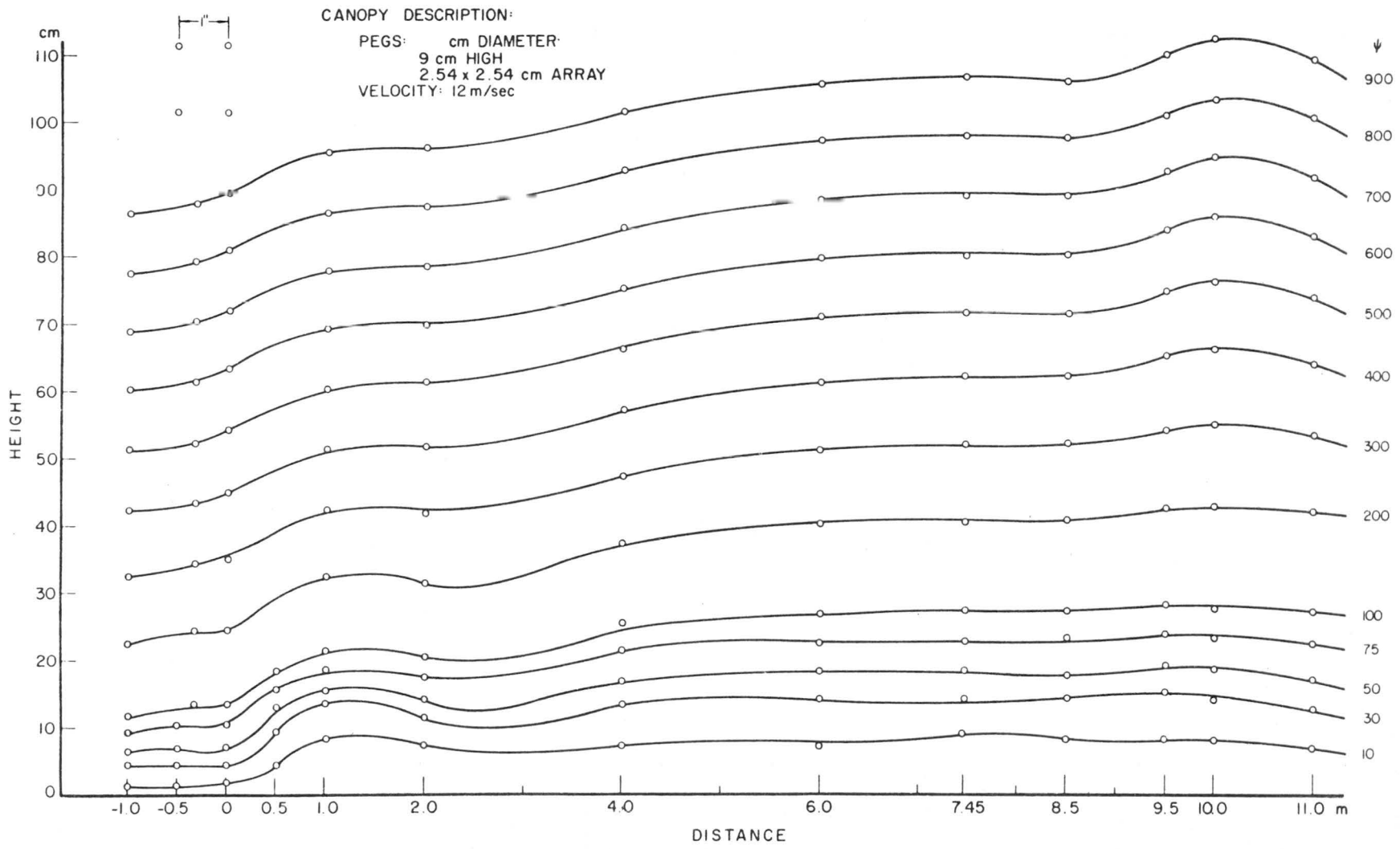


Fig. 8. Streamline flow in and above a model canopy

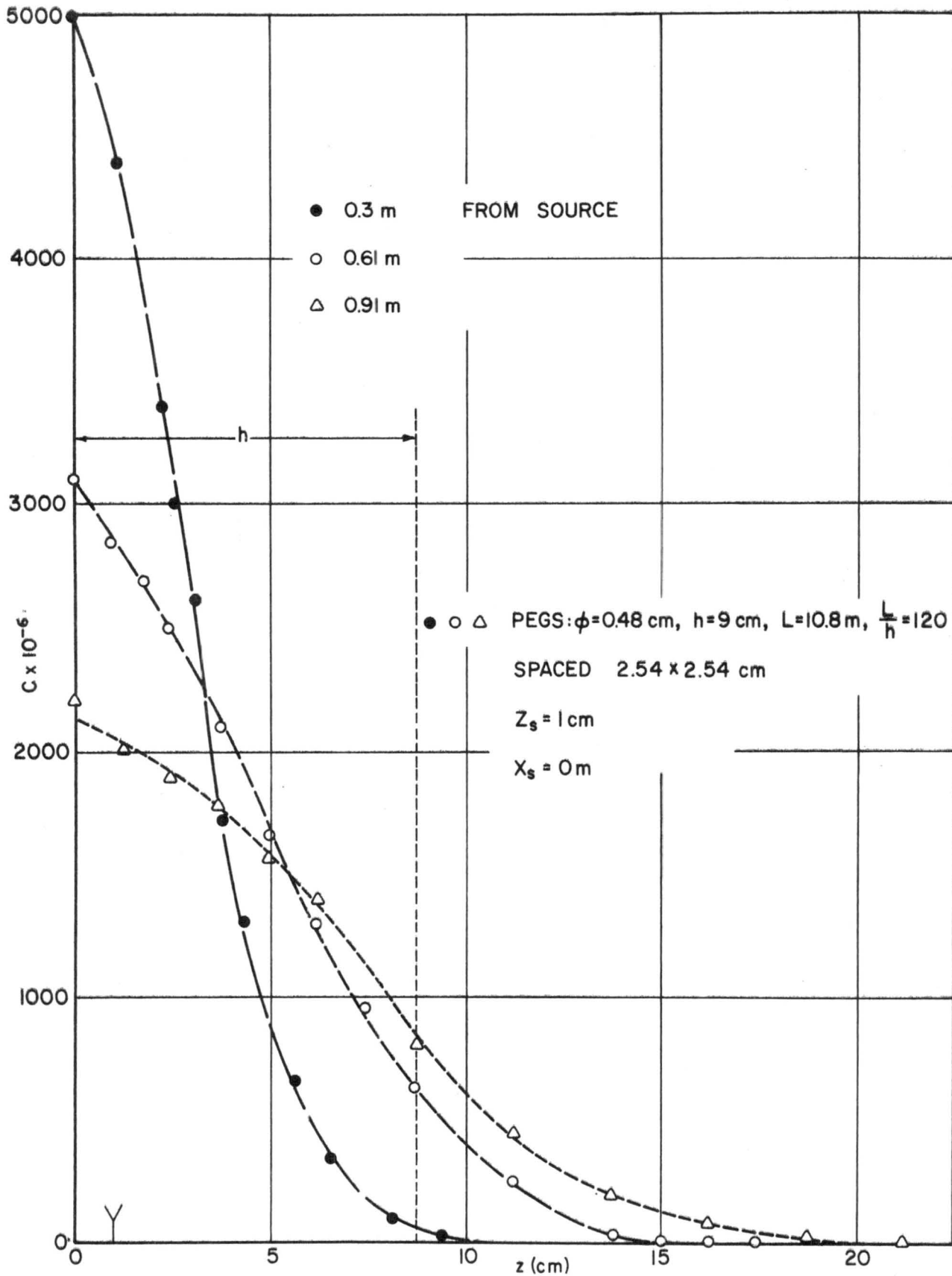


Fig. 9. Vertical dispersion of a continuous point source in a model peg canopy (2.54×2.54 cm). $x_s = 0$, $z_s = 1$ cm

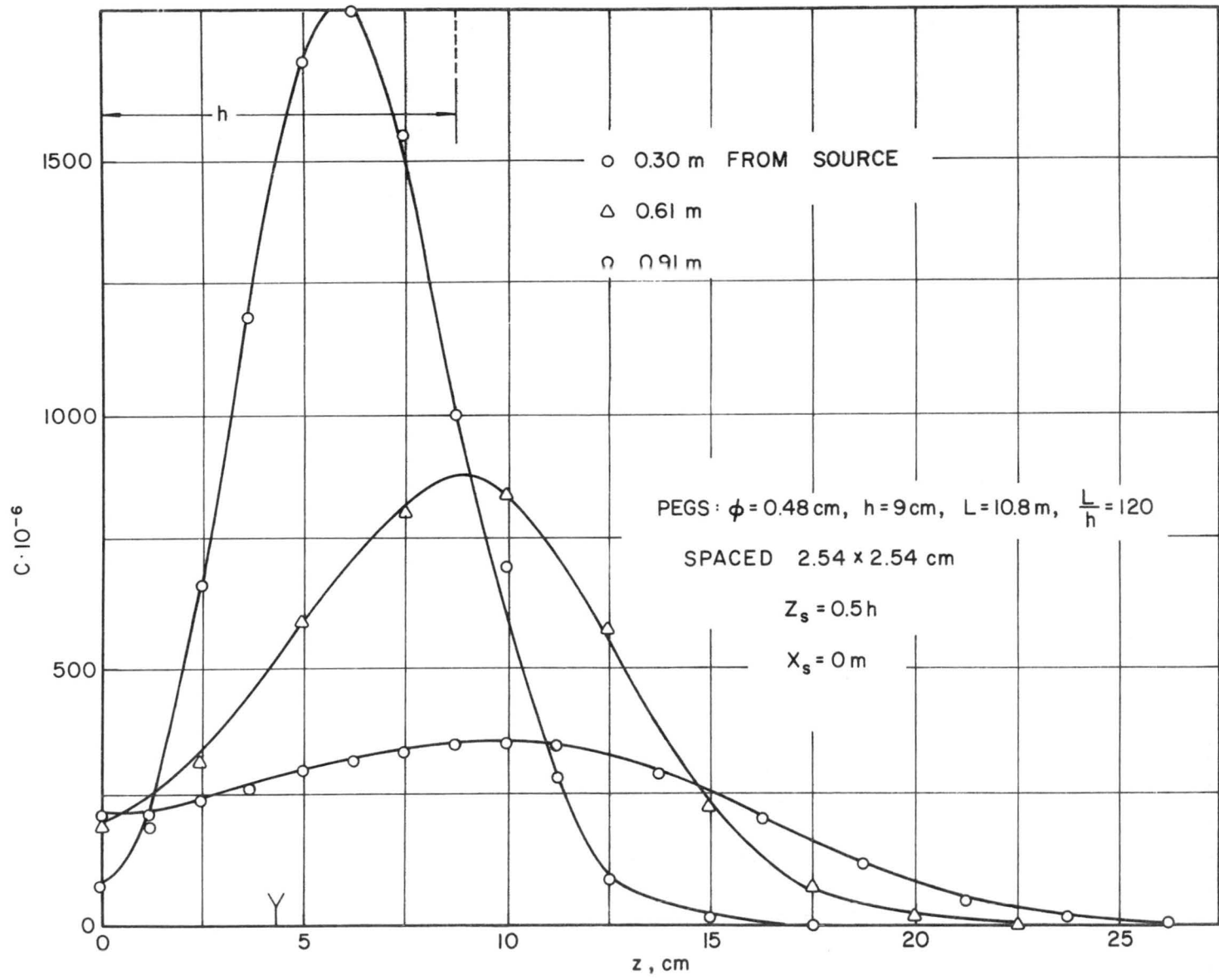


Fig. 10. Vertical dispersion of a continuous point source in a model peg canopy
 (2.54×2.54 cm). $x_s = 0$, $z_s = 0.5h$

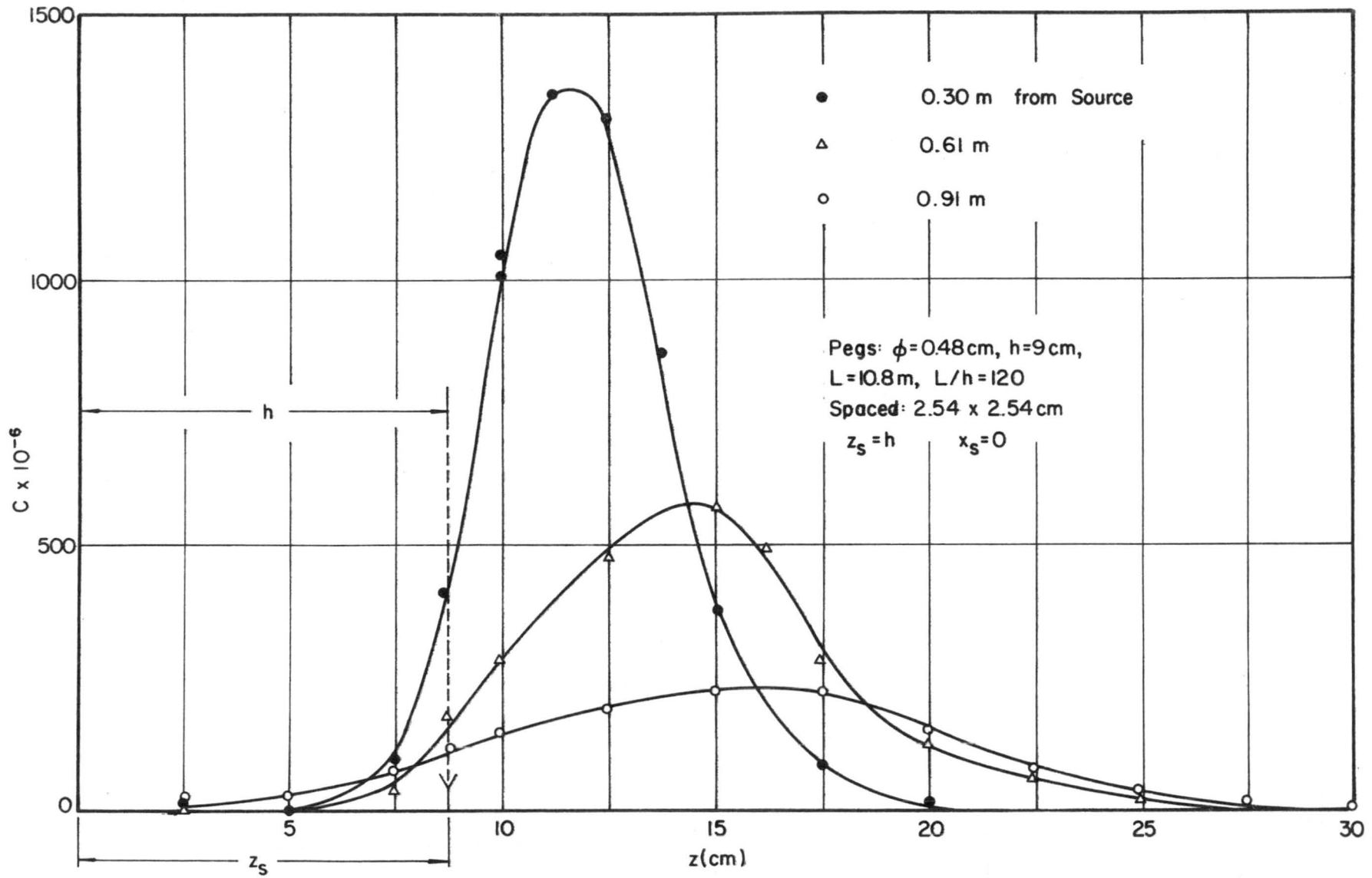


Fig. 11. Vertical dispersion of a continuous point source in a model peg canopy (2.54 x 2.54 cm). $x_s = 0$, $z_s = h$

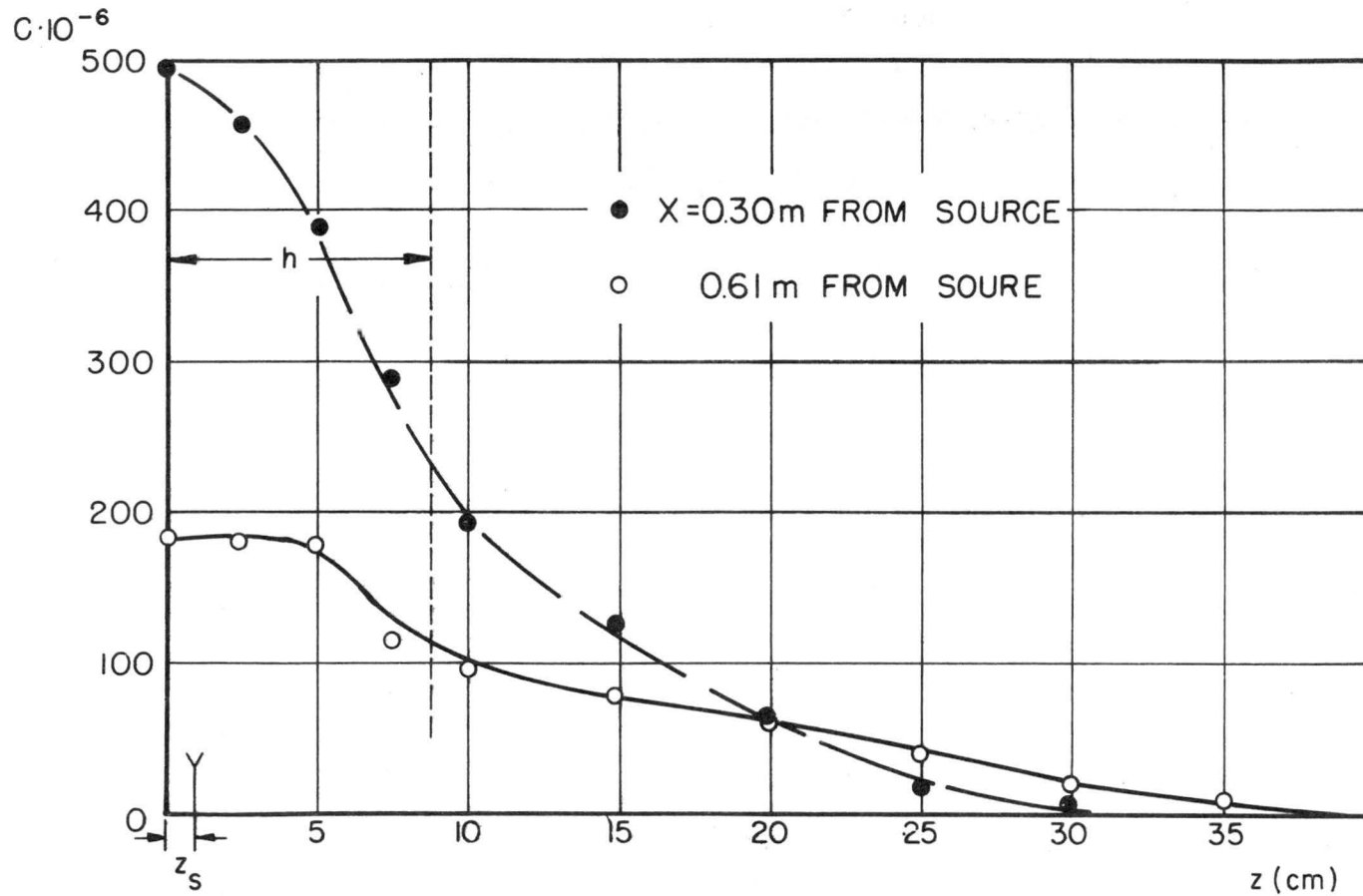


Fig. 12. Vertical dispersion of a continuous point source in a model peg canopy (2.54 x 2.54 cm). $x_s = 6$ m, $z_s = 1$ cm

PEGS: $\phi = 0.48$ cm, $h = 9$ cm, $L = 10.8$ m, $\frac{L}{h} = 120$, SPACED 2.54 x 2.54 cm

$Z_s = 1$ cm

$X_s = 6$

$V_\infty = 12$ m/sec

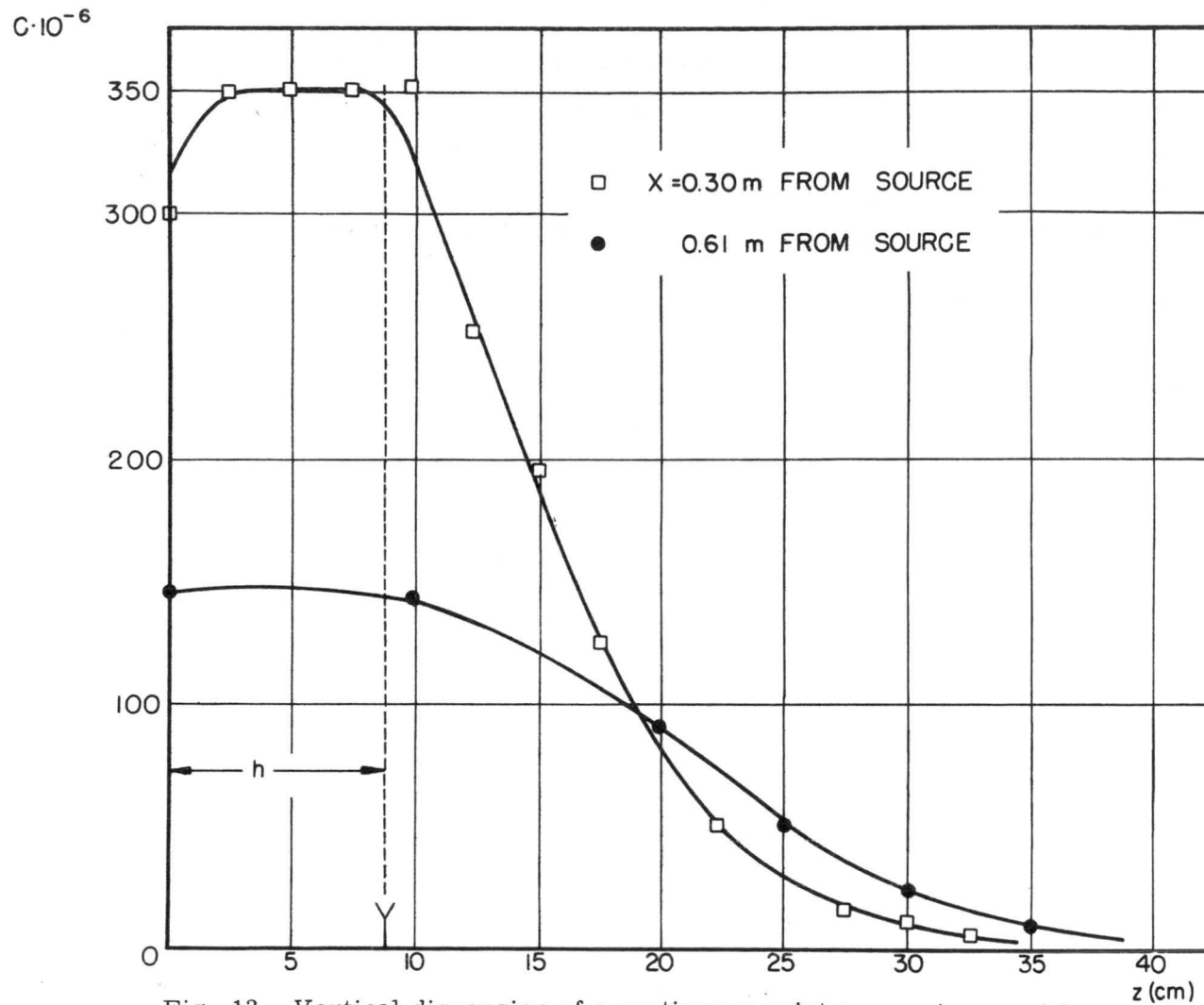


Fig. 13. Vertical dispersion of a continuous point source in a model peg canopy (2.54 x 2.54 cm). $x_s = 6$ m, $z_s = h$

PEGS: $\phi = 0.48$ cm, $h = 9$ cm, $L = 10.8$ m, $\frac{L}{h} = 120$, SPACED 2.54 x 2.54 cm

$Z_s = h$ $V_\infty = 12$ m/sec

$X_s = 6$ m

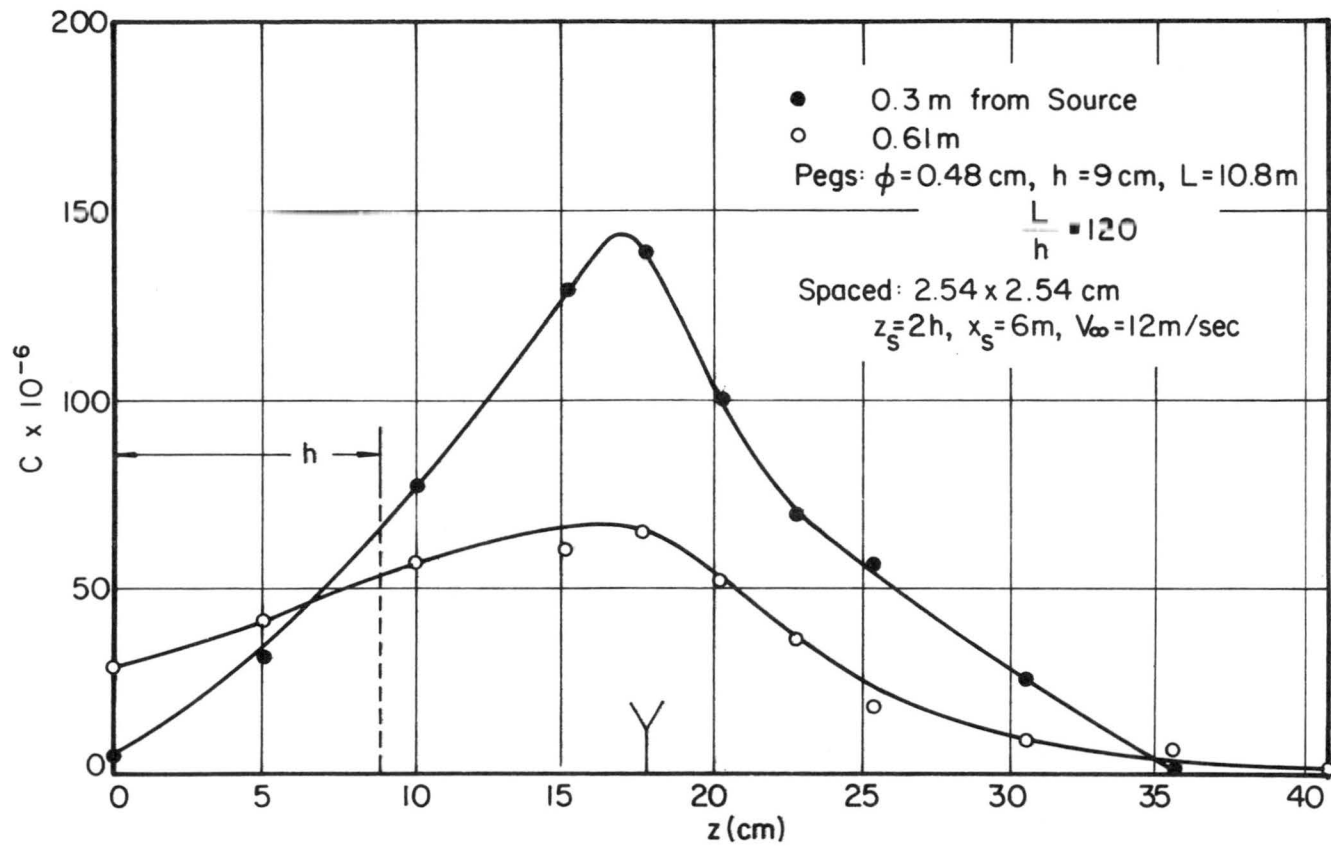


Fig. 14. Vertical dispersion of a continuous point source in a model peg canopy (2.54 x 2.54 cm). $x_s = 6$ m, $z_s = 2h$

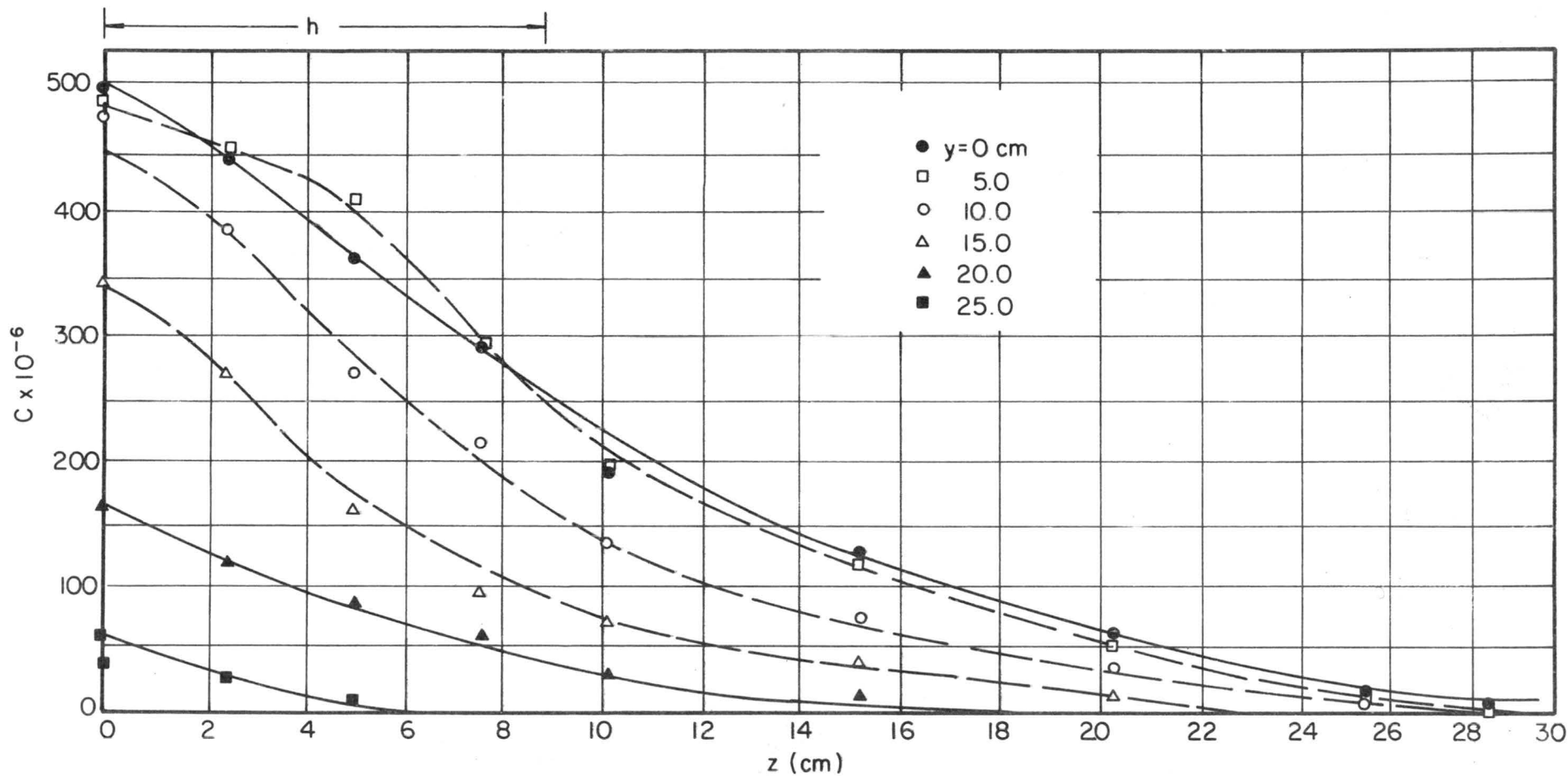


Fig. 15. Lateral dispersion of a continuous point source in a model peg canopy (2.54 x 2.54 cm). $x_s = 6$ m, $z_s = 1$ cm

Pegs: $\phi = 0.48$ cm, $h = 9$ cm, $L = 10.8$ m, $\frac{L}{h} = 120$
 Spaced: 2.54 x 2.54 cm

$z_s = 1$ cm
 $x_s = 6$ m
 $\bar{x} = 0.3$ m

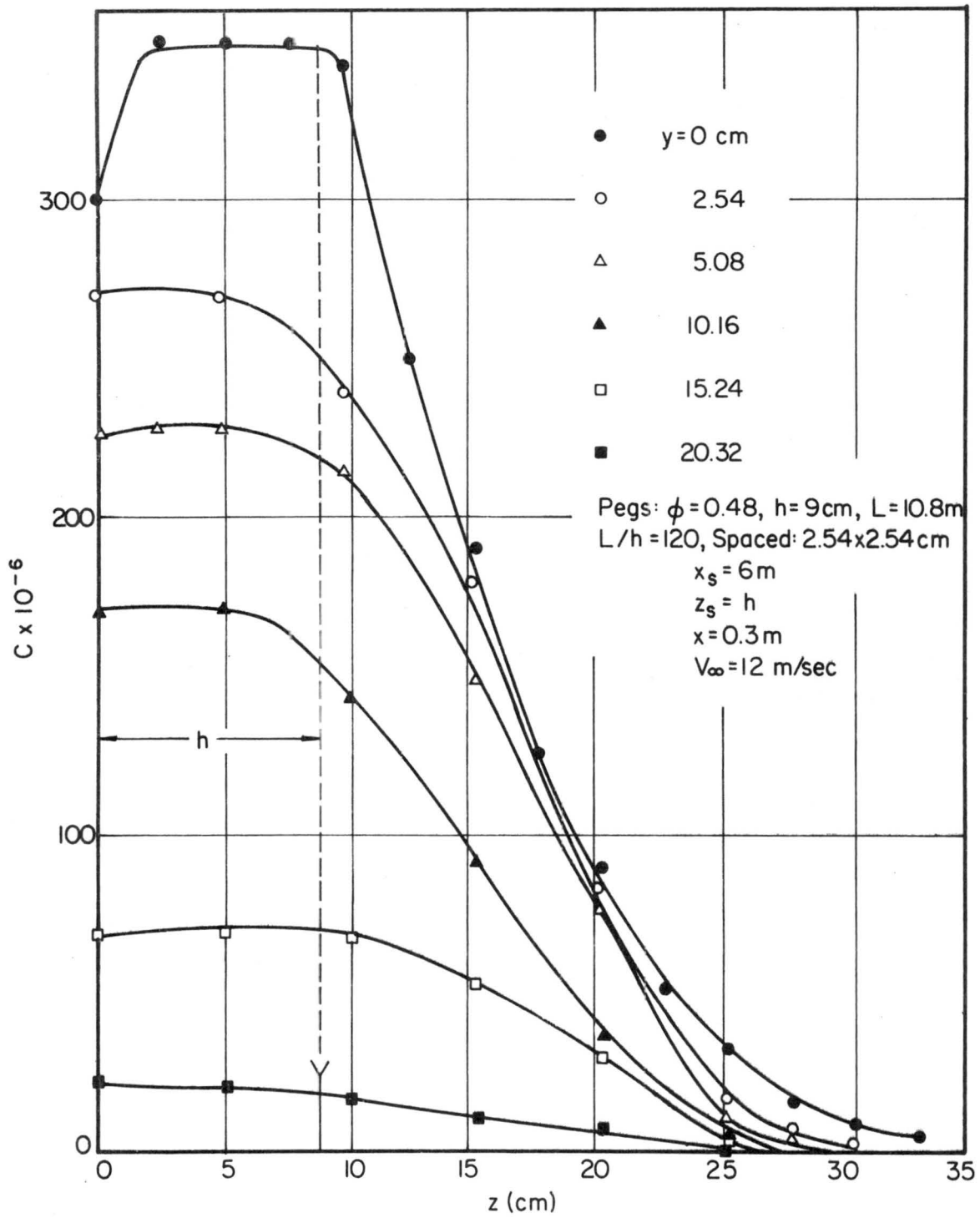


Fig. 16. Lateral dispersion of a continuous point source in a model peg canopy (2.54×2.54 cm). $x_s = 6$ m, $z_s = h$

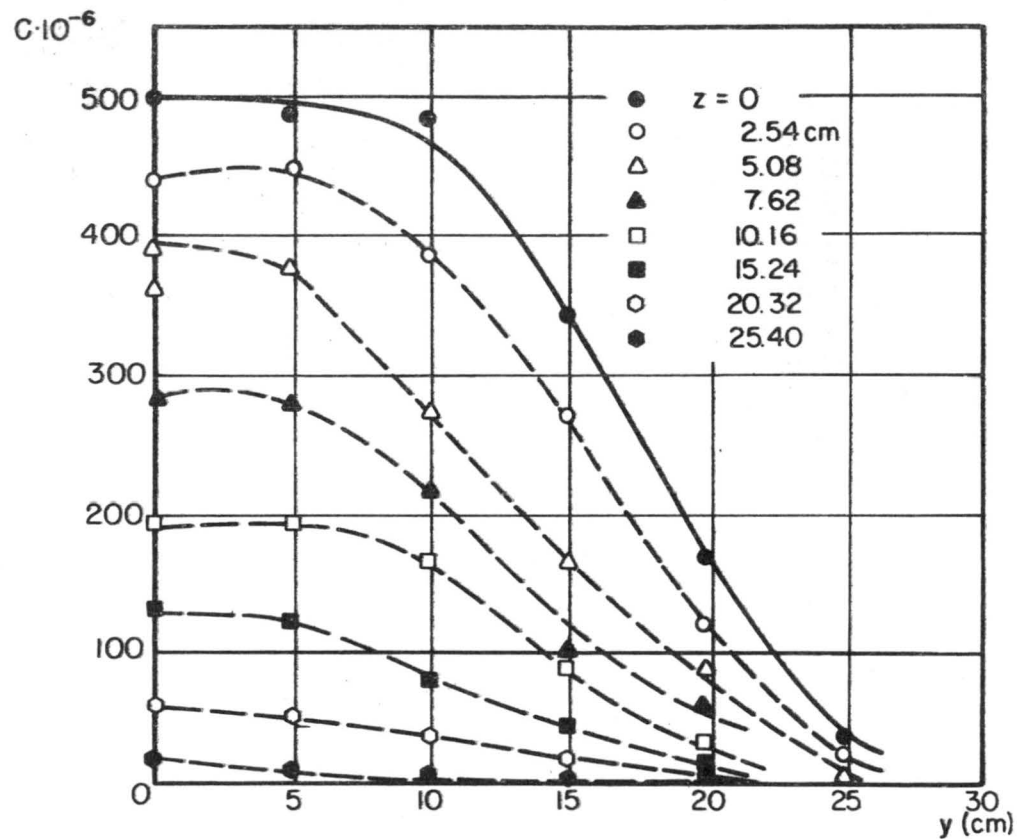


Fig. 17. Lateral dispersion of a continuous point source in a model peg canopy (2.54 x 2.54 cm). $x_s = 6$ m, $z_s = 1$ cm

PEGS: $\phi = 0.48$ cm, $h = 9$ cm, $L = 10.8$ m, $\frac{L}{h} = 120$, SPACED 2.54 x 2.54 cm

$Z_s = 1$ cm
 $X_s = 6$ m
 $V_\infty = 12$ m/sec

0.30m FROM SOURCE

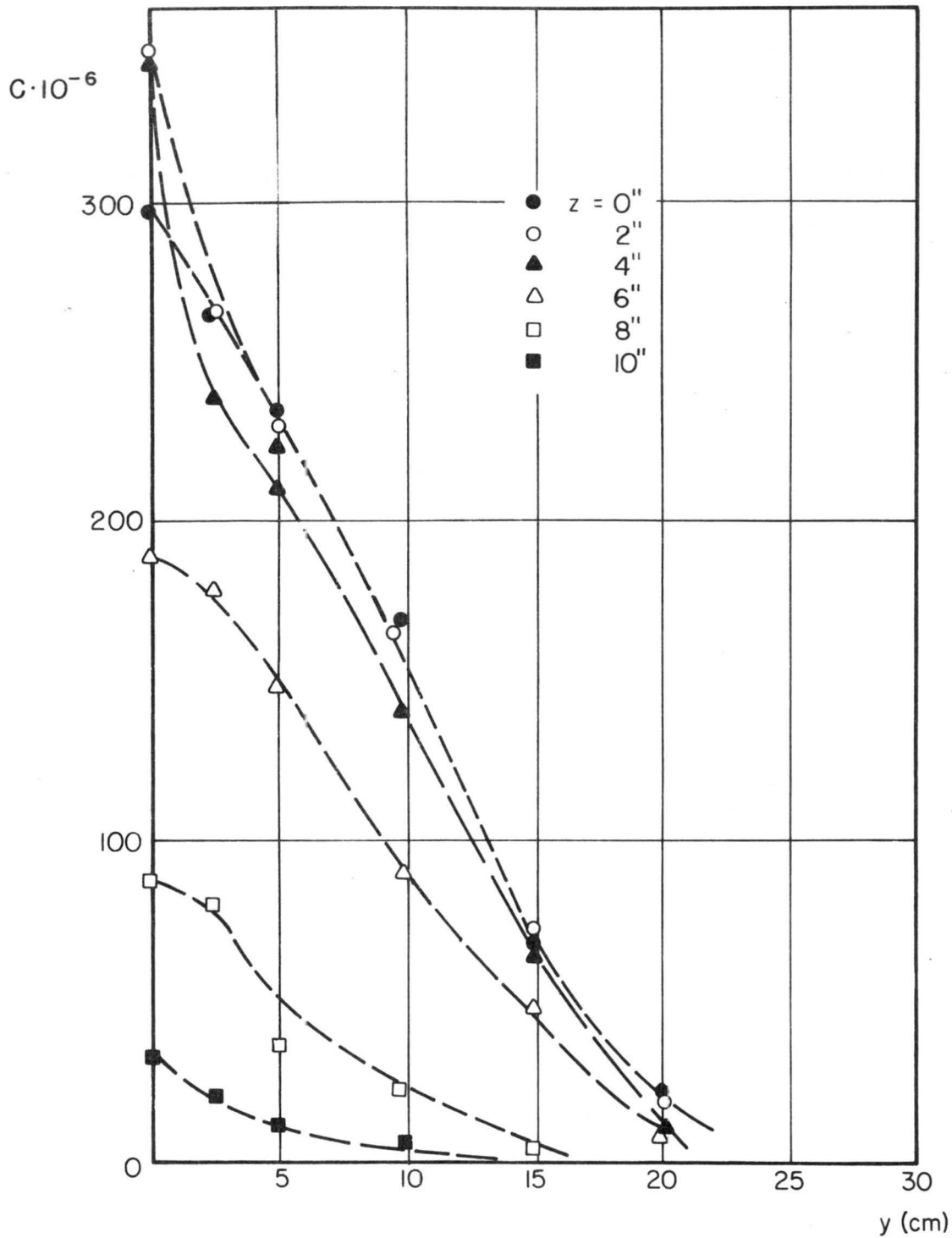


Fig. 18. Lateral dispersion of a continuous point source in a model peg canopy (2.54 x 2.54 cm). $x_s = 6$ m, $z_s = h$

PEGS: $\phi = 0.48$ cm, $h = 9$ cm, $L = 10.8$ m, $\frac{L}{h} = 120$, SPACED 2.54 x 2.54 cm

$Z_s = h$
 $X_s = 6$ m 0.3 m FROM SOURCE
 $V_\infty = 12$ m/sec

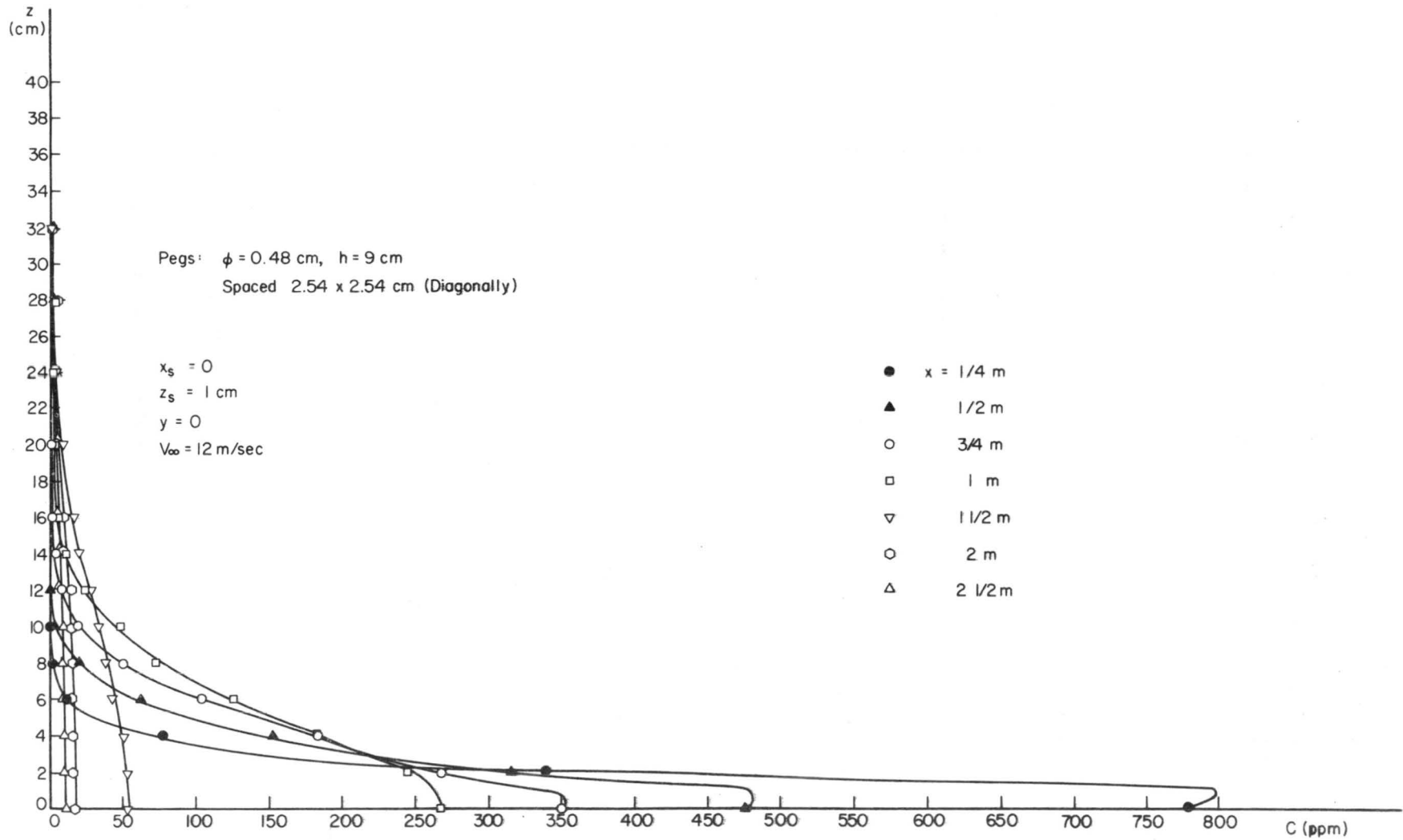


Fig. 19. Vertical dispersion of a continuous point source in a model peg canopy (2.54×2.54 cm diagonal). $x_s = 0$, $z_s = 1$ cm

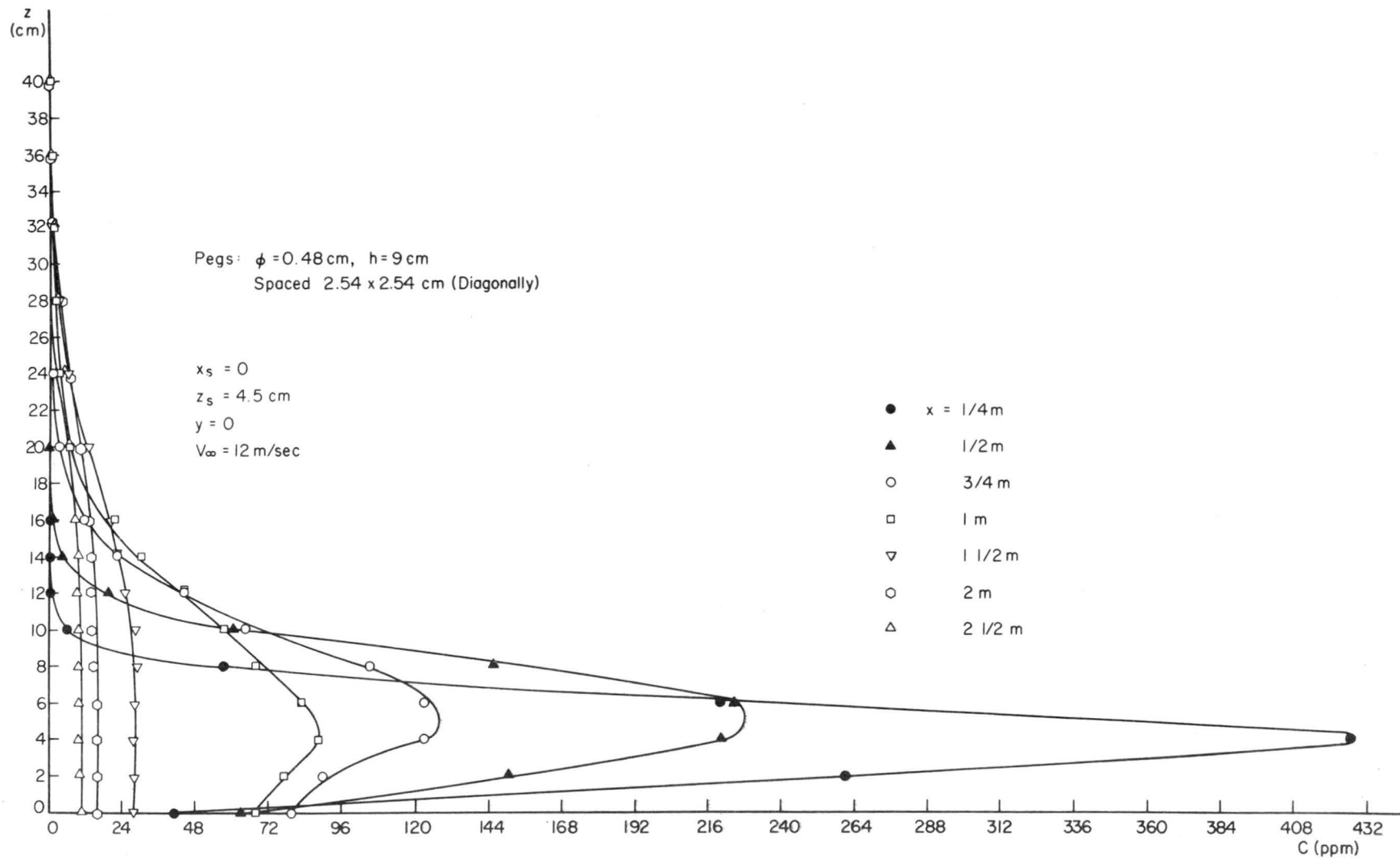


Fig. 20. Vertical dispersion of a continuous point source in a model peg canopy (2.54 x 2.54 diagonal). $x_s = 0$, $z_s = 0.5 h$

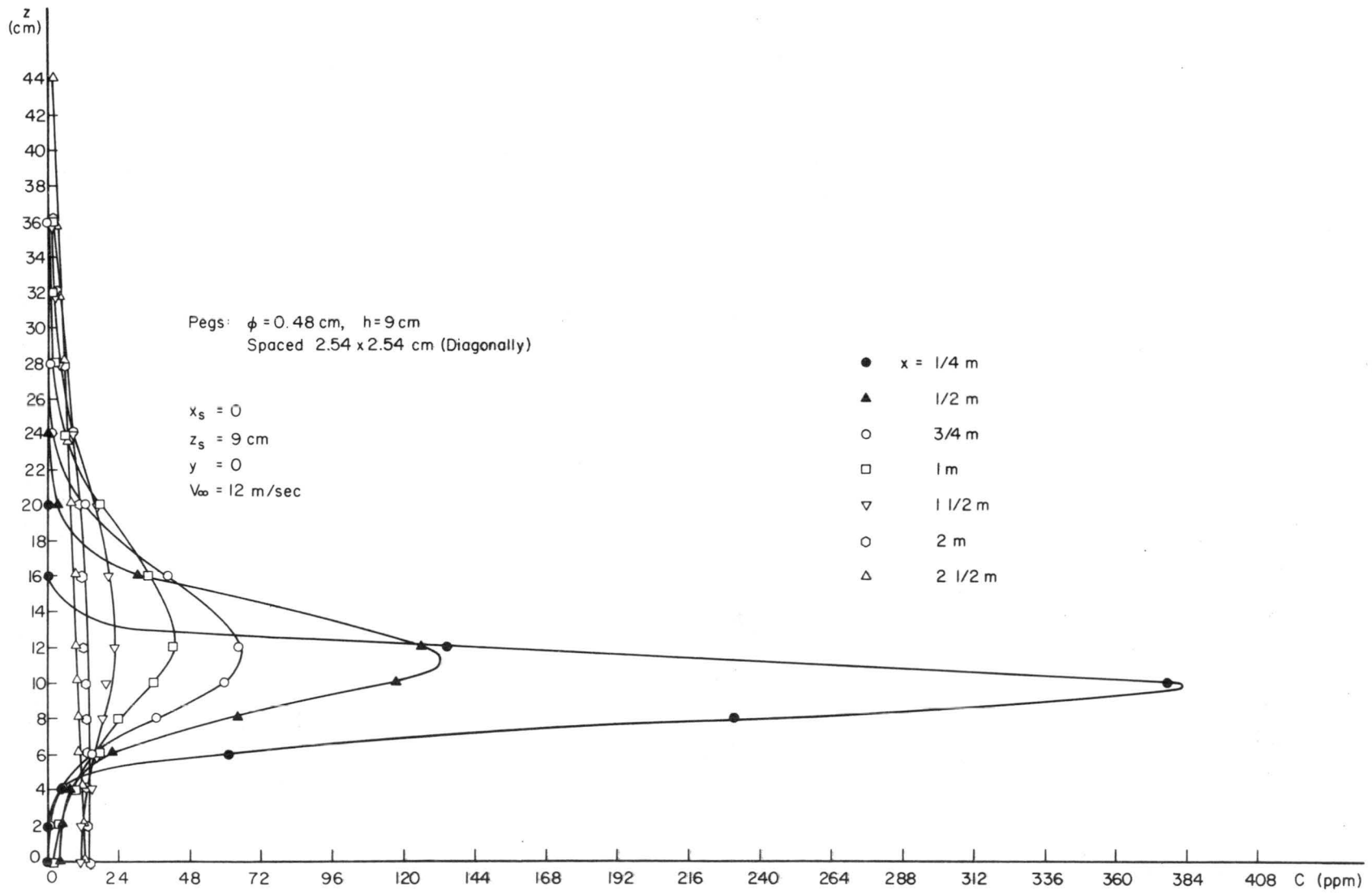


Fig. 21. Vertical dispersion of a continuous point source in a model peg canopy
 (2.54×2.54 diagonal). $x_s = 0$, $z_s = h$

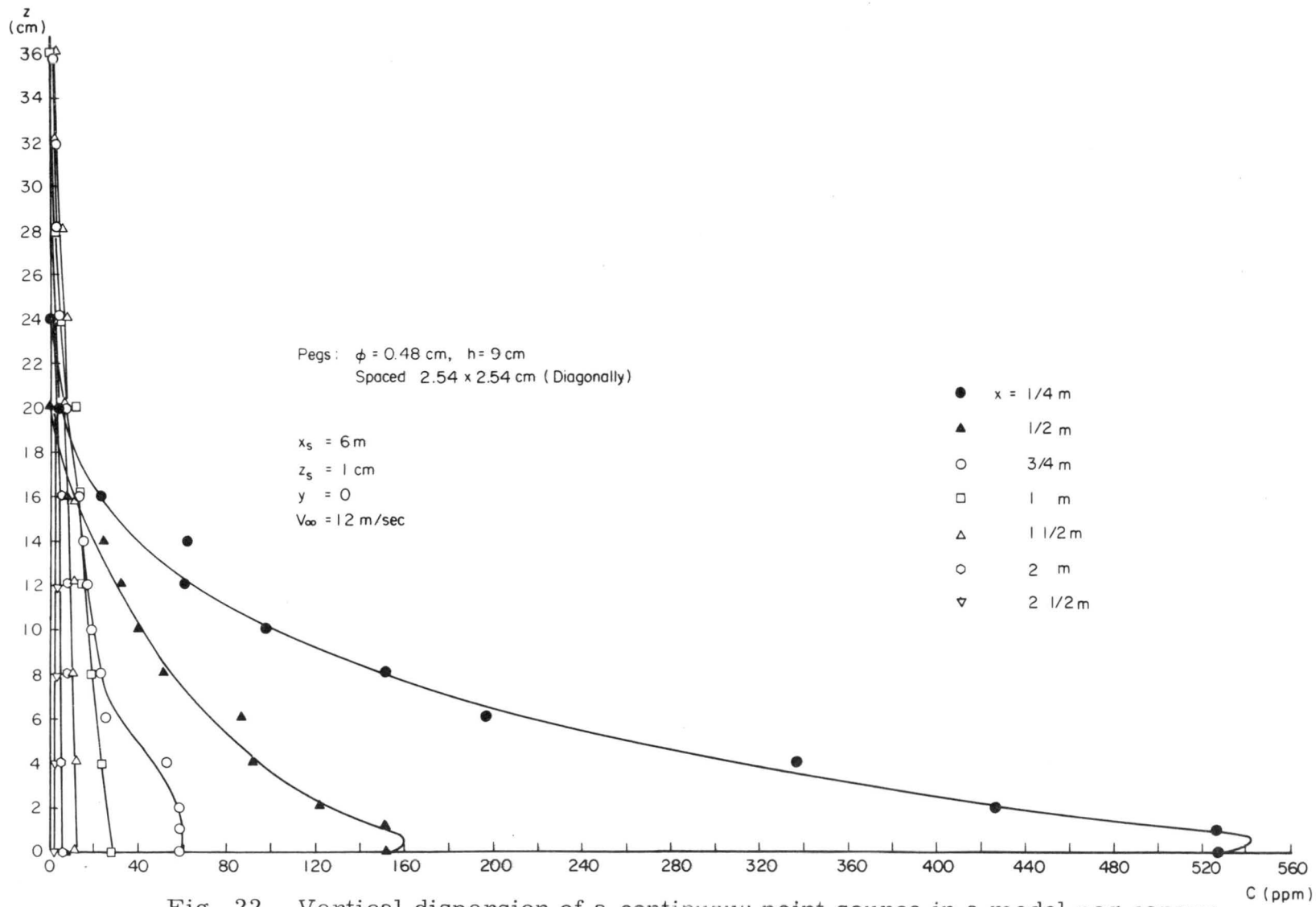


Fig. 22. Vertical dispersion of a continuous point source in a model peg canopy (2.54 x 2.54 diagonal). $x_s = 6$ m, $z_s = 1$ cm

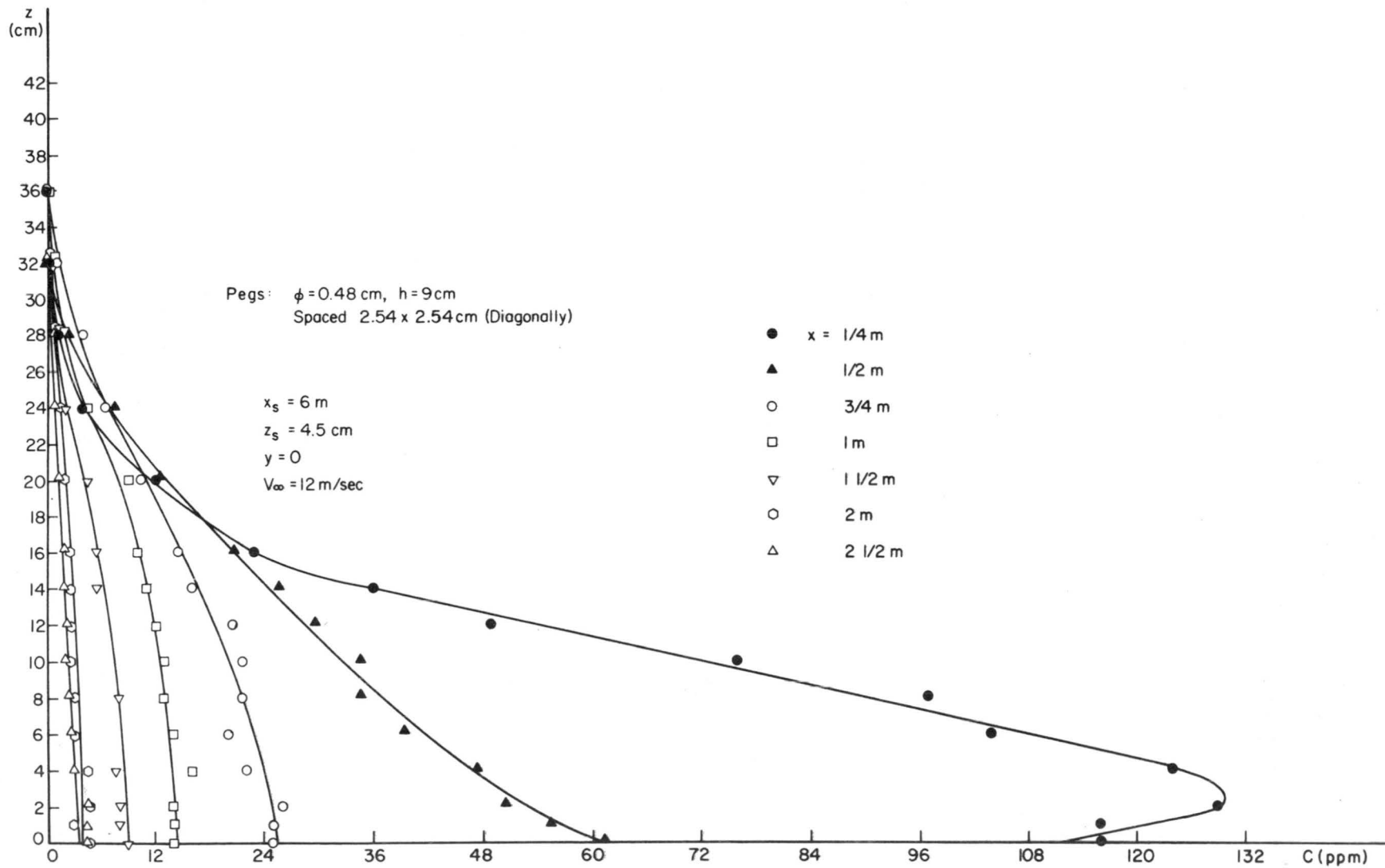


Fig. 23. Vertical dispersion of a continuous point source in a model peg canopy
 (2.54×2.54 diagonal). $x_s = 6$ m, $z_s = 0.5$ h

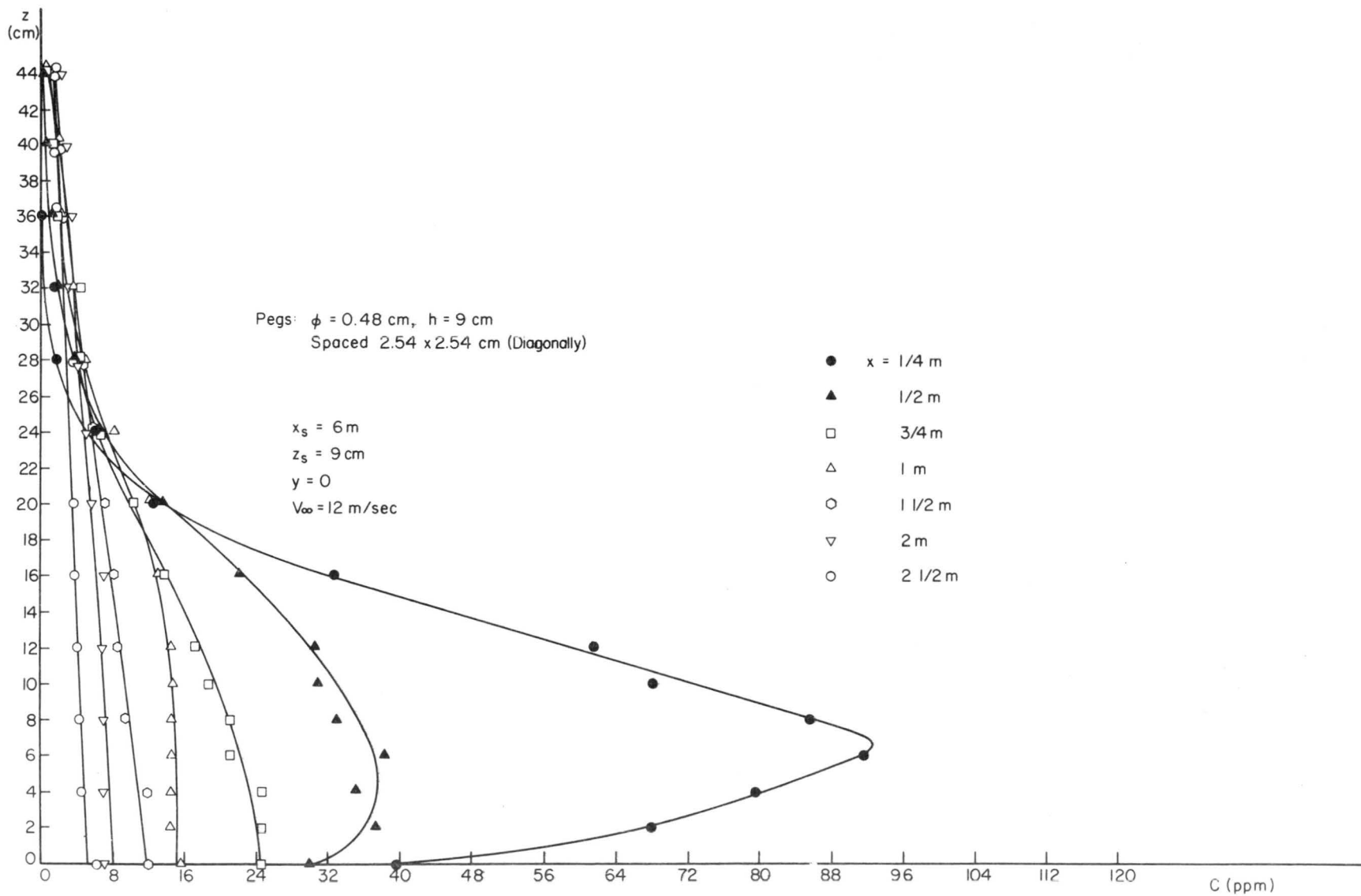


Fig. 24. Vertical dispersion of a continuous point source in a model peg canopy
 (2.54×2.54 diagonal). $x_s = 6$ m, $z_s = h$

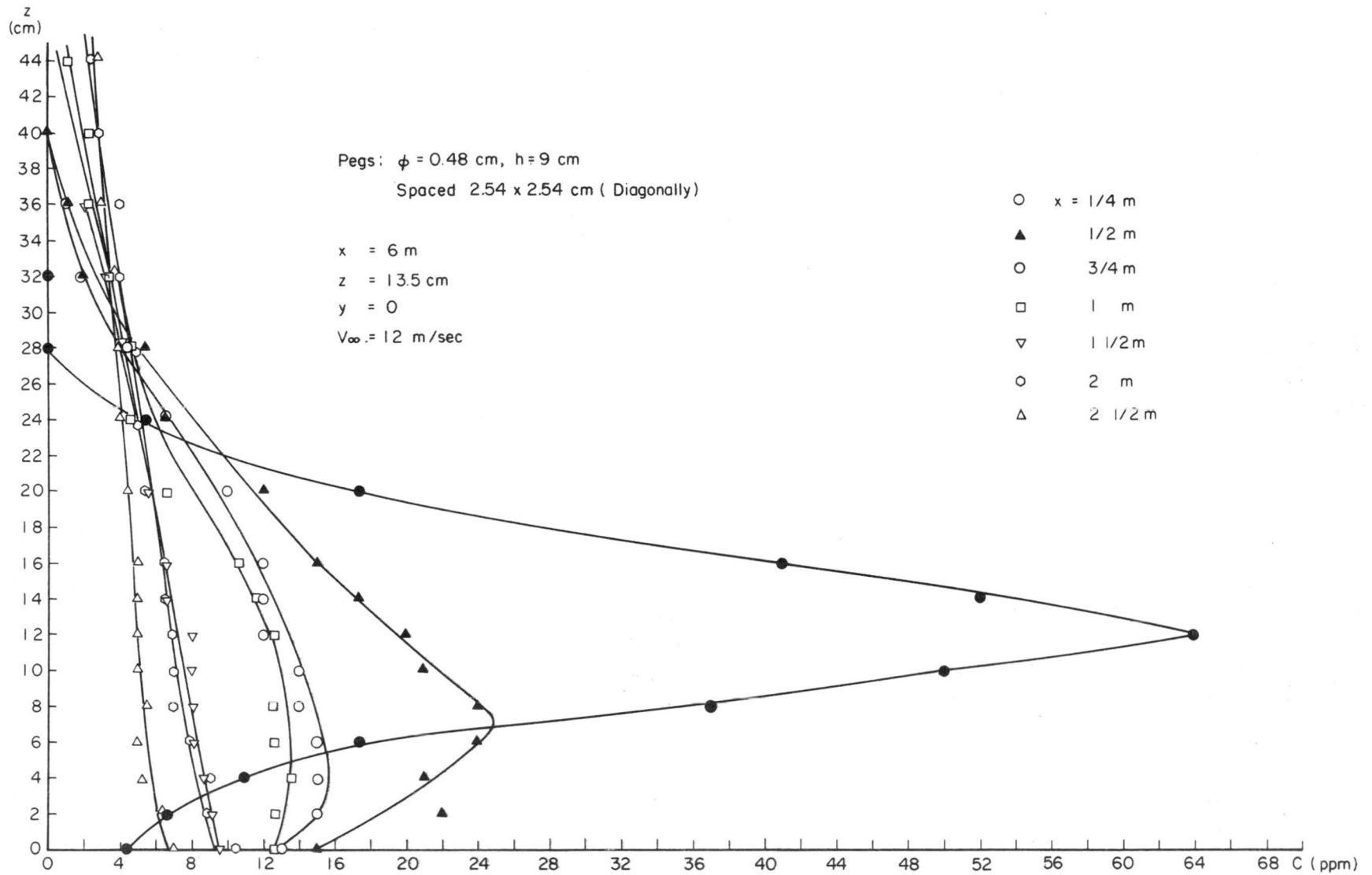


Fig. 25. Vertical dispersion of a continuous point source in a model peg canopy (2.54×2.54 diagonal). $x_s = 6$ m, $z_s = 1.5$ h

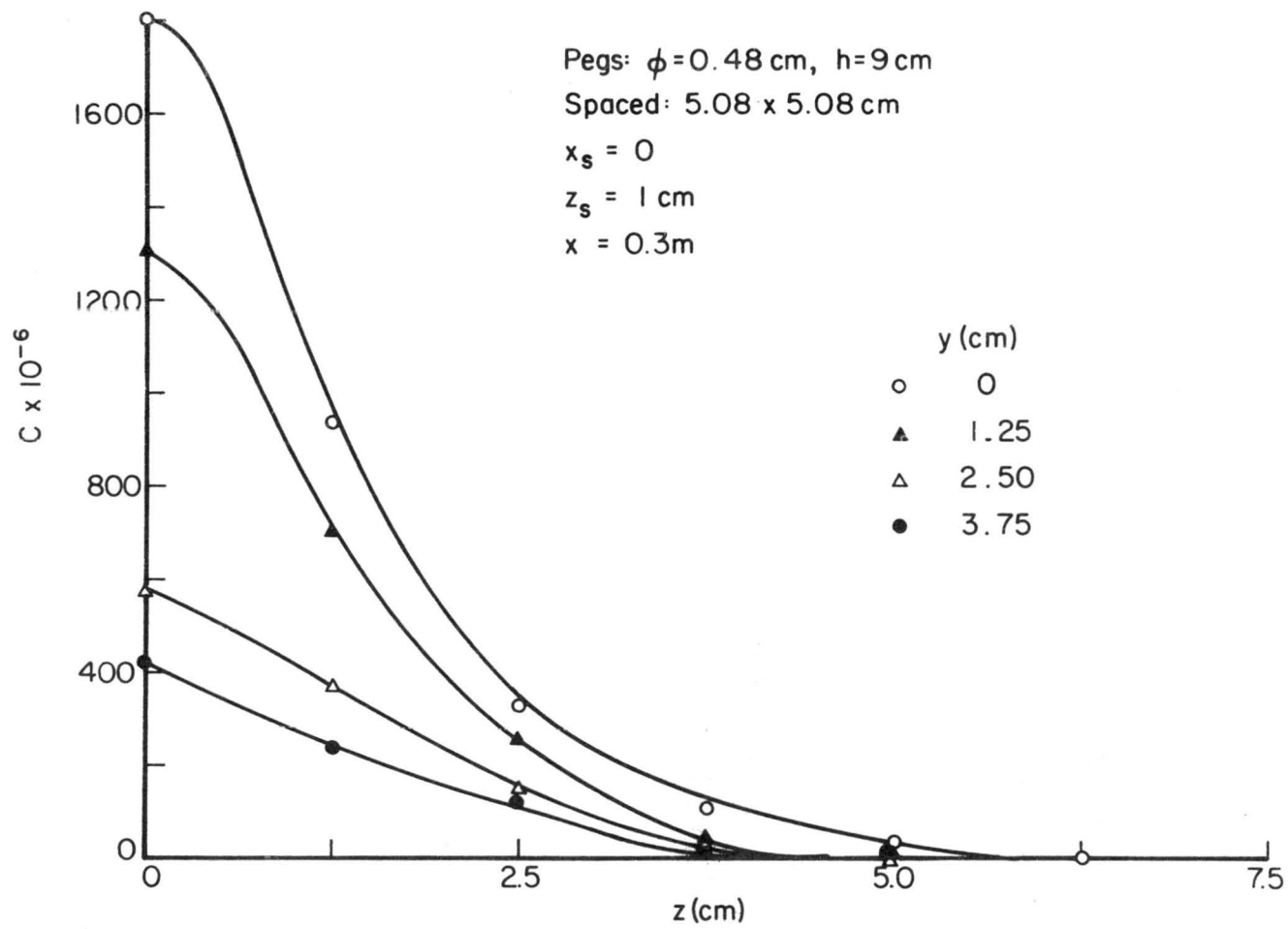


Fig. 26. Vertical dispersion of a continuous point source in a model peg canopy (5.08×5.08 cm). $x_s = 0$, $z_s = 1$ cm, $x = 0.3$ m

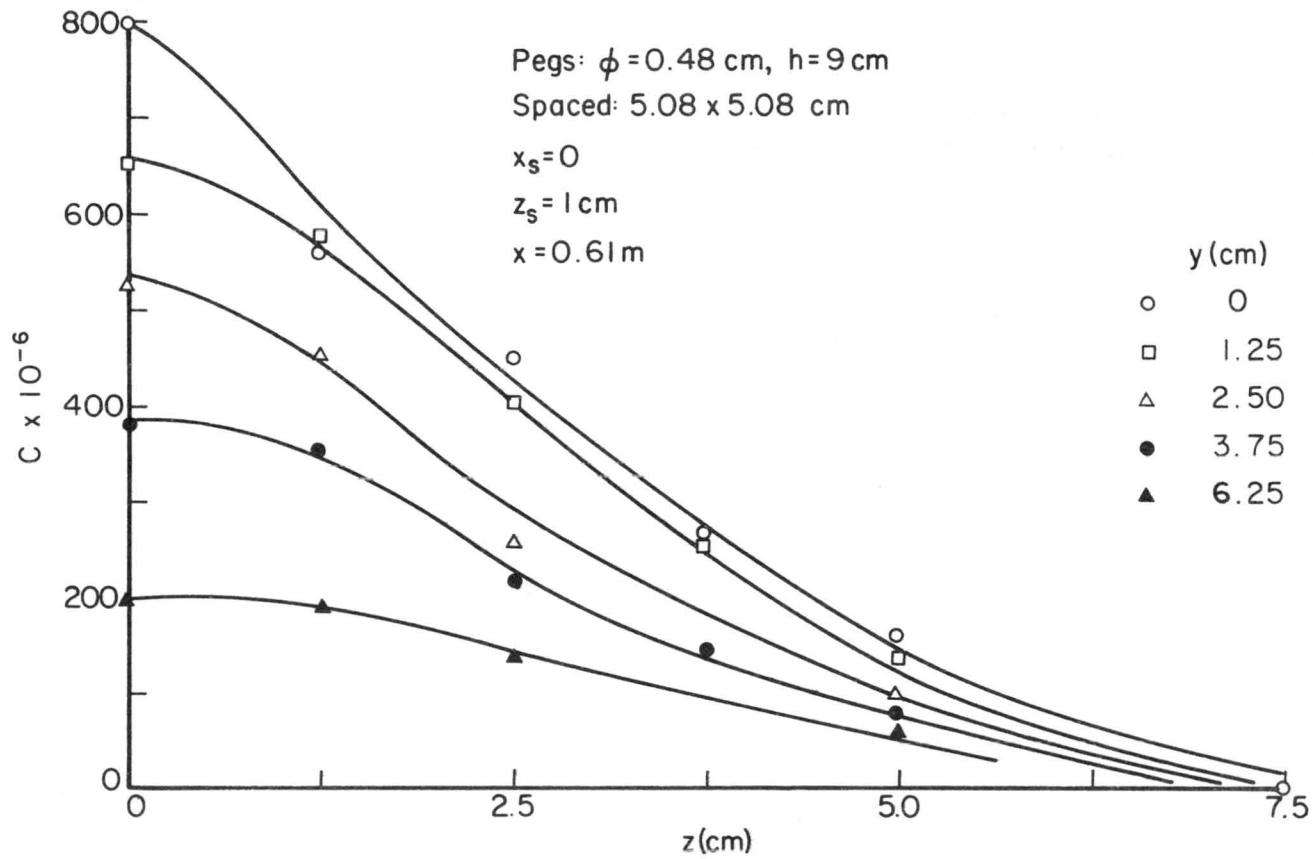


Fig. 27. Vertical dispersion of a continuous point source in a model peg canopy (5.08×5.08 cm). $x_s = 0$, $z_s = 1$ cm, $x = 0.6$ m

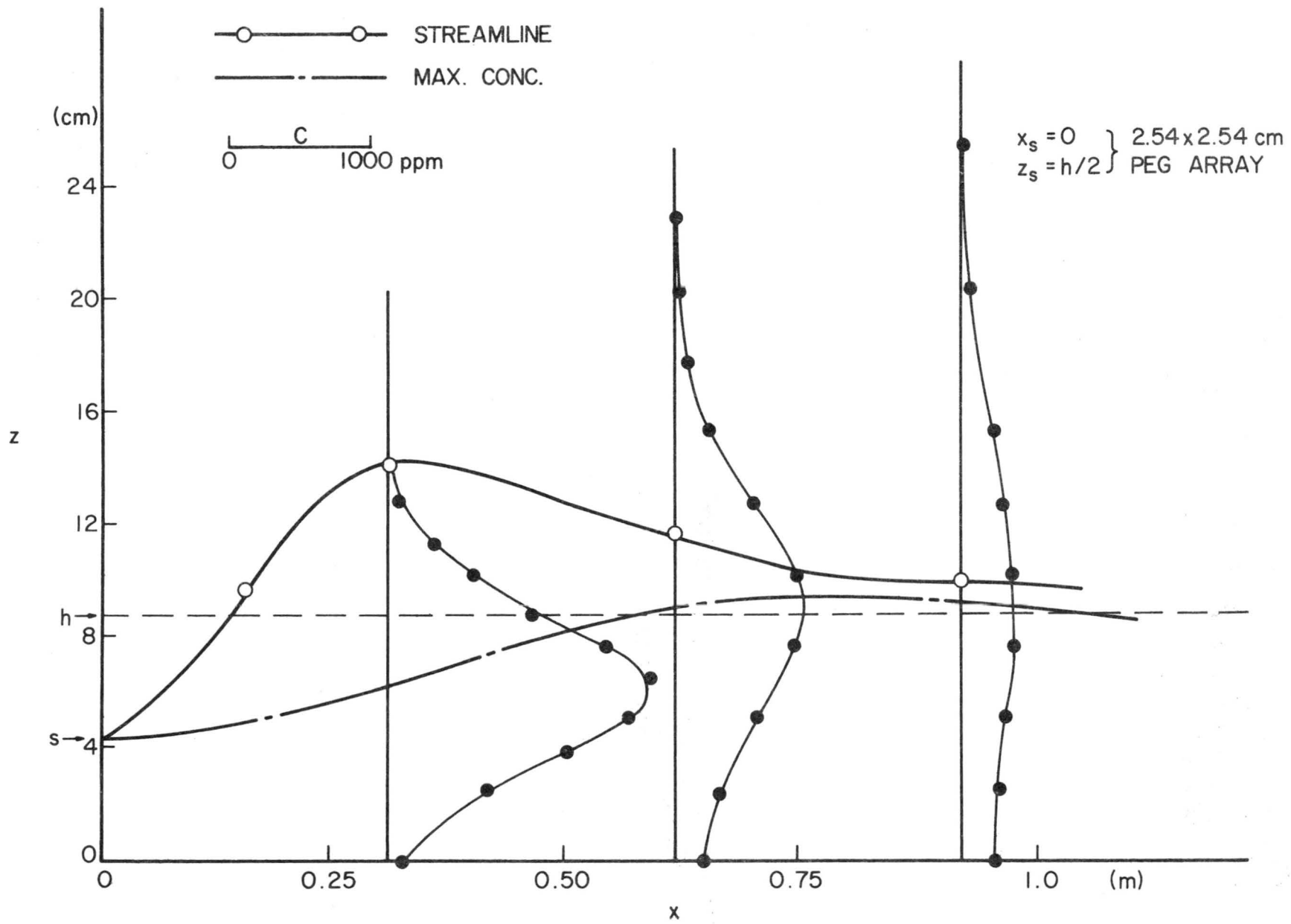


Fig. 28. Traces of maximum concentration from a point source (2.54 x 2.54 cm).
 $x_s = 0, z_s = 0.5 h.$

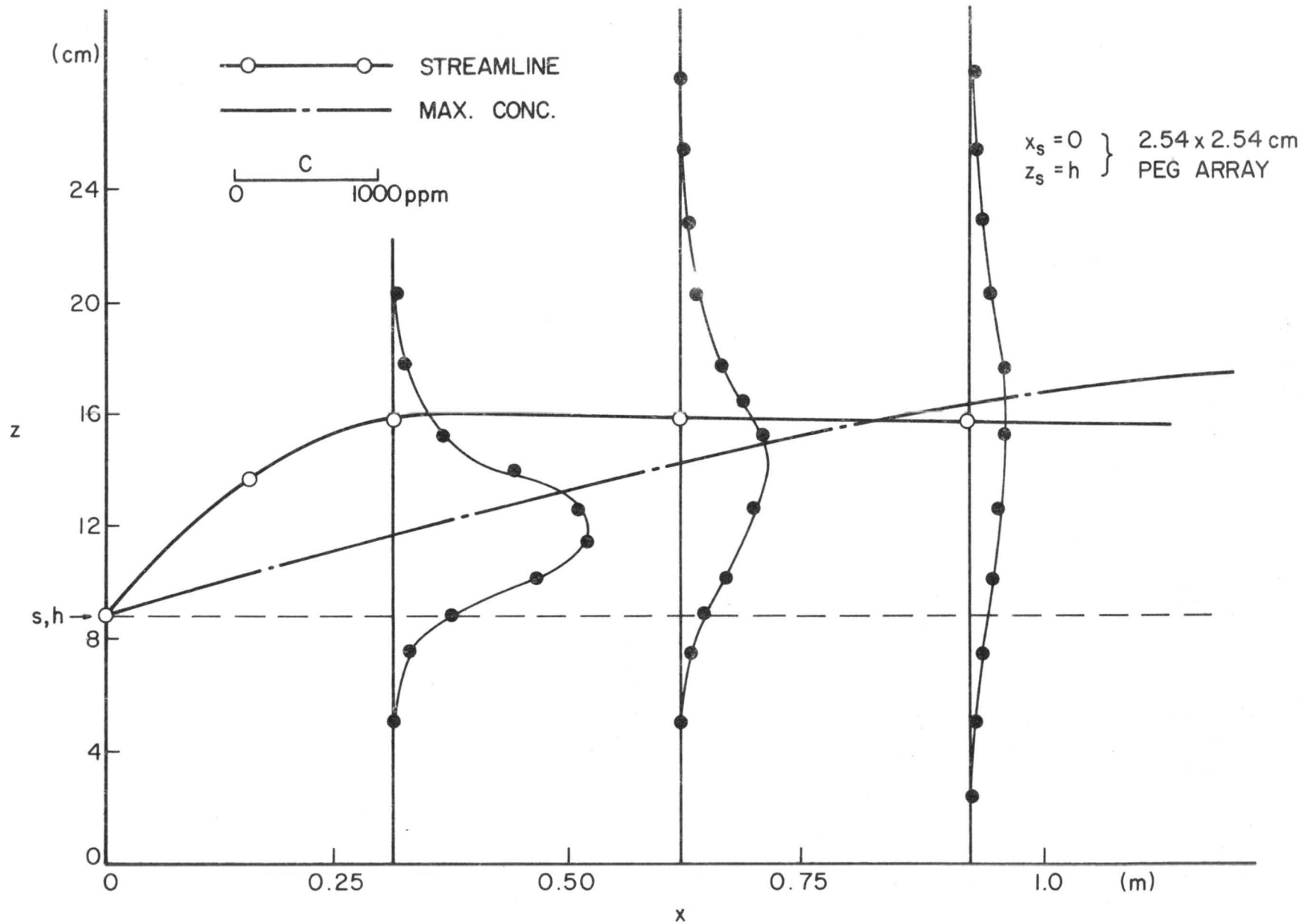


Fig. 29. Traces of maximum concentration from a point source (2.54 x 2.54 cm). $x_s = 0$, $z_s = h$

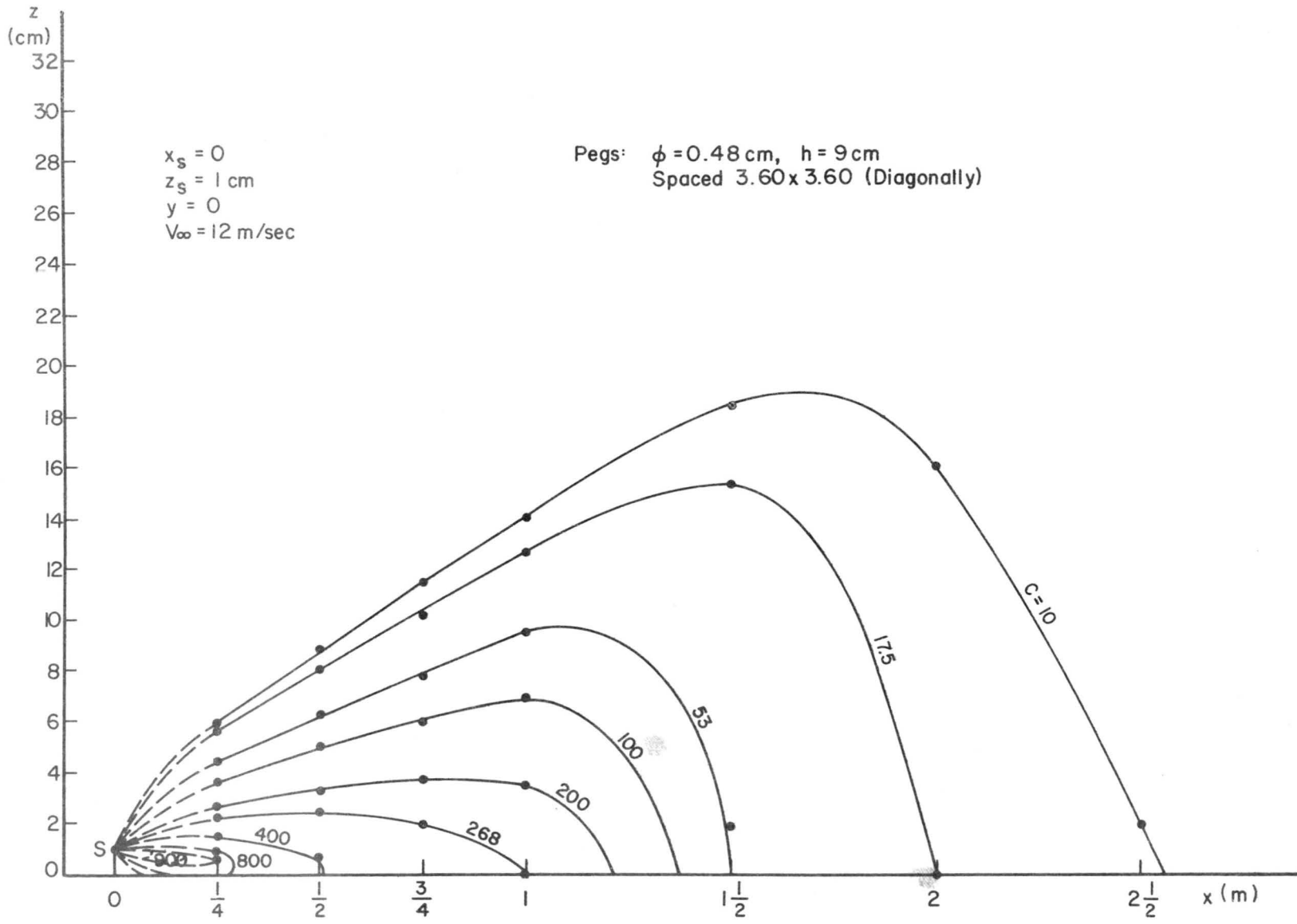


Fig. 30. Diffusion in the canopy-isoconcentration lines (2.54 x 2.54 diagonal).
 $x_s = 0, z_s = 1 \text{ cm}$

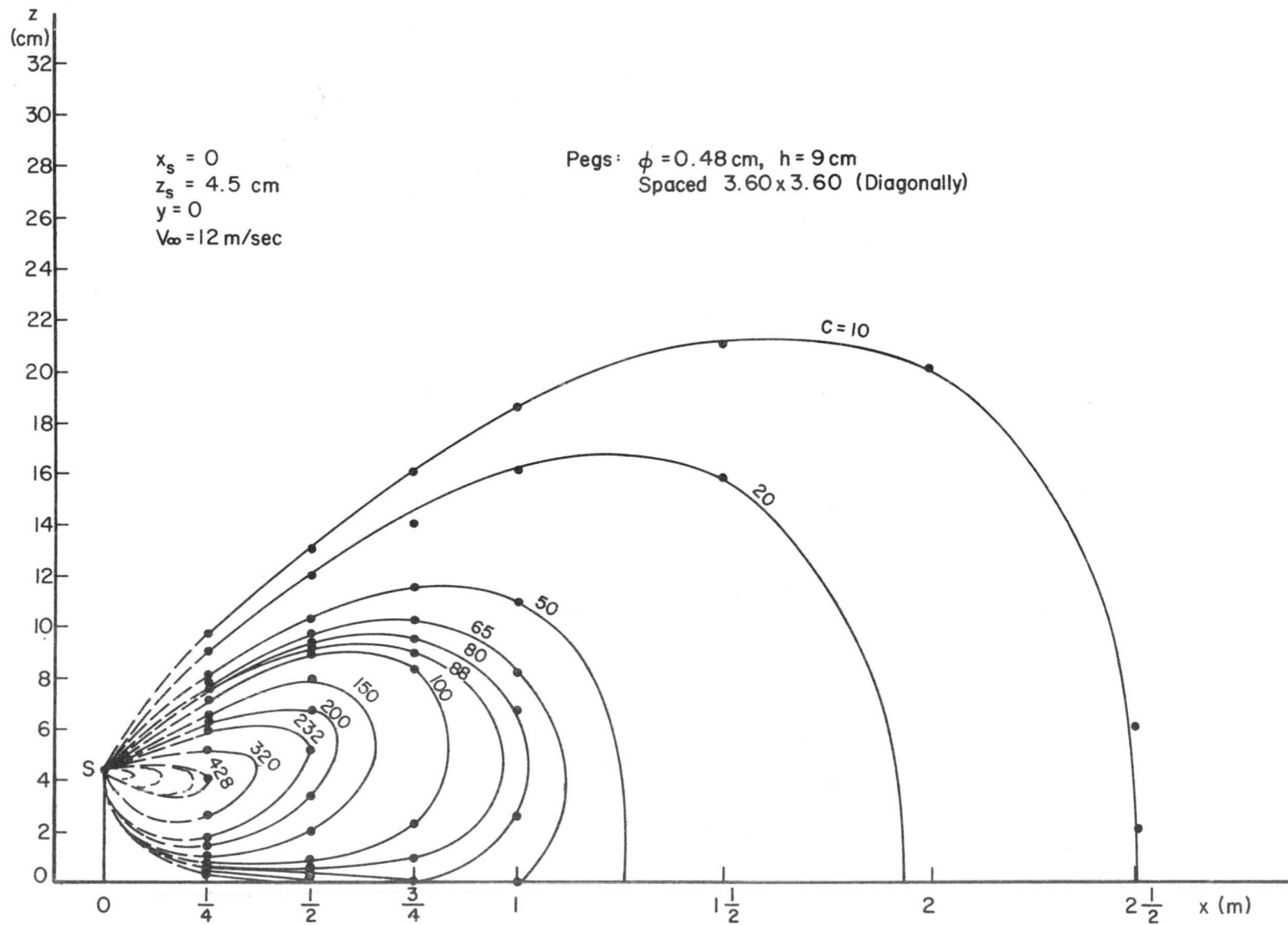


Fig. 31. Diffusion in the canopy-isoconcentration lines (2.54×2.54 diagonal).
 $x_s = 0$, $z_s = 0.5 \text{ h}$.

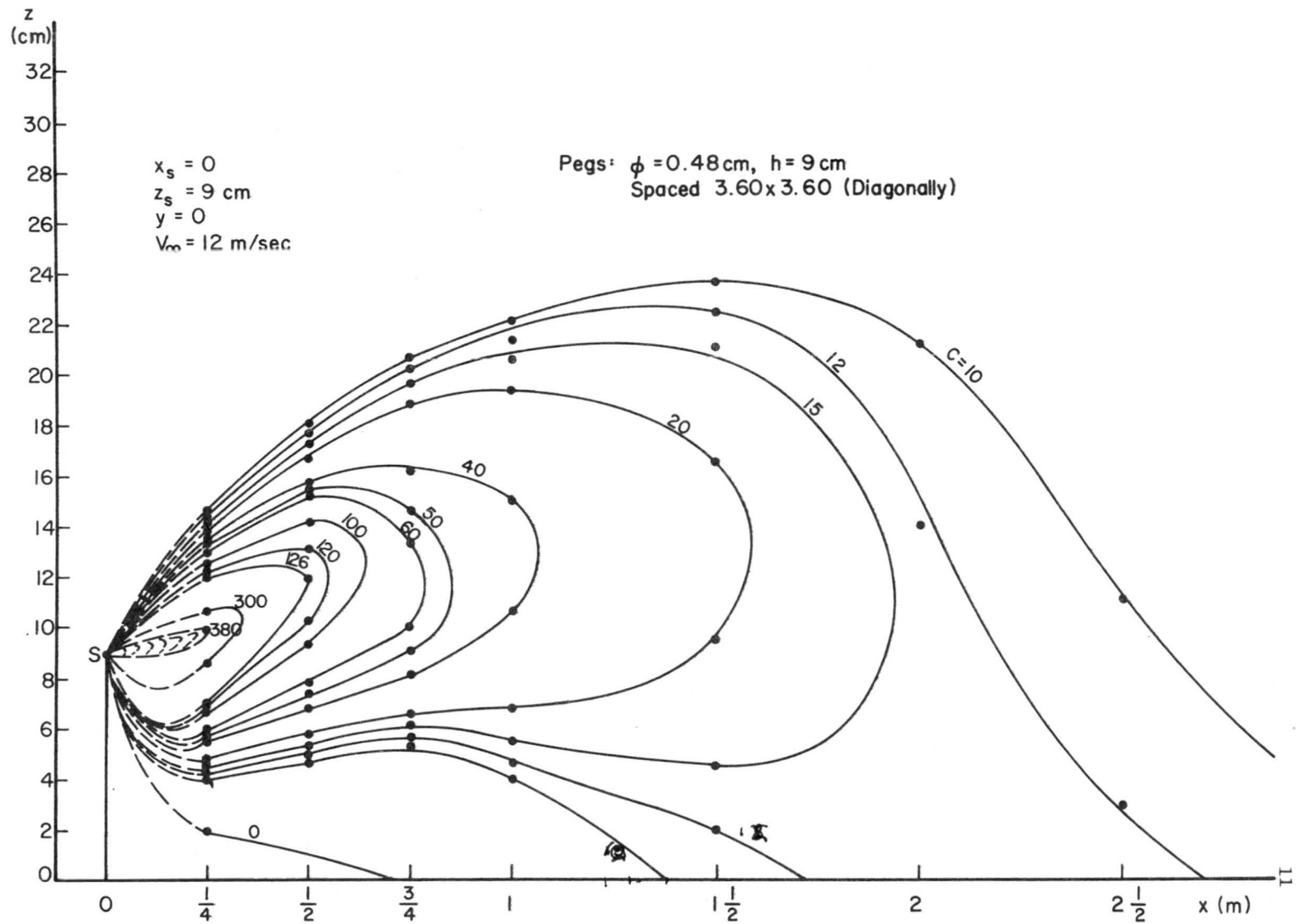


Fig. 32. Diffusion in the canopy-isoconcentration lines (2.54×2.54 diagonal).
 $x_s = 0$, $z_s = h$

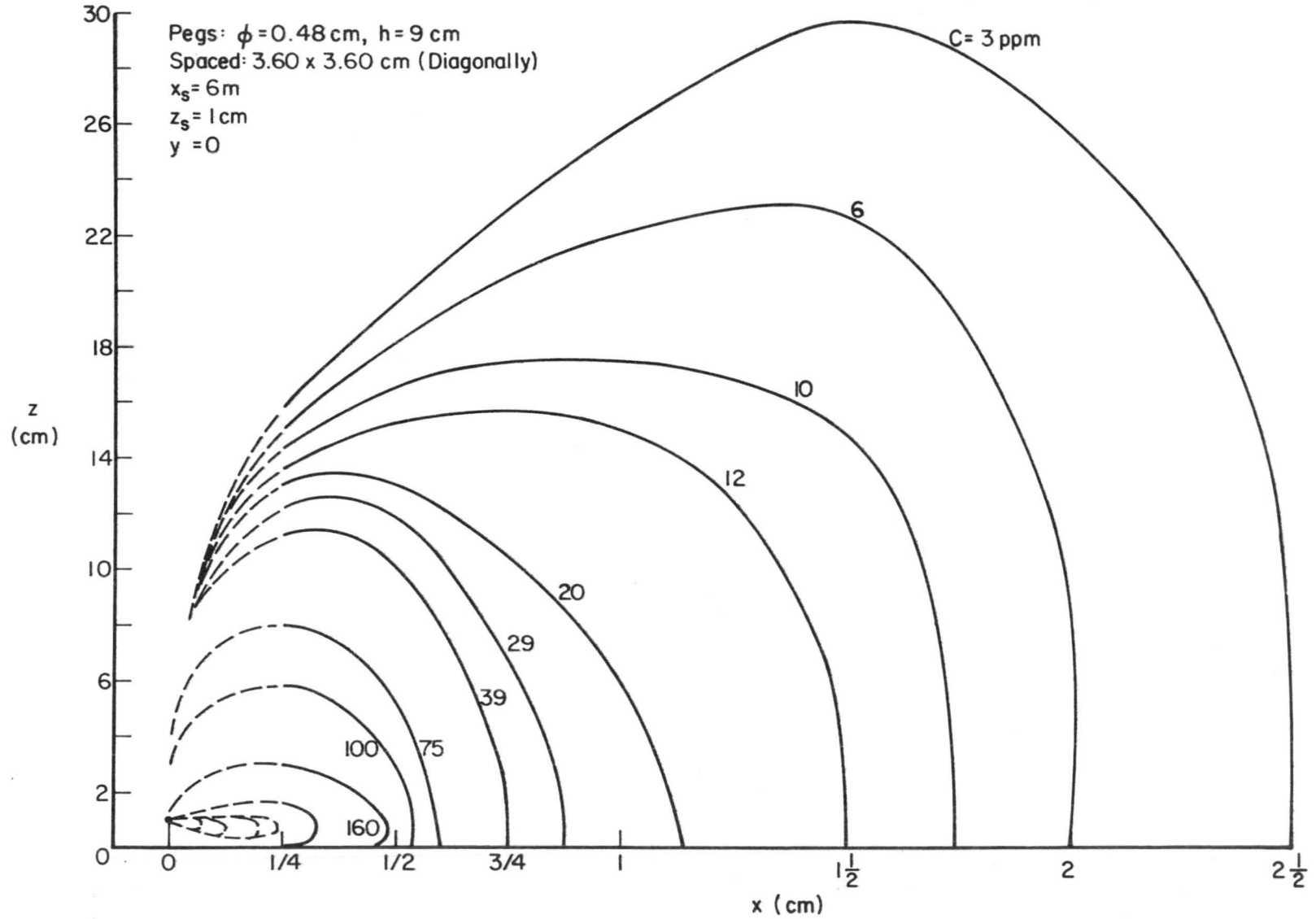


Fig. 33. Diffusion in the canopy-isoconcentration lines (2.54×2.54 diagonal).
 $x_s = 6$, $z_s = 1$ cm

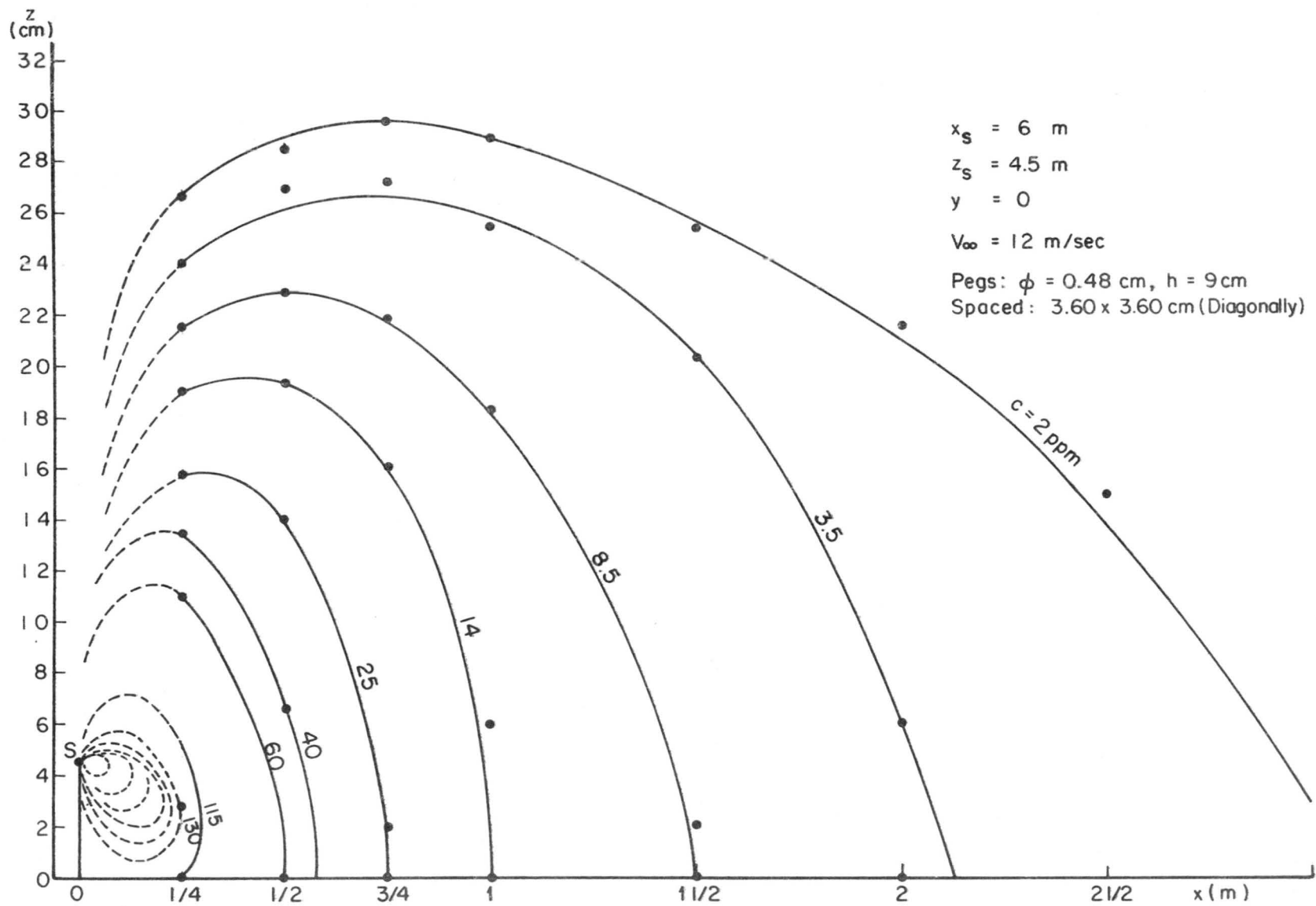


Fig. 34. Diffusion in the canopy-isoconcentration lines (2.54×2.54 diagonal).
 $x_s = 6$, $z_s = 0.5 \text{ h}$

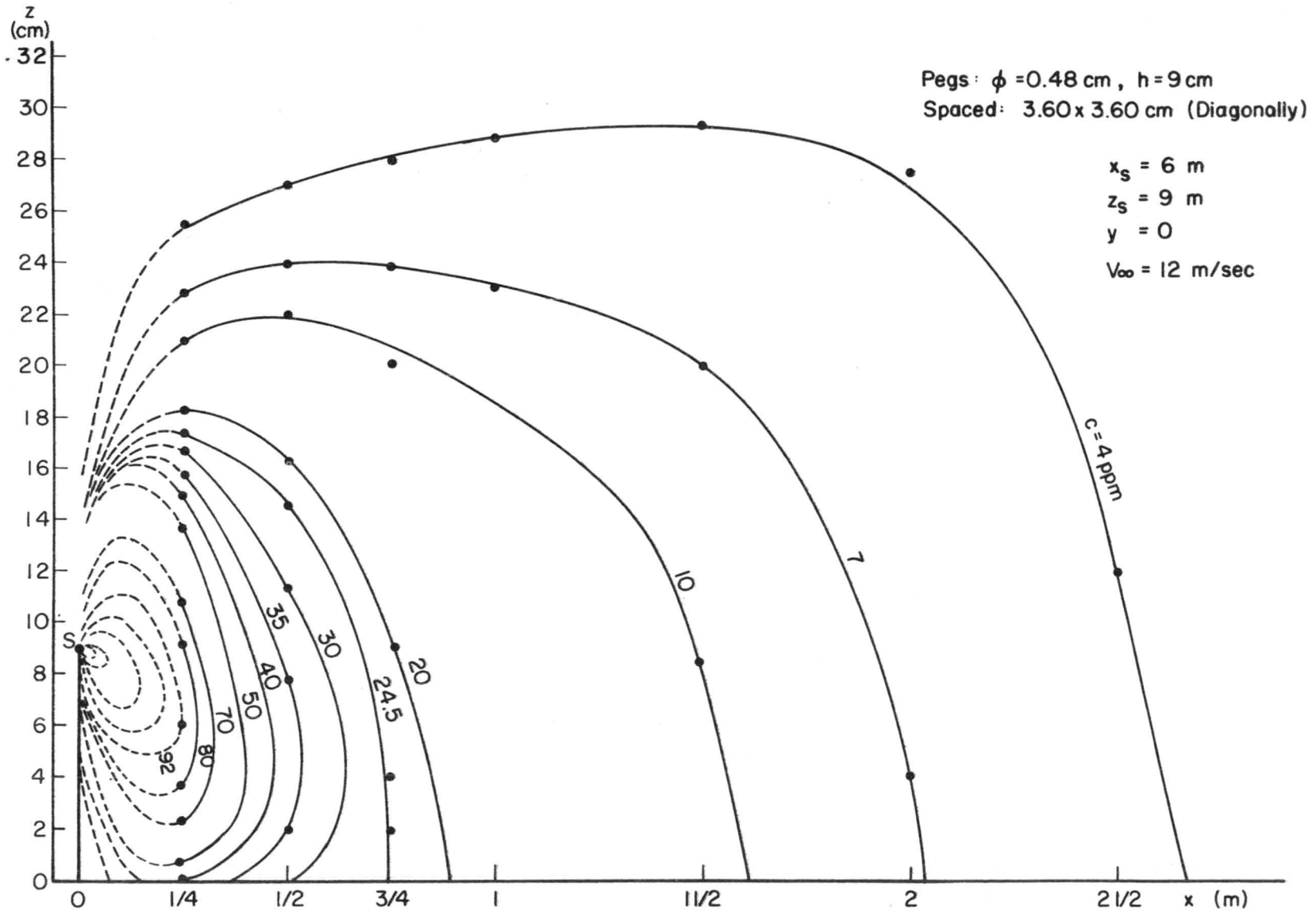


Fig. 35. Diffusion in the canopy-isoconcentration lines (2.54 x 2.54 diagonal).
 $x_s = 6$, $z_s = h$

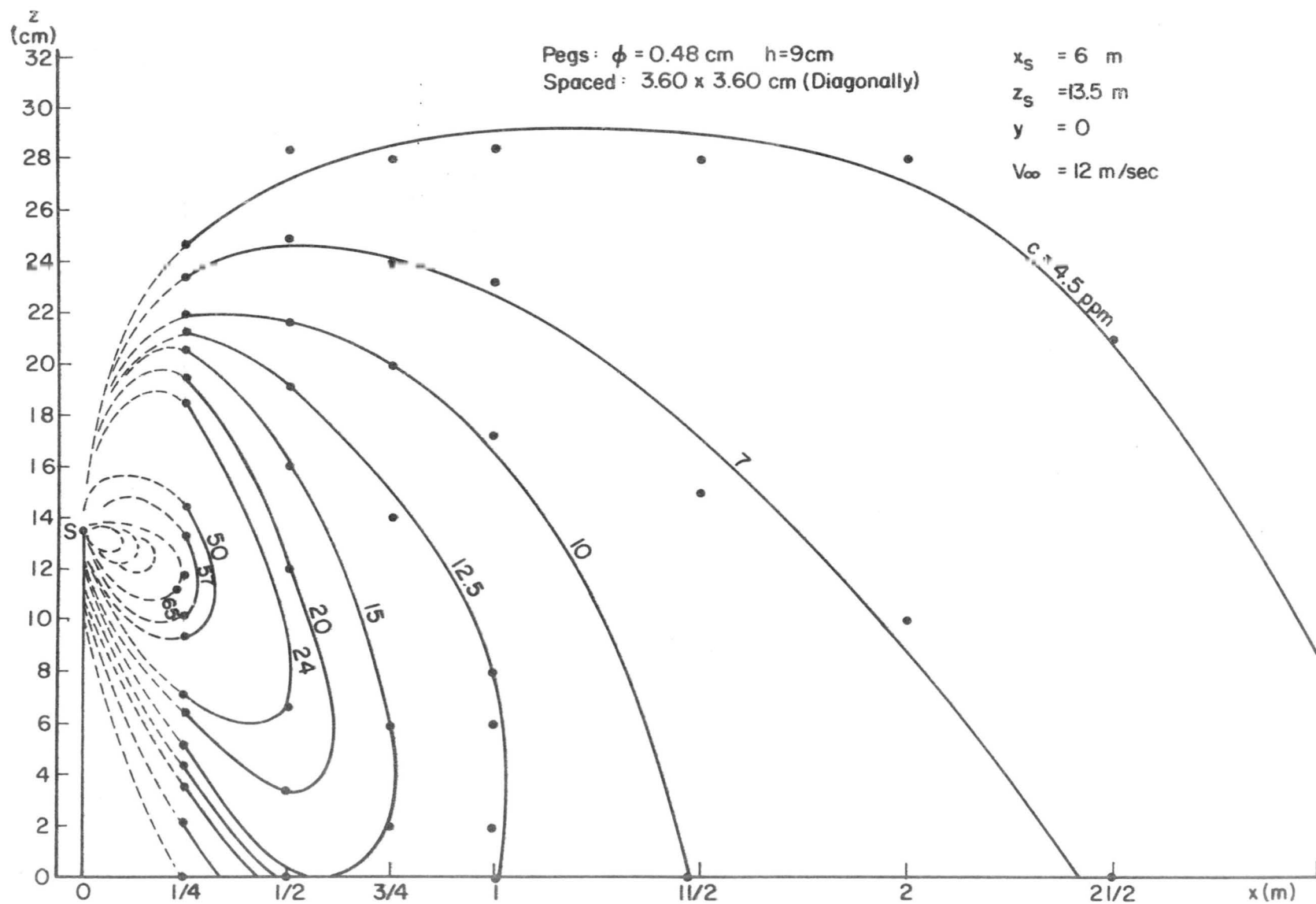


Fig. 36. Diffusion in the canopy-isoconcentration lines (2.54×2.54 diagonal).
 $x_s = 6$, $z_s = 1.5 h$

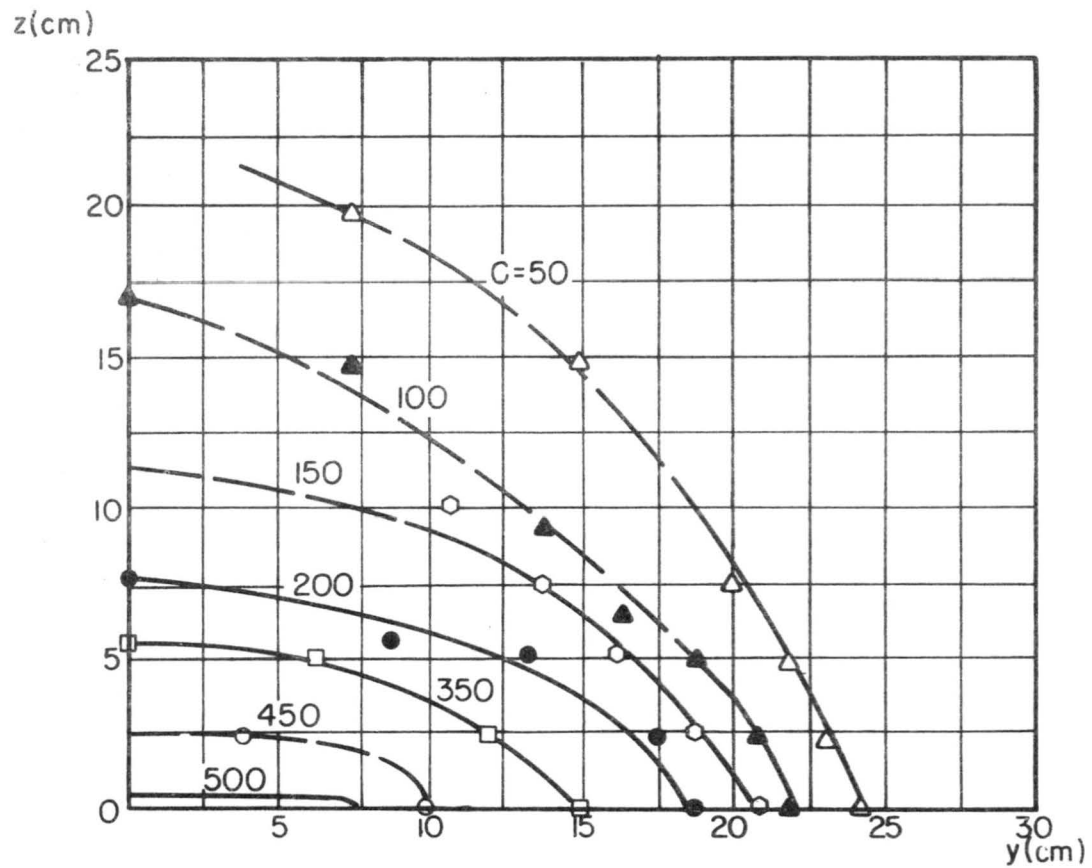


Fig. 37. Gaseous plume cross-section of a continuous point source in a model peg canopy (2.54 x 2.54 cm). $x_s = 6$ m, $z_s = 1$ cm, $x = 0.3$ m

PEGS: $\phi = 0.48$, $h = 9$ cm, $L = 10.8$ m, $\frac{L}{h} = 120$,
 SPACED: 2.54 x 2.54 cm

$Z_s = 1$ cm
 $X_s = 6$ m
 $X = 0.30$ m

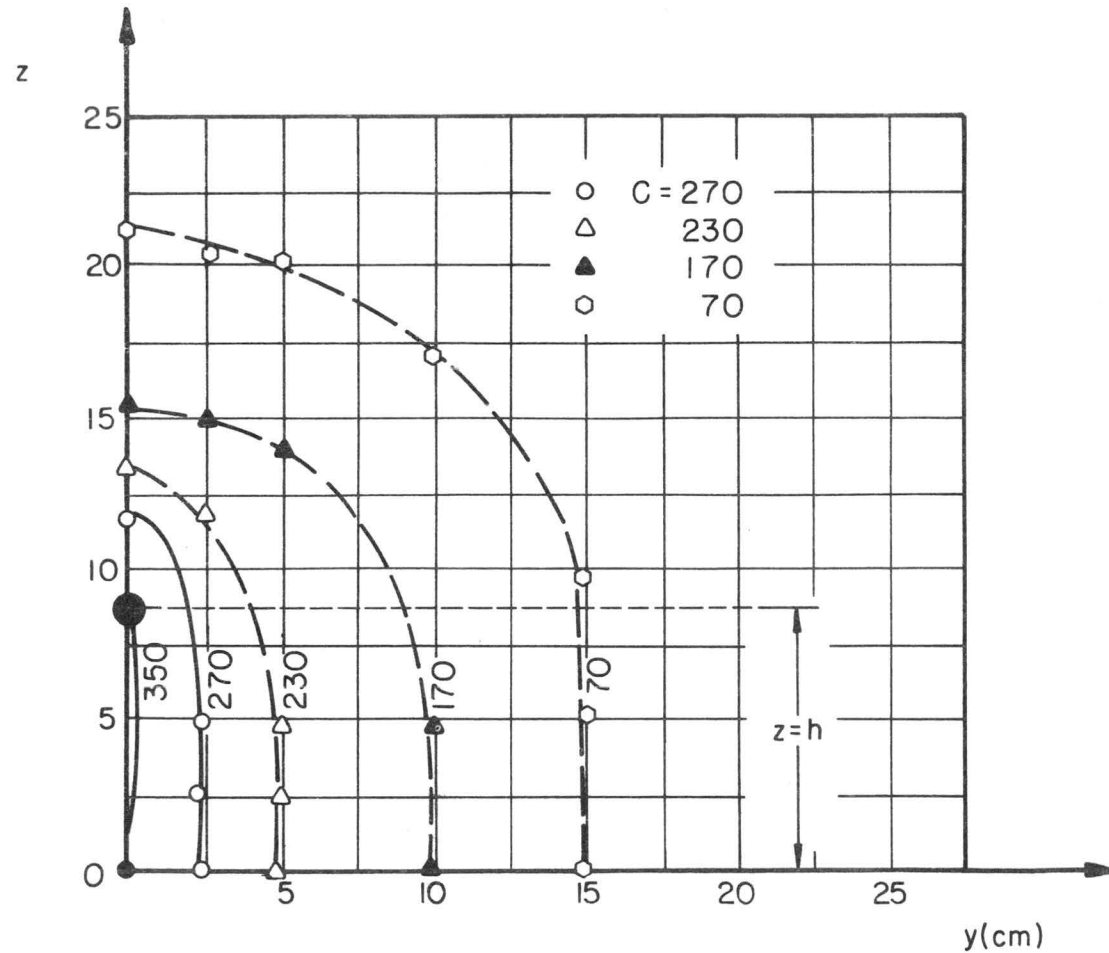


Fig. 38. Gaseous plume cross-section of a continuous point source in a model peg canopy (2.54 x 2.54 cm). $x_s = 6$ m, $z_s = h$, $x = 0.3$ m

PEGS: $\phi = 0.48$, $h = 9$ cm, $L = 10.8$ m, $\frac{L}{h} = 120$,
Spaced: 2.54 x 2.54 cm

$$Z_s = h$$

$$X_s = 6$$
 m

$$X = 0.3$$
 m

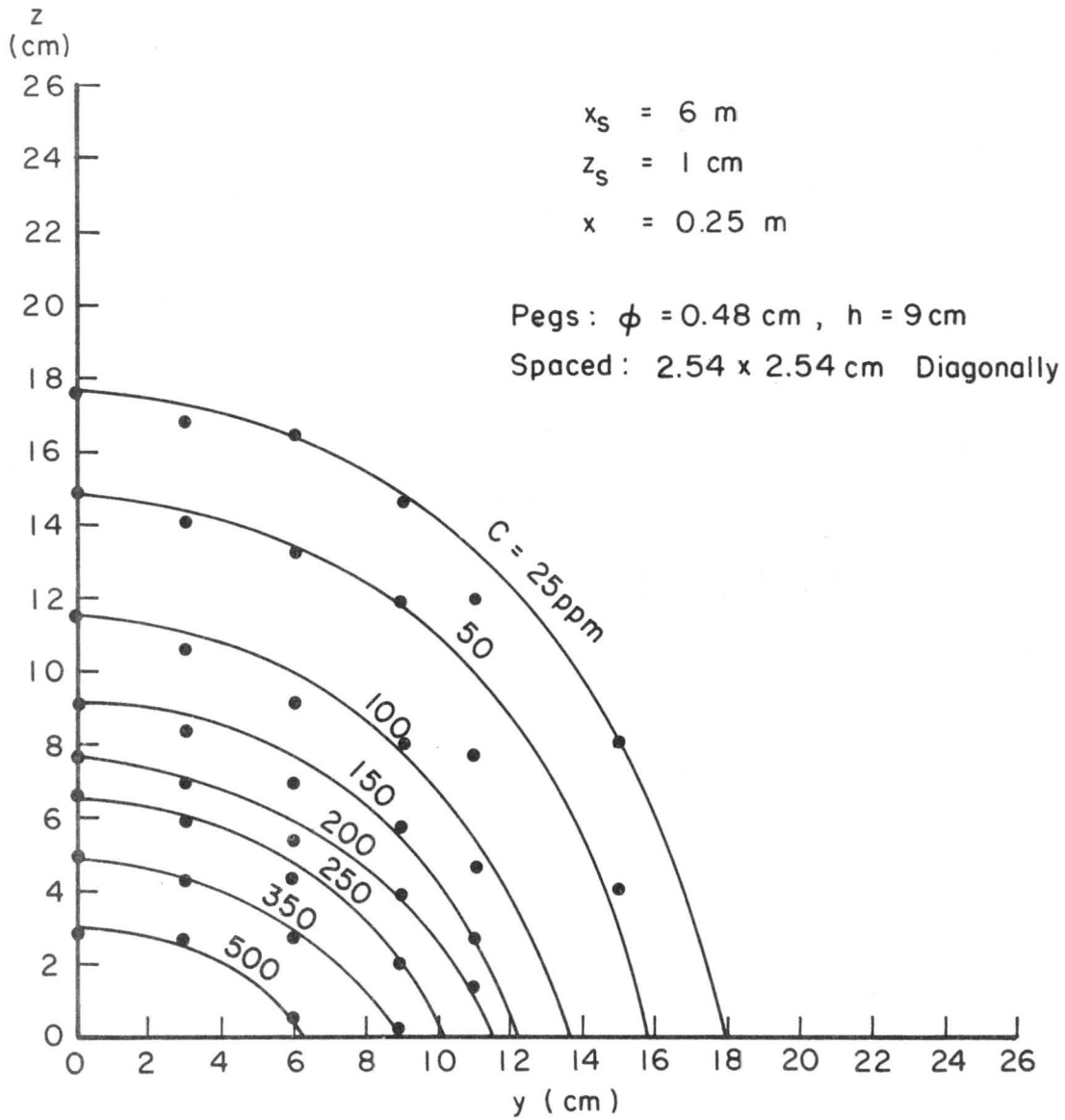


Fig. 39. Gaseous plume cross-section of a continuous point source in a model peg canopy ($2.54 \times 2.54 \text{ cm}$ diagonal). $x_s = 6 \text{ m}$, $z_s = 1 \text{ cm}$, $x = 0.25 \text{ m}$

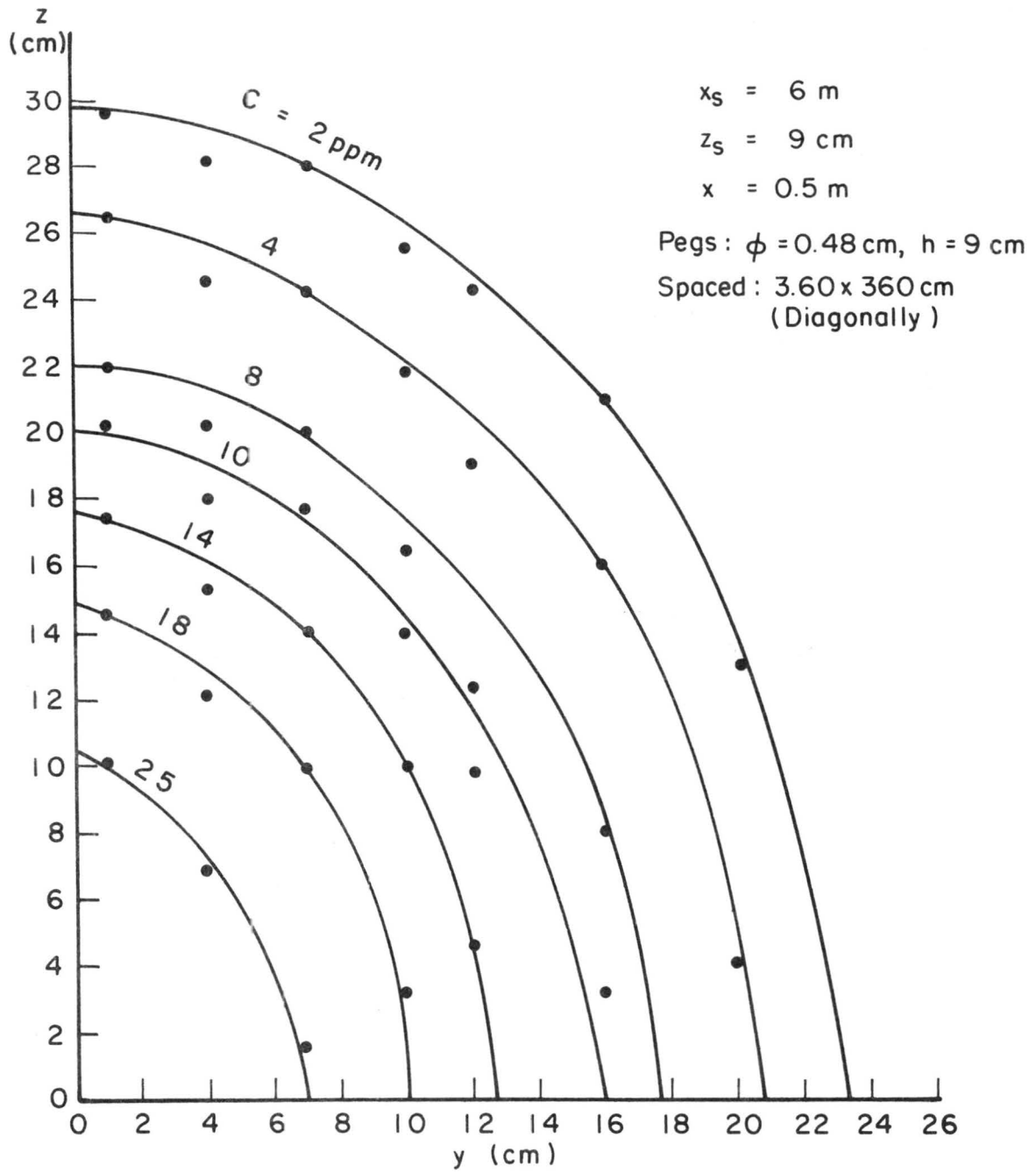


Fig. 40. Gaseous plume cross-section of a continuous point source in a model peg canopy ($2.54 \times 2.54 \text{ cm}$ diagonal). $x_s = 6 \text{ m}$, $z_s = h$, $x = 0.5 \text{ m}$

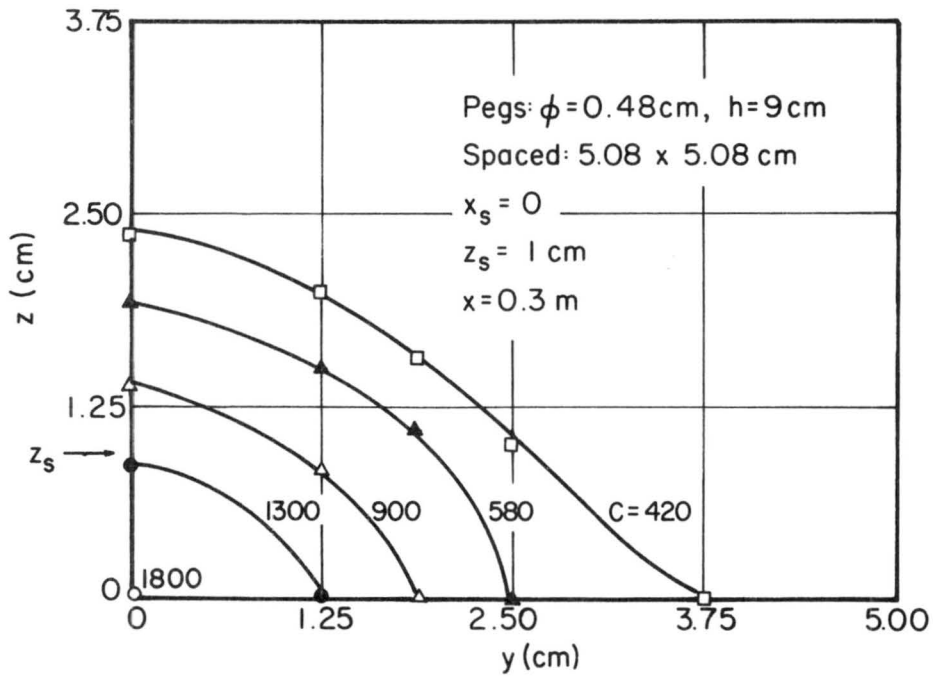


Fig. 41. Gaseous plume cross-section of a continuous point source in a model peg canopy ($5.08 \times 5.08 \text{ cm}$).
 $x_s = 0 \text{ m}$, $z_s = 1 \text{ cm}$, $x = 0.3 \text{ m}$

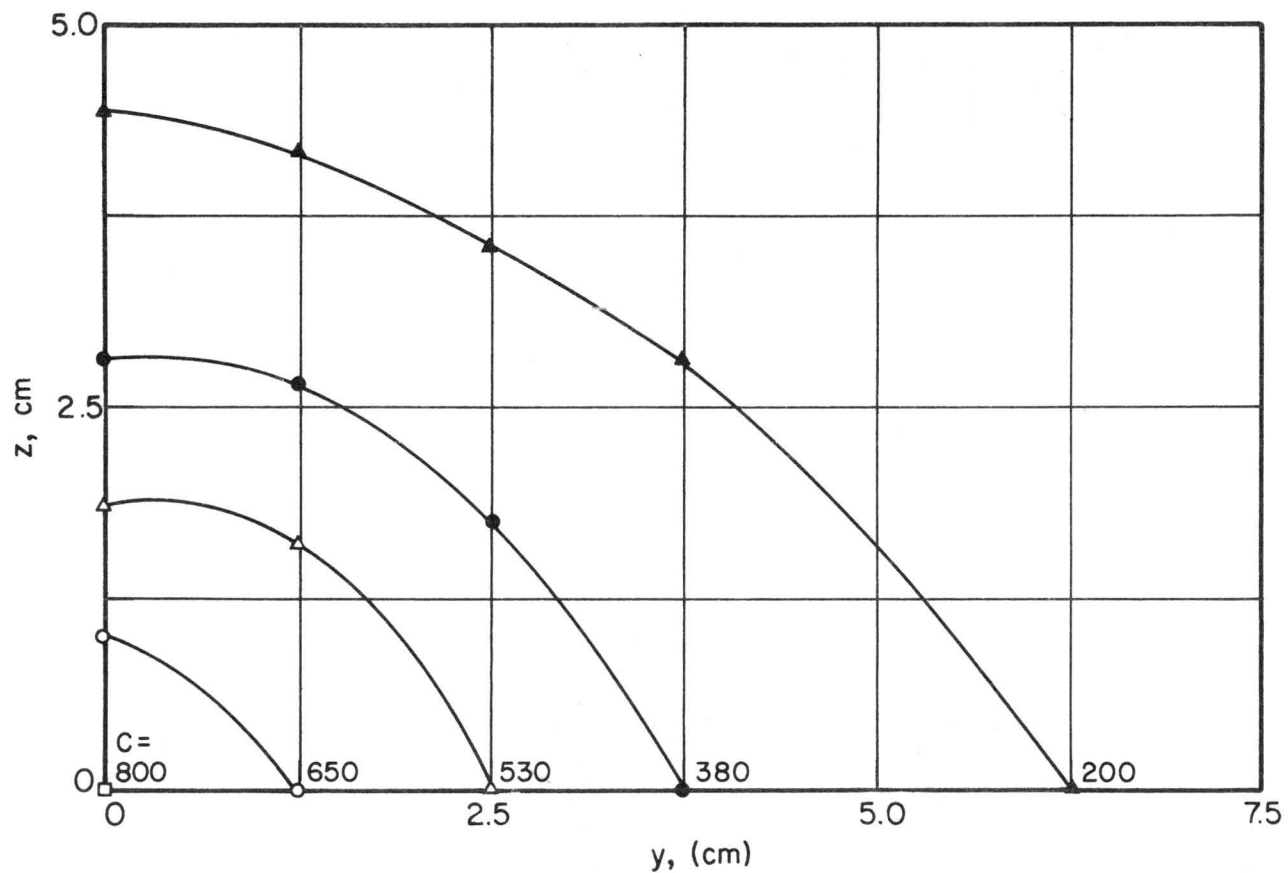


Fig. 42. Gaseous plume cross-section of a continuous point source in a model peg canopy (5.08 x 5.08 cm). $x_s = 0$ m, $z_s = 1$ cm, $x = 0.6$ m

PEGS: $\phi = 0.48$, $h = 9$ cm, SPACED 5.08 x 5.08 cm

LINE OF CONSTANT CONCENTRATION

$Z_s = 1$ cm

$X_s = 0$ cm

$X = 0.61$ m

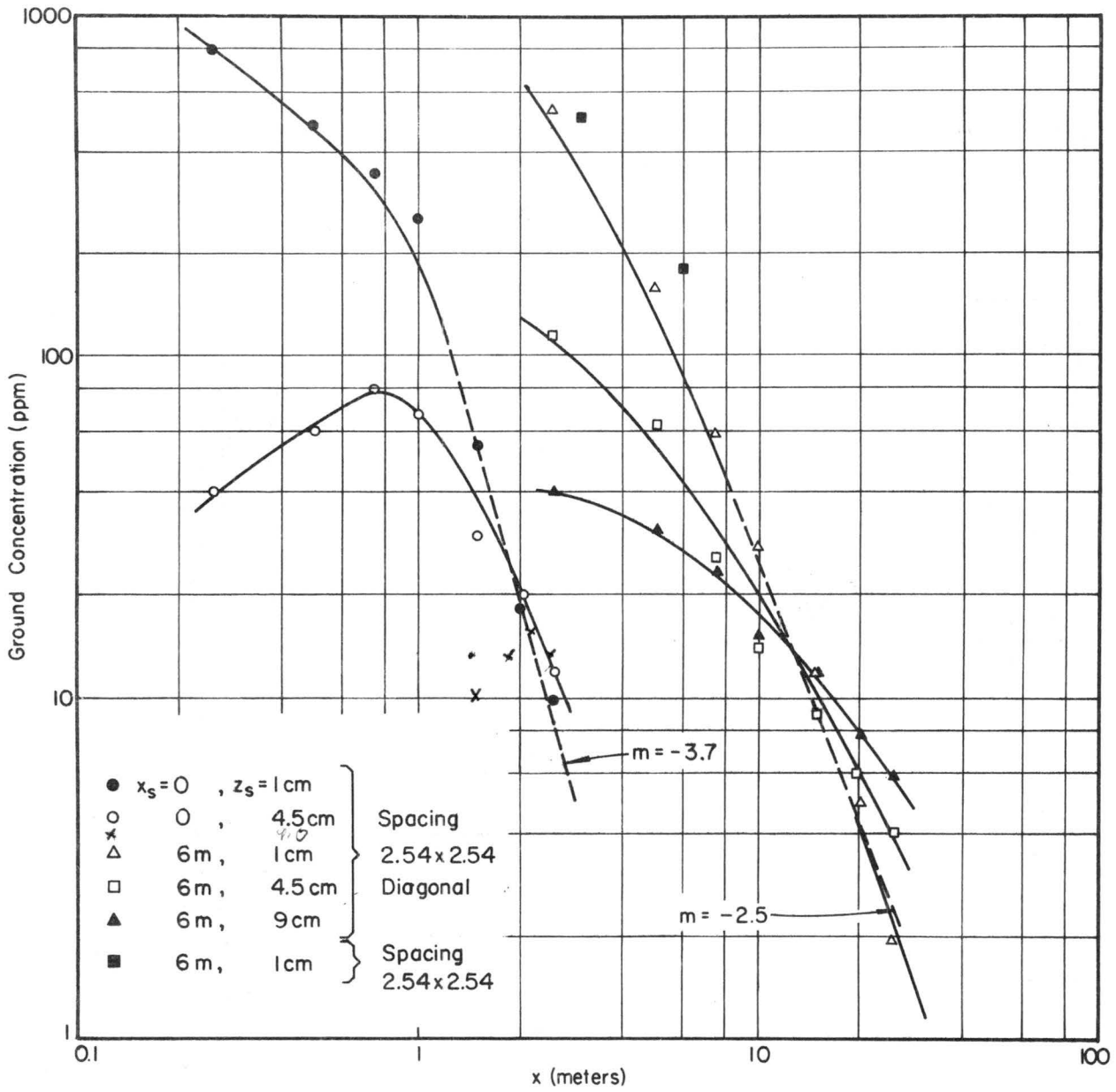


Fig. 43. Variation of ground level concentration with downstream distance

Pegs $\phi = 0.48 \text{ cm}, h = 9 \text{ cm}$

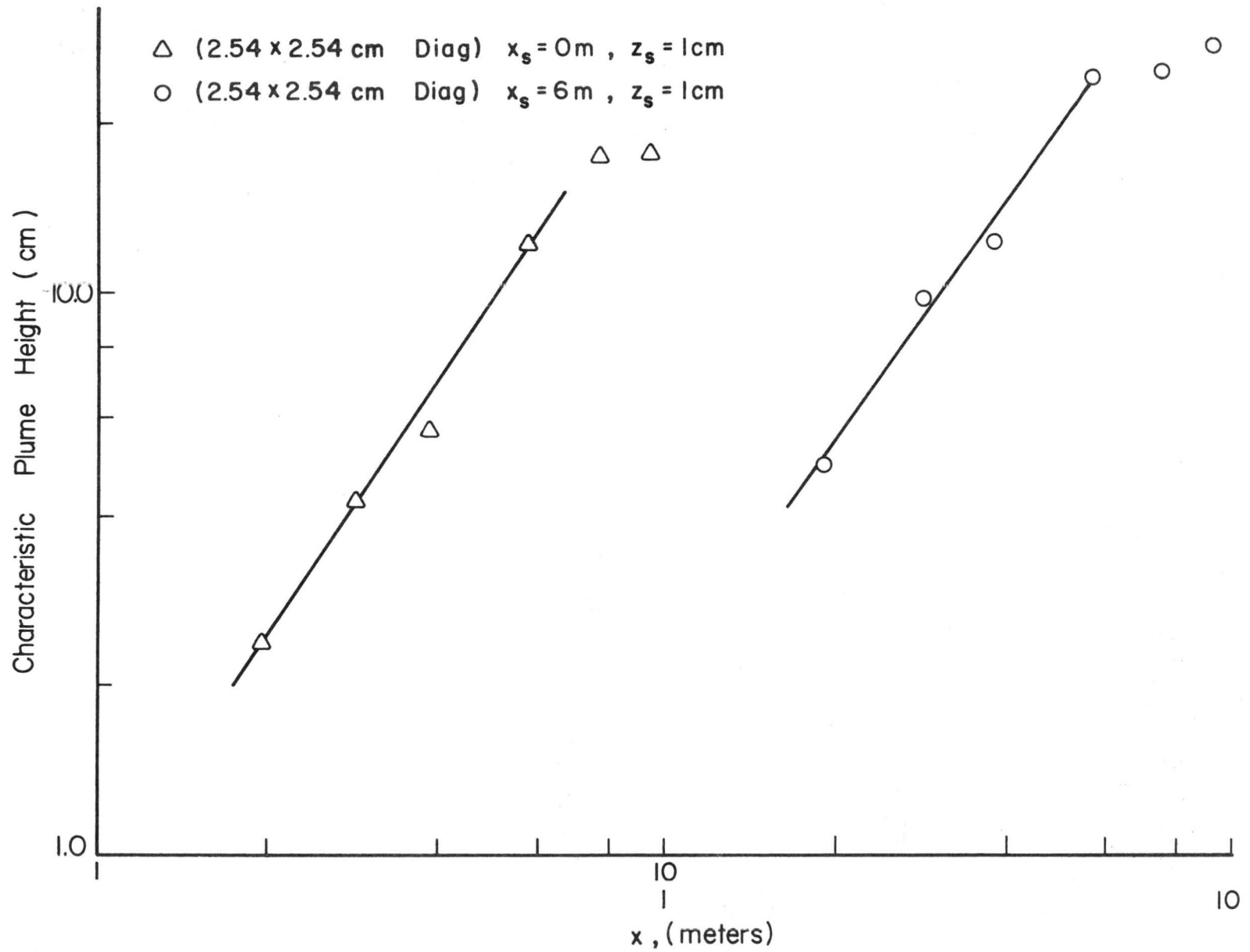


Fig. 44. Variation of characteristic plume height with downstream distance

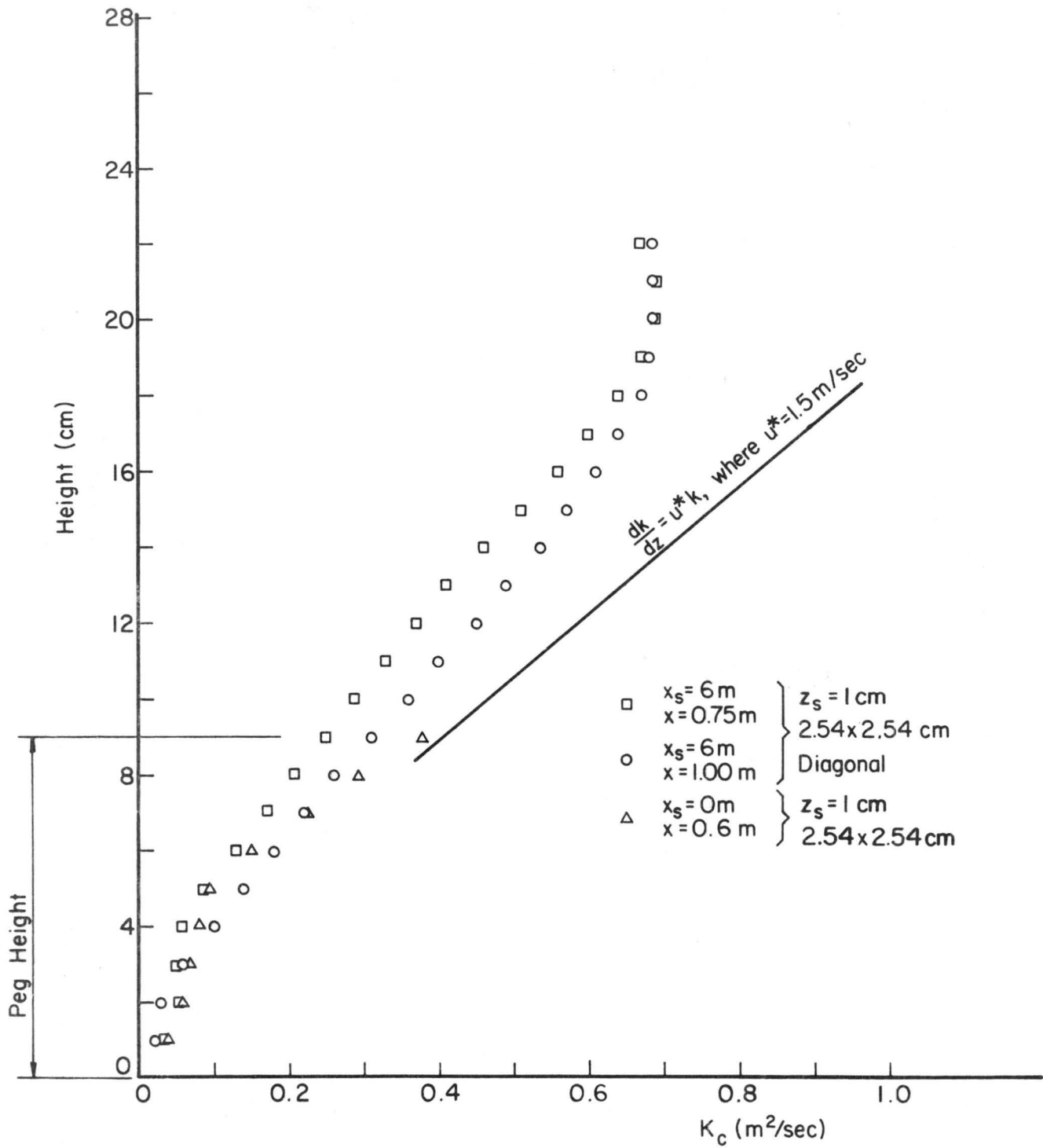


Fig. 45. Coefficient of turbulent diffusion

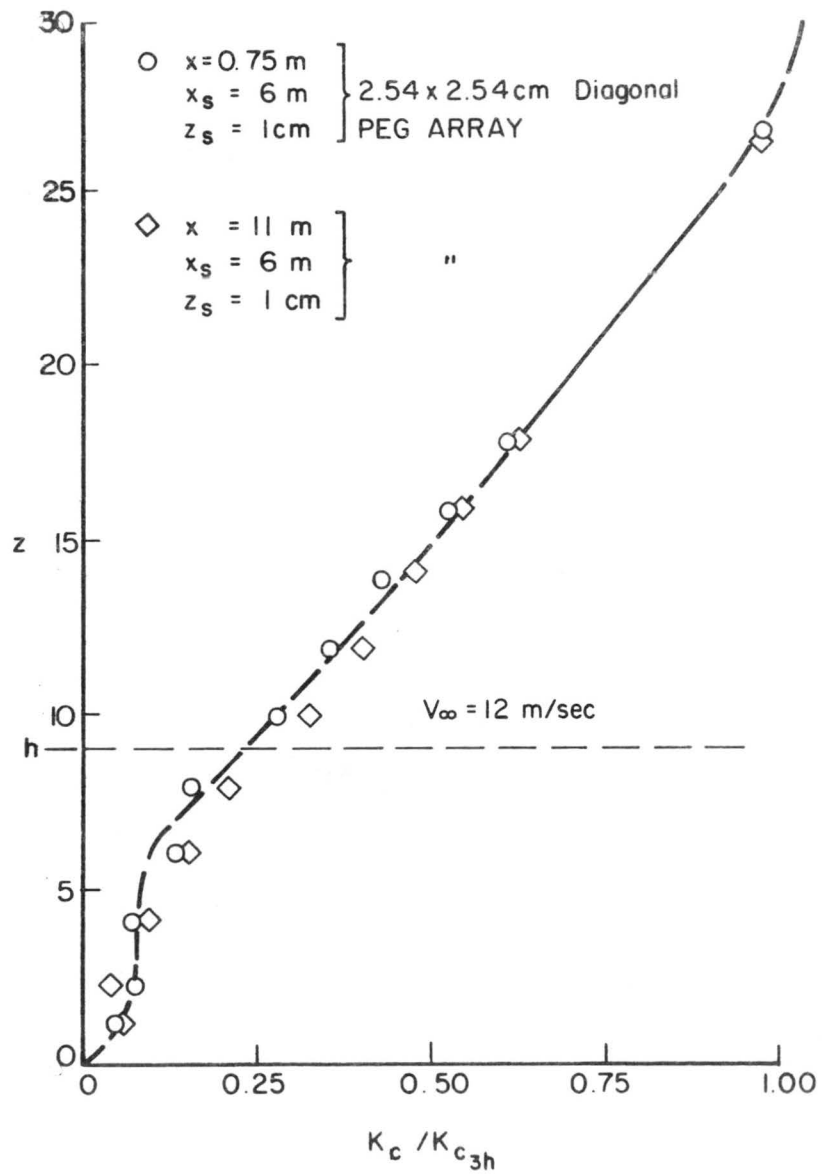
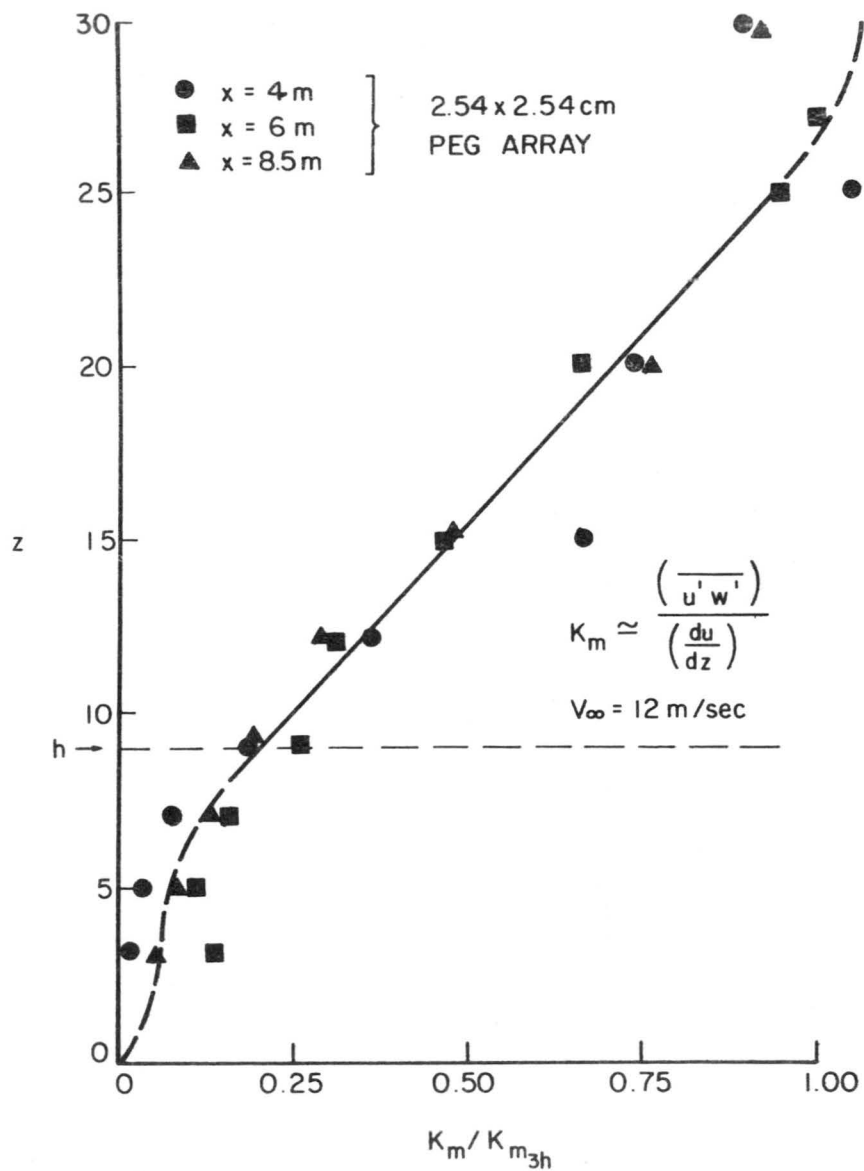


Fig. 46. Mass and momentum turbulent diffusion coefficients

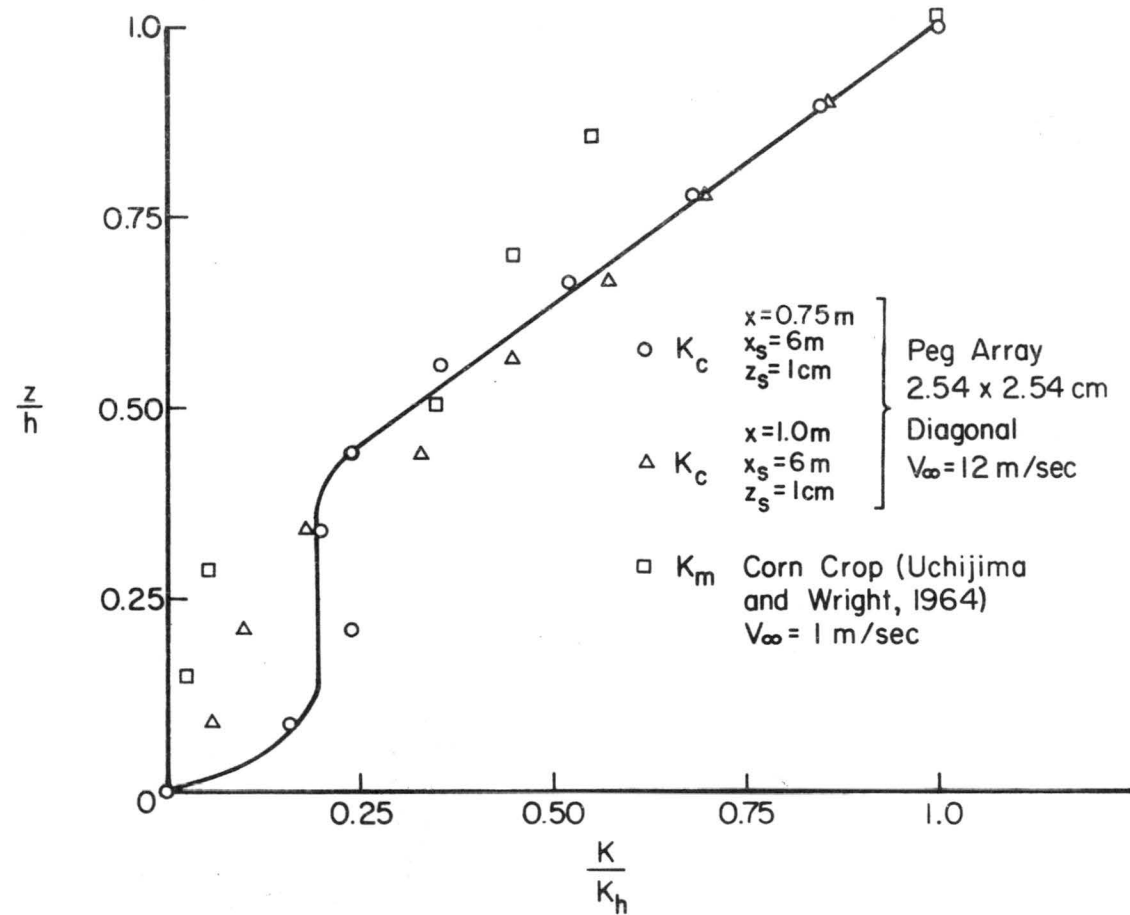


Fig. 47. Dimensionless eddy diffusion coefficient

DOCUMENT CONTROL DATA - R&D		
<i>(Security classification of title, body of abstract and indexing annotation must be entered when the overall report is classified)</i>		
1. ORIGINATING ACTIVITY (Corporate author) Colorado State University Foothills Campus Fort Collins, Colorado 80521		2a. REPORT SECURITY CLASSIFICATION Unclassified
		2b. GROUP
3. REPORT TITLE "GASEOUS PLUME DIFFUSION CHARACTERISTICS WITHIN MODEL PEG CANOPIES"		
4. DESCRIPTIVE NOTES (Type of report and inclusive dates) Technical Report		
5. AUTHOR(S) (Last name, first name, initial) Meroney, R. N.; Kesic, D.; and Yamada, T.		
6. REPORT DATE July, 1968	7a. TOTAL NO. OF PAGES 71	7b. NO. OF REFS 22
8a. CONTRACT OR GRANT NO. DAAB07-68-C-0423 b. PROJECT NO. 2275 c. d.	9a. ORIGINATOR'S REPORT NUMBER(S) CER68-69RNM- DK-TY-3 9b. OTHER REPORT NO(S) (Any other numbers that may be assigned this report)	
10. AVAILABILITY/LIMITATION NOTICES Distribution of this report is unlimited		
11. SUPPLEMENTARY NOTES	12. SPONSORING MILITARY ACTIVITY U. S. Army Materiel Command	
13. ABSTRACT A point source of an air-helium mixture was released continuously at various positions within a simulated canopy composed of 9 cm high pegs, 0.48 cm diameter, spaced in several arrays (2.54 x 2.54, 3.55 x 3.55, and 5.08 x 5.08 cm). Variations of the vertical location of the source revealed the strongly nonisotropic character of diffusion within a canopy with respect to the relative diffusion rates in the lateral and vertical directions. When the source was placed at various downstream distances from the edge of the canopy, it displayed a tendency to exhale the plume near the front of the model canopy and to inhale the plume at distances further downstream. Calculations of the turbulent diffusion coefficient, K, within and above the canopy from the experimental data, reveal both a constant region and a region of linear increase with height increase as suggested by previous authors.		

14. KEY WORDS	LINK A		LINK B		LINK C	
	ROLE	WT	ROLE	WT	ROLE	WT
	Simulation Atmospheric Modeling Wind-Tunnel Laboratory Turbulent Flow Diffusion Fluid Mechanics Micrometeorology Forest Meteorology Vegetative Canopies					

INSTRUCTIONS

1. **ORIGINATING ACTIVITY:** Enter the name and address of the contractor, subcontractor, grantee, Department of Defense activity or other organization (*corporate author*) issuing the report.
- 2a. **REPORT SECURITY CLASSIFICATION:** Enter the overall security classification of the report. Indicate whether "Restricted Data" is included. Marking is to be in accordance with appropriate security regulations.
- 2b. **GROUP:** Automatic downgrading is specified in DoD Directive 5200.10 and Armed Forces Industrial Manual. Enter the group number. Also, when applicable, show that optional markings have been used for Group 3 and Group 4 as authorized.
3. **REPORT TITLE:** Enter the complete report title in all capital letters. Titles in all cases should be unclassified. If a meaningful title cannot be selected without classification, show title classification in all capitals in parenthesis immediately following the title.
4. **DESCRIPTIVE NOTES:** If appropriate, enter the type of report, e.g., interim, progress, summary, annual, or final. Give the inclusive dates when a specific reporting period is covered.
5. **AUTHOR(S):** Enter the name(s) of author(s) as shown on or in the report. Enter last name, first name, middle initial. If military, show rank and branch of service. The name of the principal author is an absolute minimum requirement.
6. **REPORT DATE:** Enter the date of the report as day, month, year; or month, year. If more than one date appears on the report, use date of publication.
- 7a. **TOTAL NUMBER OF PAGES:** The total page count should follow normal pagination procedures, i.e., enter the number of pages containing information.
- 7b. **NUMBER OF REFERENCES:** Enter the total number of references cited in the report.
- 8a. **CONTRACT OR GRANT NUMBER:** If appropriate, enter the applicable number of the contract or grant under which the report was written.
- 8b, 8c, & 8d. **PROJECT NUMBER:** Enter the appropriate military department identification, such as project number, subproject number, system numbers, task number, etc.
- 9a. **ORIGINATOR'S REPORT NUMBER(S):** Enter the official report number by which the document will be identified and controlled by the originating activity. This number must be unique to this report.
- 9b. **OTHER REPORT NUMBER(S):** If the report has been assigned any other report numbers (*either by the originator or by the sponsor*), also enter this number(s).

10. **AVAILABILITY/LIMITATION NOTICES:** Enter any limitations on further dissemination of the report, other than those imposed by security classification, using standard statements such as:

- (1) "Qualified requesters may obtain copies of this report from DDC."
- (2) "Foreign announcement and dissemination of this report by DDC is not authorized."
- (3) "U. S. Government agencies may obtain copies of this report directly from DDC. Other qualified DDC users shall request through _____."
- (4) "U. S. military agencies may obtain copies of this report directly from DDC. Other qualified users shall request through _____."
- (5) "All distribution of this report is controlled. Qualified DDC users shall request through _____."

If the report has been furnished to the Office of Technical Services, Department of Commerce, for sale to the public, indicate this fact and enter the price, if known.

11. **SUPPLEMENTARY NOTES:** Use for additional explanatory notes.
12. **SPONSORING MILITARY ACTIVITY:** Enter the name of the departmental project office or laboratory sponsoring (*paying for*) the research and development. Include address.
13. **ABSTRACT:** Enter an abstract giving a brief and factual summary of the document indicative of the report, even though it may also appear elsewhere in the body of the technical report. If additional space is required, a continuation sheet shall be attached.

It is highly desirable that the abstract of classified reports be unclassified. Each paragraph of the abstract shall end with an indication of the military security classification of the information in the paragraph, represented as (*TS*), (*S*), (*C*), or (*U*).

There is no limitation on the length of the abstract. However, the suggested length is from 150 to 225 words.

14. **KEY WORDS:** Key words are technically meaningful terms or short phrases that characterize a report and may be used as index entries for cataloging the report. Key words must be selected so that no security classification is required. Identifiers, such as equipment model designation, trade name, military project code name, geographic location, may be used as key words but will be followed by an indication of technical context. The assignment of links, rules, and weights is optional.

MINIMUM BASIC DISTRIBUTION LIST FOR USAMC SCIENTIFIC AND
TECHNICAL REPORTS IN METEOROLOGY AND ATMOSPHERIC SCIENCES

Commanding General U. S. Army Materiel Command Attn: AMCRD-RV-A Washington, D. C. 20315	(1)	Chief of Research and Development Department of the Army Attn: CRD/M Washington, D. C. 20310	(1)	Commanding General U. S. Army Combat Development Command Attn: CDCMR-E Fort Belvoir, Virginia 22060	(1)
Commanding General U. S. Army Electronics Command Attn: AMSEL-EW Fort Monmouth, New Jersey 07703	(1)	Commanding General U. S. Army Missile Command Attn: AMSMI-RRR Redstone Arsenal, Alabama 35809	(1)	Commanding General U. S. Army Munitions Command Attn: AMSMU-RE-R Dover, New Jersey 07801	(1)
Commanding General U. S. Army Test and Evaluation Command Attn: NBC Directorate Aberdeen Proving Ground, Maryland 21005	(1)	Commanding General U. S. Army Natick Laboratories Attn: Earth Sciences Division Natick, Massachusetts 01762	(1)	Commanding Officer U. S. Army Ballistics Research Laboratories Attn: AMXBR-B Aberdeen Proving Ground, Maryland 21005	(1)
Commanding Officer U. S. Army Ballistics Research Laboratories Attn: AMXBR-IA Aberdeen Proving Ground, Maryland 21005	(1)	Director, U. S. Army Engineer Waterways Experiment Station Attn: WES-FV Vicksburg, Mississippi 39181	(1)	Director Atmospheric Sciences Laboratory U. S. Army Electronics Command Fort Monmouth, New Jersey 07703	(2)
Chief, Atmospheric Physics Division Atmospheric Sciences Laboratory U. S. Army Electronics Command Fort Monmouth, New Jersey 07703	(2)	Chief, Atmospheric Sciences Research Division Atmospheric Sciences Laboratory U. S. Army Electronics Command Fort Huachuca, Arizona 85613	(5)	Chief, Atmospheric Sciences Office Atmospheric Sciences Laboratory U. S. Army Electronics Command White Sands Missile Range, New Mexico 88002	(2)
U. S. Army Munitions Command Attn: Irving Solomon Operations Research Group Edgewood Arsenal, Maryland 21010	(1)	Commanding Officer U. S. Army Frankford Arsenal Attn: SMUFA-1140 Philadelphia, Pennsylvania 19137	(1)	Commanding Officer U. S. Army Picatinny Arsenal Attn: SMUPA-TV-3 Dover, New Jersey 07801	(1)
Commanding Officer U. S. Army Dugway Proving Ground Attn: Meteorology Division Dugway, Utah 84022	(1)	Commandant U. S. Army Artillery and Missile School Attn: Target Acquisition Department Fort Sill, Oklahoma 73504	(1)	Commanding Officer U. S. Army Communications - Electronics Combat Development Agency Fort Monmouth, New Jersey 07703	(1)
Commanding Officer U. S. Army CDC, CBR Agency Attn: Mr. N. W. Bush Fort McClellan, Alabama 36205	(1)	Commanding General U. S. Army Electronics Proving Ground Attn: Field Test Department Fort Huachuca, Arizona 85613	(1)	Commanding General Deseret Test Center Attn: Design and Analysis Division Fort Douglas, Utah 84113	(1)
Commanding General U. S. Army Test and Evaluation Command Attn: AMSTE-EL Aberdeen Proving Ground, Maryland 21005	(1)	Commanding General U. S. Army Test and Evaluation Command Attn: AMSTE-BAF Aberdeen Proving Ground, Maryland 21005	(1)	Commandant U. S. Army CBR School Micrometeorological Section Fort McClellan, Alabama 36205	(1)
Commandant U. S. Army Signal School Attn: Meteorological Department Fort Monmouth, New Jersey 07703	(1)	Office of Chief Communications - Electronics Department of the Army Attn: Electronics Systems Directorate Washington, D. C. 20315	(1)	Assistant Chief of Staff for Intelligence Department of the Army Attn: ACSI-DERSI Washington, D. C. 20310	(1)
Assistant Chief of Staff for Force Development CBR Nuclear Operations Directorate Department of the Army Washington, D. C. 20310	(1)	Chief of Naval Operations Department of the Navy Attn: Code 427 Washington, D. C. 20350	(1)	Officer in Charge U. S. Naval Weather Research Facility U. S. Naval Air Station, Building 4-28 Norfolk, Virginia 23500	(1)
Director Atmospheric Sciences Programs National Sciences Foundation Washington, D. C. 20550	(1)	Director Bureau of Research and Development Federal Aviation Agency Washington, D. C. 20553	(1)	Chief, Fallout Studies Branch Division of Biology and Medicine Atomic Energy Commission Washington, D. C. 20545	(1)
Assistant Secretary of Defense Research and Engineering Attn: Technical Library Washington, D. C. 20301	(1)	Director of Meteorological Systems Office of Applications (FM) National Aeronautics and Space Administration Washington, D. C. 20546	(1)	Director U. S. Weather Bureau Attn: Librarian Washington, D. C. 20235	(1)
R. A. Taft Sanitary Engineering Center Public Health Service 4676 Columbia Parkway Cincinnati, Ohio	(1)	Director Atmospheric Physics and Chemistry Laboratory Environmental Science Services Administration Boulder, Colorado	(1)	Dr. Albert Miller Department of Meteorology San Jose State College San Jose, California 95114	(1)
Dr. Hans A. Panofsky Department of Meteorology The Pennsylvania State University University Park, Pennsylvania	(1)	Andrew Morse Army Aeronautical Activity Ames Research Center Moffett Field, California 94035	(1)	Mrs. Francis L. Wheedon Army Research Office 3045 Columbia Pike Arlington, Virginia 22201	(1)
Commanding General U. S. Continental Army Command Attn: Reconnaissance Branch ODCS for Intelligence Fort Monroe, Virginia 23351	(1)	Commanding Officer U. S. Army Cold Regions Research and Engineering Laboratories Attn: Environmental Research Branch Hanover, New Hampshire 03755	(2)	Commander Air Force Cambridge Research Laboratories Attn: CRXL L. G. Hanscom Field Bedford, Massachusetts	(1)
Commander Air Force Cambridge Research Laboratories Attn: CRZW 1065 Main Street Waltham, Massachusetts	(1)	Mr. Ned L. Kragness U. S. Army Aviation Materiel Command SMOSM-E 12th and Spruce Streets Saint Louis, Missouri 63166	(1)	Harry Moses, Asso. Meteorologist Radiological Physics Division Argonne National Laboratory 9700 S. Cass Avenue Argonne, Illinois 60440	(1)
President U. S. Army Artillery Board Fort Sill, Oklahoma 73504	(1)	Commanding Officer, U. S. Army Artillery Combat Development Agency Fort Sill, Oklahoma 73504	(1)	Defense Documentation Center Cameron Station Alexandria, Virginia 22314	(20)
National Center for Atmospheric Research Attn: Library Boulder, Colorado	(1)	Commander, USAR Air Weather Service (MATS) Attn: AWSS/TIPD Scott Air Force Base, Illinois	(1)	Office of U. S. Naval Weather Service U. S. Naval Air Station Washington, D. C. 20390	(1)
Dr. J. E. Cermak, Head Fluid Mechanics Program Colorado State University Fort Collins, Colorado 80521	(15)	Dr. John Bogusky 7310 Cedardale Drive Alexandria, Virginia 22308	(1)	Dr. Gerald Gill University of Michigan Ann Arbor, Michigan 48103	(1)
Author	(1)				